



**HAL**  
open science

## Contribution to extension of energy approach to distributed parameter systems

Catalin-Marian Chera

► **To cite this version:**

Catalin-Marian Chera. Contribution to extension of energy approach to distributed parameter systems. Other. Ecole Centrale de Lille; Universitatea politehnica (Bucarest), 2009. English. NNT : 2009ECLI0013 . tel-00578842

**HAL Id: tel-00578842**

**<https://theses.hal.science/tel-00578842>**

Submitted on 22 Mar 2011

**HAL** is a multi-disciplinary open access archive for the deposit and dissemination of scientific research documents, whether they are published or not. The documents may come from teaching and research institutions in France or abroad, or from public or private research centers.

L'archive ouverte pluridisciplinaire **HAL**, est destinée au dépôt et à la diffusion de documents scientifiques de niveau recherche, publiés ou non, émanant des établissements d'enseignement et de recherche français ou étrangers, des laboratoires publics ou privés.

N° d'ordre : 104

ECOLE CENTRALE DE LILLE

## THESE

présentée en vue d'obtenir le grade de

## DOCTEUR

en

Spécialité : AUTOMATIQUE ET INFORMATIQUE INDUSTRIELLE

par

**CHERA Catalin Marian**

DOCTORAT DELIVRE CONJOINTEMENT  
PAR L'ECOLE CENTRALE DE LILLE ET L'UNIVERSITE «POLITEHNICA» DE BUCAREST

Titre de la thèse :

# Contribution à l'extension de l'approche énergétique à la représentation des systèmes à paramètres distribués

Soutenue le 01.07.2009 devant le jury d'examen :

<b>Président</b>	<b>Florin Filip</b> , Académicien, Academia Romana
<b>Rapporteur</b>	<b>Abdellah El Moudni</b> , Professeur, Université de Technologie de Belfort-Montbéliard
<b>Rapporteur</b>	<b>Jorge Luis Balino</b> , Professeur, Departamento Engenharia Mecanica, Escola Politécnica, Universidade de São Paulo
<b>Examineur</b>	<b>Florin Filip</b> , Académicien, Academia Romana
<b>Examineur</b>	<b>Adina Magda Florea</b> , Professeur, Department of Computer Science, University Politehnica of Bucharest
<b>Examineur</b>	<b>Arun Kumar Samantaray</b> , Associate Professor, Department of Mechanical Engineering, Indian Institute of Technology (IIT-Kharagpur)
<b>Directeur de thèse</b>	<b>Geneviève Dauphin-Tanguy</b> , Professeur, Ecole Centrale de Lille
<b>Directeur de thèse</b>	<b>Dumitru Popescu</b> , Professeur, Department of Control and Computers, University Politehnica of Bucharest
<b>Co-encadrant</b>	<b>Aziz Nakrachi</b> , Maître de Conférences, Polytech'Lille, Université de Sciences et Technologies Lille1
<b>Invité</b>	<b>Hassane Abouaissa</b> , Maître de Conférence, LGI2A, Faculté des Sciences Appliquées, Université d'Artois

Thèse préparée au Laboratoire d'Automatique,  
de Génie Informatique et Signal, LAGIS, UMR 8146  
Ecole Centrale de Lille

Ecole Doctorale SPI 072 (Lille I, Lille III, Artois, ULCO, UVHC, EC Lille)



## Acknowledgements

“The end is always a new beginning” says a Chinese proverb. After a very beautiful and fruitful period I have reached the end of the thesis. Next to the scientific aspect there is always a human one, so I would like to express my gratitude for the special people who were on my side me along this road.

I want to thank my two advisers, Mr. Dumitru Popescu and Mrs. Genevieve Dauphin Tanguy, for offering me the opportunity to pursue my PhD, and always having a good advice when I needed one. The research period I have spent at Ecole Centrale has been particularly productive.

My deep respect and gratitude go to my adviser Mr. Aziz Nakrachi for all his help He was near me and offered me the best advice when I need it.

I would like to thank Mr. Jorge Balino for the good advice he offered me during the period he spent at Ecole Centrale de Lille, and for helping me finalize the thesis.

Mr. Abdellah El Moudni reviewed this PhD report before publication and helped me shape its final form.

I am grateful to Mr. Florin Filip, Mrs. Adina Magda Florea and Mr. Arun Kumar Samantaray for accepting to be a part of the PhD defense committee.

I want to thank all my PhD students colleagues: Stefan, Anca, Catalin, Roberto, Dapeng, Hicham etc. I want to express my gratitude to the Romanian students I met here in Lille and next to whom I spent a nice and pleasant time: Cristina, Raluca, Marinela, Cosmin, Vicentiu, Laura, etc.

I want to give special tanks to my friends Radu Vatavu and Adriana Bacila, with whom I spent many evenings and days discussing technical problems.

A special thank you goes to my family which was always close to me in the difficult moments of my life, supported me and gave me the strength to finish this thesis. They offered me all support and made me not realize the physical distance that separated us.

## **Contribution à l'extension de l'approche énergétique à la représentation des systèmes à paramètres distribués**

Tout phénomène, qu'il soit biologique, géologique ou mécanique peut être décrit à l'aide des lois de la physique en termes d'équations différentielles, algébriques ou intégrales, mettant en relation différentes variables physiques.

L'étude des phénomènes physiques implique deux tâches importantes : la formulation d'un modèle mathématique et une analyse numérique pour le modèle considéré.

La conception du modèle mathématique nécessite de bonnes connaissances dans les domaines concernés (lois de la physique), et, très souvent, sur certains outils mathématiques. C'est une tâche difficile et parfois longue, qui demande du temps et des efforts afin d'obtenir un modèle réaliste qui est capable de satisfaire les demandes de l'utilisateur.

Les résultats, sous forme d'équations différentielles pour l'étude dynamique, établissent un lien entre les variables nécessaires à la compréhension et/ou la conception des systèmes. Dans l'accomplissement de cette tâche, des hypothèses concernant le fonctionnement du processus sont faites. Dans la simulation numérique nous utilisons des algorithmes numériques et l'ordinateur pour évaluer

le modèle mathématique et faire l'estimation des caractéristiques du processus.

L'approche bond graph a une place importante parmi les approches utilisées pour la représentation des systèmes. C'est un langage graphique qui utilise le principe d'analogie, pour différents domaines physiques, permettant la modélisation et la simulation. Il est basé sur l'étude des échanges de puissance au sein du système et entre le système et son environnement.

Souvent on suppose que le système à modéliser est à paramètres localisés. Mais si cette hypothèse n'est pas vérifiée, des outils spécifiques seront utilisés.

Les systèmes à paramètres distribués ont en général un nombre réduit d'entrées et de sorties, mais l'espace d'état est de dimension infinie. La représentation mathématique est faite à l'aide d'équations différentielles partielles (EDP). La forme (parabolique, hyperbolique) des équations détermine les propriétés du modèle (en termes de stabilité, contrôlabilité, observabilité etc.).

Les objectifs de la thèse sont de montrer comment les systèmes à paramètres distribués peuvent être modélisés par un modèle bond graph, qui est par sa nature un modèle à paramètres localisés. Deux approches sont possibles:

- la première approche consiste à utiliser une technique d'approximation qui discrétise le modèle dans le domaine spatial, en supposant que les phénomènes physiques distribués peuvent être considérés comme homogènes dans certaines parties de l'espace, donc localisés. Différents modèles bond graphs peuvent être obtenus en fonction de la technique utilisée.
- la deuxième approche consiste à déterminer la solution des EDP qui dépend du temps et de l'espace, puis à approximer cette solution avec différents outils numériques.

Le premier chapitre rappelle quelques méthodes classiques utilisées pour l'approximation des EDP et les modèles bond graphs correspondants.

Obtenir une solution exacte pour une EDP est une tâche difficile. Des méthodes d'approximation existent, elles peuvent être classées en deux grandes familles : les méthodes d'approximation des équations (ex. volumes finis) et les méthodes d'approximation des solutions (ex. éléments finis).

La méthode des éléments finis [STR 04], [GUE 63], [GER 87] est une méthode où les dérivées partielles sont remplacées par des quotients qui utilisent les valeurs de la solution en certains points particuliers du domaine. Le résultat est un système d'équations algébriques qui peut être résolu si les conditions aux frontières sont fixes.

Les méthodes variationnelles [WAN 07], [GER 87] sont des méthodes où les équations aux dérivées partielles sont représentées sous une forme intégrale et les solutions sont approchées par une combinaison linéaire  $\sum_i b_i \phi_i$ , où  $\phi_i$  sont les fonctions d'approximation et  $b_i$  les coefficients inconnus. A titre d'exemples, on peut citer la méthode des résidus pondérés, la méthode de Galerkin, la méthode de Ritz. Le principal désavantage de ces méthodes concerne la difficulté à sélectionner les fonctions d'approximation. Il n'y a pas de procédure unique pour les construire et cela devient très difficile quand le domaine a une géométrie complexe et les conditions aux frontières compliquées.

La méthode des éléments finis est similaire aux méthodes spectrales ; la différence majeure réside dans le choix des fonctions d'approximation. Les éléments finis découpent l'intervalle spatial en sous intervalles, et prennent  $\phi_i(x)$  comme des fonctions locales sous forme polynomiale non nulle avec un degré fixe. Les méthodes spectrales utilisent des fonctions de base globales où les  $\phi_i(x)$  sont polynomiales avec un haut degré qui sont non nulles sur tout le domaine sauf en quelques points isolés.

Les méthodes spectrales produisent des équations algébriques avec des matrices pleines, et l'ordre élevé des fonctions de base donne une grande précision. Les éléments finis produisent des matrices bandes.

Le deuxième chapitre présente l'approche port-Hamiltonienne et son extension aux systèmes à paramètres distribués est proposée.

Quelques résultats de la littérature sont rappelés pour les systèmes dissipatifs et non dissipatifs. Nous proposons un nouveau résultat pour la modélisation bond graph de l'équation du télégraphiste dans le cas avec phénomènes dissipatifs.

Le système port Hamiltonien a été utilisé pour la représentation des systèmes à paramètres distribués. Sur l'exemple de l'équation du télégraphiste, on a montré [Che 09] que si on utilise une forme spéciale de discrétisation pour l'espace, on fait le calcul seulement pour un élément local et puis en concaténant les éléments on peut calculer la ligne de transmission entière.

Le système port-Hamiltonien est dérivé de la fonction d'énergie (Hamiltonien) qui peut être prise comme fonction de Lyapunov, utilisée pour la commande.

La modélisation du trafic routier a été choisie comme le champ d'application de nos travaux.

Le troisième chapitre présente un résumé des différents types des modèles de trafic routier trouvés dans la littérature. Nous avons mis en œuvre certains d'entre eux et comparé les résultats obtenus par simulation pour quelques modèles et quelques algorithmes.

Le modèle LWR [Lig 55], [Ric 56] a été considéré pendant de nombreuses années comme un des meilleurs modèles proposés pour la représentation du trafic routier. Mais dans les dernières années quelques auteurs ont mis en évidence des problèmes, et proposé de nouveaux modèles. Nous avons retenu quelques modèles macroscopiques par lesquels ceux de Zhang, Aw et Rasclé [Aw 00].

A l'aide de simulations on a montré les avantages et les inconvénients de ces modèles, et déterminé les méthodes numériques les mieux adaptées à la discrétisation des modèles.

Dans le chapitre quatre, on a proposé une approche originale par l'extension de la représentation bond graph développée dans le domaine des Computational Fluid Dynamics pour la modélisation des flux de trafic, en utilisant le modèle de Jiang [Jia 02] .

Les principaux résultats que nous avons obtenus sont:

- la construction d'un modèle bond graph à paramètres distribués où toutes les variables sont distribuées ;
- la dérivation du modèle d'état à partir du modèle bond graph comme un modèle ODE de dimension infinie.

Ce modèle bond graph doit être discrétisé pour la simulation. Un modèle bond graph générique est proposé pour chaque partie de l'espace (appelé « section »), qui doit être reproduit un nombre suffisant de fois pour obtenir une solution stable.

On a développé une approche théorique de l'approche bond graph pour représenter le modèle à deux équations EDP, une pour la densité et l'autre pour la vitesse. Les équations d'état sont exprimées en termes de variables d'état, associées aux valeurs nodales de masse et de vitesse.

L'ensemble des variables de l'effort et de flux généralisés a été déduit à l'aide de considérations énergétiques, tandis que les équations d'état ont été obtenues conformément à la formulation Petrov-Galerkin pour les phénomènes liés à la masse et la formulation Galerkin pour ceux liés à la vitesse; en conséquence, les outils de calcul développés pour la méthode de éléments finis, aussi que pour d'autres méthodes numériques, peuvent être utilisés pour résoudre les équations d'état obtenues.

Concernant l'approche CFD, il y a encore quelques problèmes à résoudre:

- développer un algorithme de calcul qui gère les singularités dans les matrices ;
- déterminer le nombre approprié de sections à utiliser pour avoir une solution stabilisée ;
- étudier plus précisément la vitesse, et comparer les résultats obtenus avec ceux déduits du modèle LWR dans différents scénarios. Les développements futurs concernant les flux de trafic sont vastes et complexes ;
- le modèle bond graph pour CFD proposé considère une seule route, maintenant il doit être étendu à des croisements;
- la route est supposée composée d'une seule voie. Les modèles peuvent être étendus à deux voies comme une autoroute ;
- nous supposons avoir le même type de véhicules. Ceci peut être étendu en considérant différents types de véhicules, avec des vitesses différentes ;
- la route est supposée être sans rampe d'accès. Nous pouvons considérer le cas où on a une rampe en entrée et/or en sortie ;
- le modèle est un modèle de circuit ouvert, sans perturbations. Une stratégie de contrôle, lié aux objectifs de flux de trafic, peut être étudiée. On peut utiliser le modèle d'espace d'état dérivée de bond graph pour cela.

## Contents

<b>Acknowledgements</b>	i
<b>Résumé en français</b>	iii
<b>Table of contents</b>	ix
<b>Introduction</b>	1
<b>Chapter 1. Classical methods for solving PDE models..... 7</b>	
1.1. Introduction .....	11
1.2. Partial differential equations.....	14
1.3. Solving PDE.....	17
1.3.1. The method of weighted residual .....	19
1.3.2. The method of separation of variables .....	20
1.3.3. Spectral methods .....	27
1.3.4. Finite element method .....	30
1.3.5. Finite difference method.....	42
1.3.6. Finite volume method.....	48
1.4. Conclusion.....	52

<b>Chapter 2. Port-Hamiltonian systems</b> .....	55
2.1. Introduction .....	58
2.2. The principle of least action.....	59
2.3. Hamiltonian formalism.....	61
2.3.1. Port Hamiltonian representation.....	62
2.4. Transmission line application.....	75
2.4.1. Without dissipation.....	75
2.4.2. With dissipation.....	76
2.4.3. Spatial discretization .....	80
2.4.4. Constitutive equations.....	86
2.5. Conclusion.....	89
<b>Chapter 3. Traffic flow models</b> .....	91
3.1. Introduction .....	95
3.2. Model classification.....	97
3.3. Microscopic and mesoscopic models .....	98
3.3. Macroscopic models.....	99
3.4. Numerical methods .....	110
3.5. Implementation .....	114
3.5.1. Riemann problem in the LWR model.....	114
3.5.2. Influence of the choice of a numerical method on LWR model.....	115

3.5.3.	Comparison of 1-equation model and 2-equation models.....	116
3.5.4.	Comparison of LWR and Jiang models.....	118
3.6.	Conclusions.....	120
<b>Chapter 4. Transport equations modeled by CFD.....</b>		<b>123</b>
4.1.	Introduction .....	127
4.1.1.	Two-equation traffic models.....	128
4.2.	Power balance per unit volume.....	128
4.2.1.	Kinetic energy .....	128
4.2.2.	Balance equations .....	129
4.3.	Discretization.....	130
4.3.1.	Description of the flow fields.....	130
4.3.2.	Integrated variables .....	131
4.4.	System integration.....	132
4.4.1.	Kinetic energy .....	132
4.4.2.	System $IC$ -field .....	134
4.4.3	Resistance field.....	135
4.5.	State equations.....	136
4.5.1.	Mass port .....	136
4.5.2.	Velocity port .....	138
4.6.	Coupling matrices .....	139
4.6.1.	Coupling between the velocity and mass ports .....	139

4.7.	System Bond Graph .....	140
4.8.	Initial and boundary conditions .....	141
4.8.1.	Initial conditions .....	141
4.8.2.	Boundary conditions .....	142
4.9.	Integrated variables .....	142
4.9.1.	Shape and weight functions .....	143
4.9.2.	Diagonal volume matrix .....	147
4.9.3.	Nodal vector of mass .....	148
4.9.4.	Inertia matrix .....	148
4.9.5.	Nodal vectors of potentials .....	148
4.9.6.	State equations, mass port .....	149
4.9.7.	State equations, velocity port .....	154
4.10.	Implementation .....	159
4.11.	Conclusions .....	165
	<b>Conclusions. Future developments</b> .....	<b>167</b>
	<b>References</b> .....	<b>173</b>
	<b>Appendices</b> .....	<b>187</b>

# **Introduction**



## Introduction

Virtually every phenomenon in nature, whether biological, geological, or mechanical, can be described with the aid of the laws of physics, in terms of algebraic, differential, or integral equations relating various quantities of interest.

The study of physical phenomena involves two major tasks: to formulate a mathematical model and to make a numerical analysis for the considered model.

The conception of a mathematical model requires background in related subjects (e.g. laws of physics) and, most often, certain mathematical tools. It is a difficult and sometimes long task, which request time and effort in order to obtain a realistic model capable to satisfy the user demands.

The results, as differential equations for dynamic study, relate quantities of interest in the understanding and/or design of the physical process. In the achievement of this task, assumptions concerning how process works are made. In numerical simulation we use numerical algorithms and computer to evaluate the mathematical model and estimate the characteristics of the process.

Among the system representation approaches, the bond graph has an important place. It is a unified graphical language, using the analogy principle, for different physical domains allowing modeling and simulation. It is based on power exchanges inside the system and between the system and its environment.

It is often assumed that the system to be modeled as lumped parameters. But if this assumption is not verified, specific tools have to be used.

The distributed parameter systems do not have in general a great number of inputs and outputs, but the state space is of infinite dimension. The mathematical representation of these systems is made using partial differential equations (PDE). The form (parabolic, hyperbolic) of equations determines the properties of the model (in terms of stability, controllability, observability etc.).

The objectives of the thesis were to show how distributed parameter systems can be modeled using a bond graph model, which is by its nature itself a lumped parameter model. Two ways are possible. They are summarized in figure 1:

- the first approach consists in using an approximation technique to discretize the model in the space domain, assuming that physical distributed phenomena can be considered as homogenous in some parts of space, and thus lumped. Different bond graph models can be obtained depending on the technique used.
- the second approach consists in determining a solution of the PDE depending on space and time, and thus to approximate this solution by means of different kinds of tools.

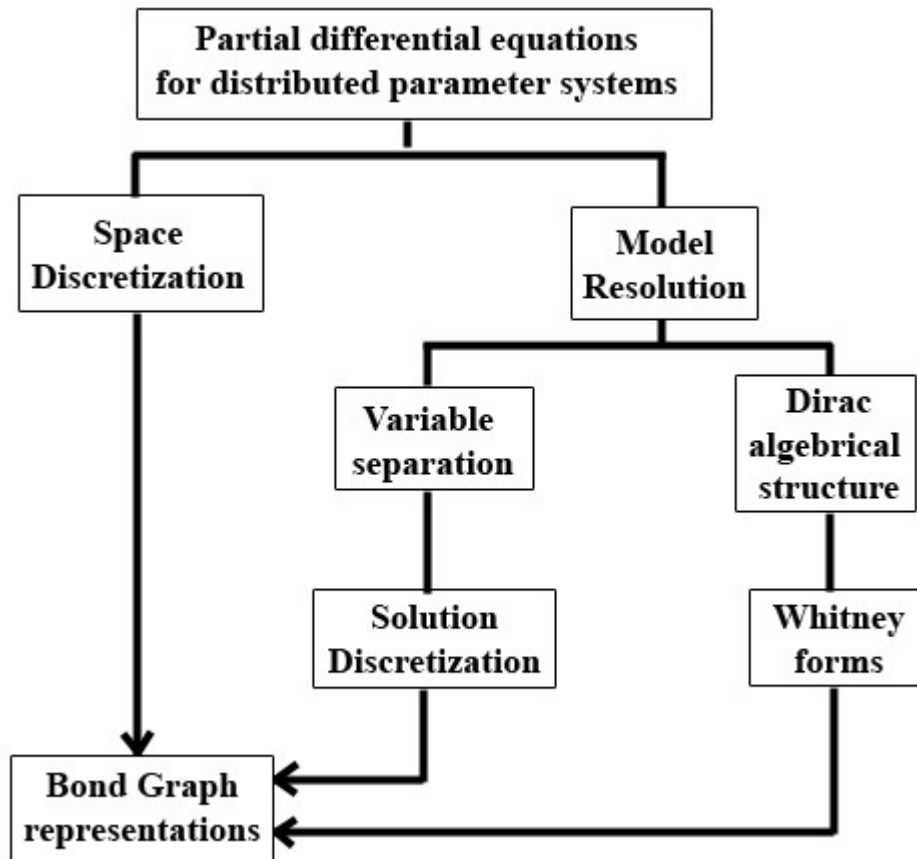


Fig. 1. Two approaches to go from PDE models to bond graph models

In the first chapter we recall the classical methods used for approximation of partial differential equations and the corresponding Bond Graph model.

The second chapter presents the port-Hamiltonian approach for distributed parameter systems.

Some results from the literature are recalled for non dissipative and dissipative systems. We propose a new result for the bond graph modeling of the telegrapher's equation in the case of dissipative phenomena.

The modeling of traffic flow was chosen as application field.

In the third chapter, we make a summary of the different types of models found in the literature. We implement some of them and compare the obtained simulation results for several models and several numerical algorithms.

The fourth chapter proposes an original approach extending Computational Fluid Dynamics bond graph representation to traffic flow. The main results of this method are:

- construction of a “distributed parameter bond graph” where all the variables are distributed variables;
- derivation from the bond graph of a state model under as an infinite dimensional ODE model.

This bond graph model has to be discretized for simulation. A “generic” bond graph model of each space subpart (called “section”) is proposed, which has to be reproduced the number of times sufficient to obtain a stabilized simulated solution.

Implementation of traffic flow CFD models is made using MATLAB software.

A bibliography and appendices are placed at the end of the report.

# **Chapter 1.**

## **Classical methods for solving PDE models**



## Contents

<b>Chapter 1. Classical methods for solving PDE models</b> .....	7
1.1. Introduction .....	11
1.2. Partial differential equations.....	14
1.3. Solving PDE.....	17
1.3.1. The method of weighted residual .....	19
1.3.2. The method of separation of variables .....	20
1.3.3. Spectral methods .....	27
1.3.4. Finite element method .....	31
1.3.5. Finite difference method .....	42
1.3.6. Finite volume method.....	48
1.4. Conclusion.....	52



## Chapter 1. Classical methods for solving PDE models

### 1.1. Introduction

Every physical system is composed of elements, dynamically interacting and exchanging power and informations.

The energy and information exchanges between components can be represented in a graphical way, which contains all is necessary to obtain the dynamical evolution of the model. The bond graph [KAR 90], [DAU 00] approach follows this concept.

In the bond graph representation, the power transfer between elements is represented by bonds. Through a bond, an element exchange power with the rest of the system; power is for all the physical domains the product of two complementary variables (effort and flow) as shown figure 1.1.

Interconnections between subsystems can be done at nodes where power can be exchanged between subsystems. Such places are called ports, and physical subsystems with one or more ports are called multiports. A system with a single port is called a 1-port, a system with two ports is called as 2-ports, and so on.

	<b>Effort <math>e</math></b>	<b>Flow <math>f</math></b>
<b>Electrical</b>	Voltage [V]	Current [A]
<b>Mechanics Translational</b>	Force [N]	Velocity [m/s]
<b>Rotational</b>	Torque [N*m]	Angular Velocity [rad/sec]
<b>Hydraulic</b>	Pressure [N/m <sup>2</sup> ]	Volume Flow rate [m <sup>3</sup> /sec]
<b>Chemical</b>	Chemical Potential [J/mole]	Molar Flow rate [mole/sec]
<b>Thermodynamic</b>	Temperature [K]	Entropy Flow rate $dS/dt$ [W/K]

Fig.1.1. Effort/flow definitions in different engineering domains

In every system (mechanical, electrical, chemical or hydraulic domain), generalized effort variable and a generalized flow variable are defined the product of which being the power exchanged between elements.

Distributed parameter systems are represented using partial differential equations (PDE).

Partial differential equations are differential equations containing independent variables (spatial variables to which we add time in evolution phenomena cases) and dependent variable.

One of the problems in the study of distributed parameter models is to find the solution of the equations, and in most cases this solution is found as an approximation of the initial problem with respect to some properties.

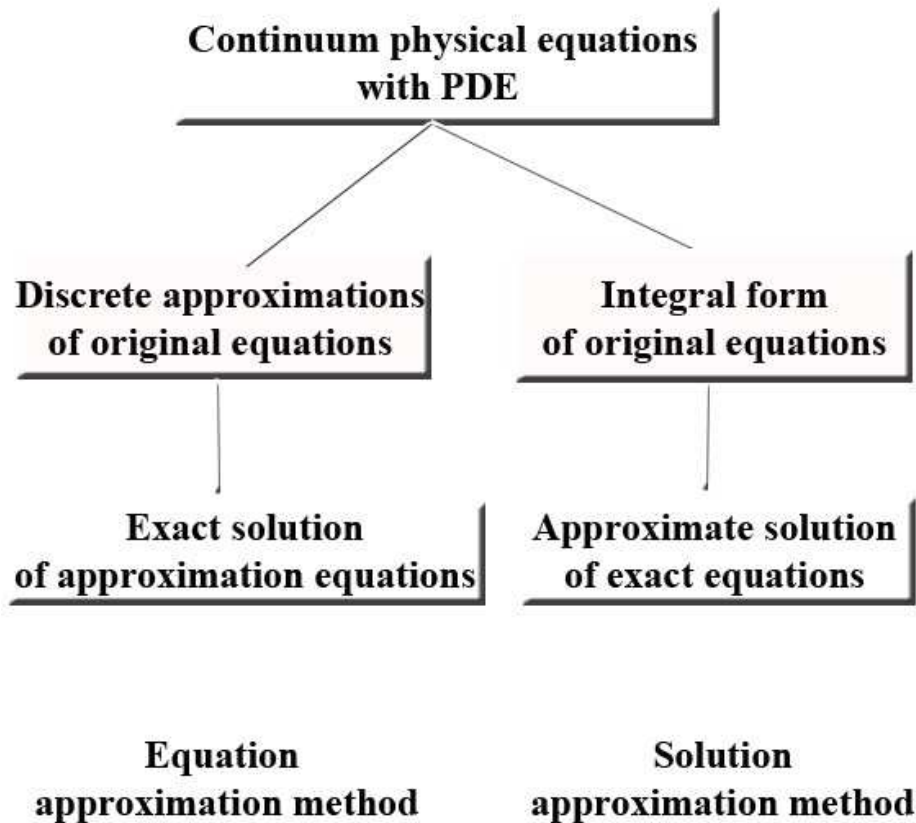


Fig.1.2. Different approaches used for solving PDE

In simulation, to obtain an exact solution of the problem is a very difficult task. Approximation methods are instead used to find a solution. There are two classes of approximation: the approximation of the equations (finite difference volumes) and the approximation of the solution (variational methods, finite elements methods).

In the finite difference methods [STR 04], [GUE 63], [GER 87] the partial derivatives of the variables are replaced by difference quotients which involve the values of the solution at discrete mesh points of the domain. The result is an algebraic equation system which is solved once boundary conditions are fixed.

In the variational methods [WAN 07], [GER 87] the partial differential equation is represented in an equivalent weighted-integral form and the approximate solution is assumed to be a linear combination  $\sum_i b_i \phi_i$ , with approximation functions  $\phi_i$  and undetermined

coefficients  $b_i$ . The coefficients  $b_i$  are determined such that the integral statement equivalent to the original partial differential equation is satisfied. The variational methods as Galerkin, Rayleigh-Ritz and least-squares, differ one from another by the choice of the integral form, weight function and/or approximation functions.

The finite element methods [RED 93], [AGO 85], [LEW 91], [SAB 86] represent the domain as a collection of geometrically simple sub domains, called finite elements. Then, over each element, the approximation functions are derived using the basic idea that any continuous function can be represented by a linear combination of algebraic polynomials. The algebraic relations among the undetermined coefficients are obtained by satisfying the governing equations, often in a weighted-integral sense, over each element.

In this chapter we will present a classical approach which will consist in a discretization followed by a bond graph representation.

## ***1.2. Partial differential equations***

A system is assumed to be an entity separable from the rest of the universe (the environment of the system) by means of a physical or conceptual boundary. The exchange of information and power with the environment is realized through the boundary. A system is decomposed into interacting parts. These are considered as subsystems and have a lower complexity level than the system.

The modeling procedure consists in trying to obtain one or more models that represent in a way the system compartment. The models are abstract entities which help us to understand, analyze and predict the system behavior. Each model must be homogenous to the system, meaning that it must have the same number of inputs and outputs.

The model structure consists in a parameter vector, a number of inputs and a number of outputs that depend of hypotheses made. The model obtained is a specific vision of the studied system. There are some

approximation methods that need to ignore some parameters in order to avoid singularities and some complexity, meaning that it is possible to find models that contain less parameters than we need. The choice of the model depends also of the study to be made. For example, a spectral model is not good for a stationary study, but is good for a frequency study with a sufficient large frequency band but not very large to avoid noise and numerical errors. These are very important in distributed parameter system study because modeling and numerical errors improve the level of approximations used to pass from partial differential equations (PDE) to ordinary differential equations (ODE).

A model represented by PDE consists in:

- a space domain  $\Omega$  represented by the space vector  $x = \{x_1, x_2, \dots, x_n\}$  in  $\mathbb{R}^n$ , with boundary  $\partial\Omega$ ;
- a time interval  $I = [0, t_f]$ ;
- one evolution equation of a variable  $u(x, t)$  in  $\Omega \times I$ :

$$\frac{\partial u(x, t)}{\partial t} = M[u(x, t)] + v(x, t) \quad (1.1)$$

where  $v(x, t)$  denotes the input variable, which can be distributed or lumped.

- boundary conditions on  $\partial\Omega \times I$  to be imposed, and written as:  $B[u(x, t)]$ ;
- initial conditions on  $\Omega$  to be defined:  $P[u(x, 0)]$ ;

M, B, P are operators (linear, differential...).

Partial differential equations (PDE) are classified according to their order, boundary condition type, and degree of linearity (yes, no or quasi). Most PDEs encountered in science and engineering are of second order, i.e. the highest derivative term is a second order partial derivative.

There are three type of PDE: elliptic, parabolic and hyperbolic.

$$a \frac{\partial^2 u}{\partial x_1^2} + 2b \frac{\partial^2 u}{\partial x_1 \partial x_2} + c \frac{\partial^2 u}{\partial x_2^2} = F\left(x_1, x_2, u, \frac{\partial u}{\partial x_1}, \frac{\partial u}{\partial x_2}\right) \quad (1.2)$$

where the coefficients  $a, b, c$  are functions of the independent variables  $x_1$  and  $x_2$  only, or constant (one spatial variable can be replaced by time  $t$ ).

The three canonical forms are determined by the following criterion:

-elliptic (example: Laplace's equation)

$$b^2 - ac < 0 \quad (1.3)$$

-parabolic (example: diffusion equation)

$$b^2 - ac = 0 \quad (1.4)$$

-hyperbolic (example: wave equation)

$$b^2 - ac > 0 \quad (1.5)$$

These classifications serve as a rough guide to the information flow in the domain. For instance, in elliptic equations, information from the boundaries is propagated instantaneously to all interior points. Thus, elliptic equations are termed "non-local", meaning that information from far away influences the given position, versus "local", where only information from nearby influences the field variable. In parabolic systems, information "diffuses", i.e. it spreads out in all directions. In hyperbolic systems, information "propagates", i.e. there is a demarcation between regions that have already received the information, regions that will receive the information, and possibly regions that will never receive the information. If the system is linear or quasi-linear (i.e. some coefficient depends on the dependent variable or a lower order partial derivative than that it multiplies), this classification system and the intuition about how information is transported serves as a robust guide to second order models. For nonlinear models, however, nonlinearity can destroy the information transport structure. In nonlinear models, information may be "bound", i.e. never transferred, beyond given attractors, or it may be created from noise (one view) or lost (a different view) by forgetting initial conditions in a given window in time.

### 1.3. Solving PDE

One method to solve these equations is to reformulate them, to find an approximate solution which is the closest to the real solution and this can be achieved using the best approximation.

There are a number of approximation methods which can be classified in three categories: exact solution method, spectral methods (TAU, collocation method), space domain discretization methods (the finite differences, the finite elements). These methods are also classified into strong and weak formulation. We will use the stationary case for sake of simplicity.

Let consider equation (1.6):

$$Au = f \quad \forall x \in \Omega, t \in I \quad (1.6)$$

with boundary conditions:

$$Bu = g \quad \forall x \in \partial\Omega, t \in I \quad (1.7)$$

where  $A$  and  $B$  are partial differential operators:

$$A = \sum_{|\alpha| \leq n+1} a_\alpha \partial^\alpha \quad (1.8)$$

with  $\alpha = (\alpha_1, \alpha_2, \dots, \alpha_{n+1}) \in \mathbb{N}^n$ .

We write:

$$|\alpha| = \sum_{j=1}^{n+1} \alpha_j \quad (1.9)$$

and

$$\partial^\alpha u = \frac{\partial^{|\alpha|}}{\partial x_1^{\alpha_1} \partial x_2^{\alpha_2} \dots \partial x_n^{\alpha_n} \partial t^{\alpha_{n+1}}} \quad (1.10)$$

If we find a solution which satisfies eq. (1.6), and in the same time eq.(1.7) in all points  $x$  in  $\Omega$  and  $\partial\Omega$ , and  $\forall t \in I$ , we say that we have a strong formulation.

But this is only possible when  $u$  is a function without discontinuities. When  $u$  admits discontinuities we cannot find the

derivatives in that points. So we must solve in another way the problem using the weak form.

This consists in using a function  $w$ , named weight function, which multiplies the equation and then integrate over the domain. Making this, we have a problem equivalent to the initial one, but now we seek the solution in a functional space which is smaller than the original.

We try to seek the solution in a class of functions, considering  $u(x,t)$  as an element of the Hilbert space  $(H)$ . On the space  $H$  is defined the internal product  $\langle u, v \rangle$ , that associates with each pair  $(u, v) \in H$  a real number:

$$\langle u, v \rangle = \int_{\Omega} uv d\Omega \quad (1.11)$$

**Definition** [Der 05]. Let  $w \in H$  with support in  $\Omega$  (the closed set of points where  $w(x) \neq 0$  is contained in  $\Omega$ ). Then an element  $u(x,t)$  is a weak solution of the eq. (1.6) if and only if

$$\langle Au, w \rangle = \langle f, w \rangle \quad (1.12)$$

The class of weak solutions is larger than the class of strong solutions because eq.(1.12) imposed only to the two integrals to be equal in  $\Omega$ .

The development of weighted-integral statement of a differential equation is made to have  $N$  linearly independent algebraic relations among the coefficient  $b_j$  of the approximation:

$$u \approx U_N = \sum_{j=1}^N b_j(t)\phi_j(x) + \phi_0(x) \quad (1.13)$$

This is accomplished by choosing  $N$  linearly independent weight functions in the integral statement.

### 1.3.1. The method of weighted residual

Let consider

$$Au = f \quad \text{in} \quad \Omega \quad (1.14)$$

where  $A$  is a partial differential operator, acting on the dependent variable  $u$  and  $f$  is a known function of the independent variables.

The function  $u$  must also satisfy the boundary conditions associated with the operator equation.

The solution  $u$  is approximated by the expression:

$$u_N = \sum_{j=1}^N b_j \phi_j + \phi_0 \quad (1.15)$$

Substituting  $u_N$  in (1.14) gives  $f_N \equiv Au_N$ . The difference  $Au_N - f$ , called the residual of the approximation, is nonzero:

$$R(x_1, x_2, b_j) \equiv Au_N - f = A \left( \sum_{j=1}^N b_j \phi_j + \phi_0 \right) - f \neq 0 \quad (1.16)$$

The parameters  $b_j$  are determined by the requiring that the residual  $R(x_1, x_2, b_j)$  is vanishing in the weighted-integral sense:

$$\int_{\Omega} \psi_i(x_1, x_2) R(x_1, x_2, b_j) dx_1 dx_2 = 0 \quad (i = 1, 2, \dots, N) \quad (1.17)$$

where  $\Omega$  is a two dimensional space domain and  $\psi_i$  are weight functions, which, in general, are not the same as the approximation functions  $\phi_i$ . The set  $\{\psi_i\}$  must be linearly independent in order to have (1.17) solvable.

Because (1.17) does not contain the natural and essential boundary conditions,  $\phi_0$  is required to satisfy all specified boundary conditions, and  $\phi_j$  are required to satisfy the homogenous form of all specified boundary conditions of the problem.

The main method is the Galerkin method as presented here after.

In this method the weight functions  $\psi_i$  is chosen equal to the approximation functions  $\phi_i$ :

$$\sum_{j=1}^N A_{ij} b_j = F_i \quad (1.18)$$

where

$$A_{ij} = \int_{\Omega} \phi_i A \phi_j dx_1 dx_2 \quad F_i = \int_{\Omega} \phi_i [f - A \phi_0] dx_1 dx_2 .$$

One physical application where this method is applied is the principle of virtual power, where the goal is to withdraw the variation of total energy, meaning to verify that the total energy is equal to the sum of internal and external energy.

When the weight functions are not equal to the approximation functions  $\psi_i \neq \phi_i$ , we have the Petrov-Galerkin method. When  $A$  is linear, (1.17) becomes

$$\sum_{j=1}^N \left[ \int_{\Omega} \psi_i A \phi_j dx_1 dx_2 \right] b_j = \int_{\Omega} \psi_i [f - A \phi_0] dx_1 dx_2 \quad (1.19)$$

or

$$\sum_{j=1}^N A_{ij} b_j = F_i \quad (1.20)$$

### 1.3.2. The method of separation of variables

#### 1.3.2.1. Principle

Let consider the equation:

$$A_t u(x, t) + A_x u(x, t) = f(x, t) \quad x \in \Omega, t \geq 0 \quad (1.21)$$

$$G(x, t) u(x, t) = 0, \quad x \in \partial\Omega, t > 0 \quad (1.22)$$

$$u(x, 0) = u_0(x), \quad x \in \Omega \quad (1.23)$$

where

$A_t$  and  $A_x$  are partial differential operators for  $t$  and  $x_1 = x$  here.

We are looking for a solution of the form:

$$u(x, t) = b(t) \cdot \phi(x) \quad (1.24)$$

where  $b(t)$  is a function of time and  $\phi(x)$  is a function of space.

Replacing  $u(x, t)$  from (1.24) in (1.21), in homogeneous case, we obtain:

$$[A_t b(t)]\phi(x) + [A_x \phi(x)]b(t) = 0 \quad (1.25)$$

For the  $(t, x)$  couples where  $b(t) \neq 0$  and  $\phi(x) \neq 0$  it is possible to write:

$$\frac{1}{b(t)}[A_t b(t)] = -\frac{1}{\phi(x)}[A_x \phi(x)] \quad (1.26)$$

Because each part depends only on  $t$  and  $x$ , we can consider them as being equal to a constant, which is defined by convention as  $-\lambda^2$ :

$$\frac{1}{b(t)}[A_t b(t)] = -\frac{1}{\phi(x)}[A_x \phi(x)] = -\lambda^2 \quad (1.27)$$

We have:

$$[A_t b(t)] + b(t)\lambda^2 = 0 \quad (1.28)$$

$$[A_x \phi(x)] + \lambda^2 \phi(x) = 0 \quad (1.29)$$

The general solution must satisfy both equations. Eq. (1.29) gives us possibility to find interesting base functions named proper functions, which have the property to be orthogonal.

$$\langle \phi_i, \phi_j \rangle = \int_{\Omega} \phi_i(x) \phi_j(x) dx = 0 \quad i \neq j \quad (1.30)$$

If, for example,  $A_x \phi(x) = \alpha \frac{\partial^2 \phi}{\partial x^2}$ , equation (1.29) has as solution:

$$\phi(x) = C \cos(\tau x) + D \sin(\tau x) \quad (1.31)$$

where

$$\tau^2 = \frac{\lambda^2}{\alpha} \quad (1.32)$$

The coefficients  $C, D$  are found using the boundary conditions. Because  $\phi(x)$  is a periodic function we have infinity of solutions:

$$\phi_i(x) = C \cos(\tau_i x) + D \sin(\tau_i x) \quad i = 1, 2, \dots, \infty \quad (1.33)$$

$\phi_i$  are the proper functions or basis functions.

Consider the non homogenous form of (1.21) and apply the approximation (1.24)

$$\sum_{i=0}^{\infty} \phi_i A_i b_i + \sum_{i=0}^{\infty} (A_x \phi_i) b_i = f(t, x) \quad (1.34)$$

where  $\phi_i$  are the proper functions of the  $A_x$  with the proper values  $\lambda_i^2 = \tau_i^2 \alpha$ . Multiplying eq. (1.34) by  $\phi_j$  and integrating on the spatial domain we obtain:

$$\sum_i \langle \phi_j, \phi_i \rangle A_i b_i + \sum_i \lambda_i^2 \langle \phi_j, \phi_i \rangle b_i = \langle \phi_j, f(t, x) \rangle \quad (1.35)$$

Using the orthogonality, it leads to a time differential equation system:

$$\left[ \langle \phi_j(x), \phi_j(x) \rangle \right] A_j b_j(t) + \left[ \alpha \tau_j^2 \langle \phi_j, \phi_j \rangle \right] b_j(t) = \langle \phi_j, f(t, x) \rangle \quad (1.36)$$

### 1.3.2.2. Bond Graph representation

In a mechanical system, if we consider  $b_i$  as a general coordinate, the construction of the bond graph depends on the  $A_i$  form: when it contains an algebraic expression we have a potential energy, when it contains a derivative we have dissipation and when it contains a second derivative we have a kinetic energy [Der 05].

Consider the compressed bar model show in figure 1.3. as:

$$\rho S \frac{\partial^2 \xi}{\partial t^2} + r S \frac{\partial \xi}{\partial t} + E S \frac{\partial^2 \xi}{\partial x^2} - F(t) \delta(x - L) = 0 \quad (1.37)$$

$$\xi(0, t) = 0 \quad \frac{\partial \xi}{\partial x}(L, t) = 0 \quad (1.38)$$

with

$S$  –the section;  $L$ - the length;  $E$ -Young’s modulus;  $\rho$  - mass density;  $r$ - resistance.

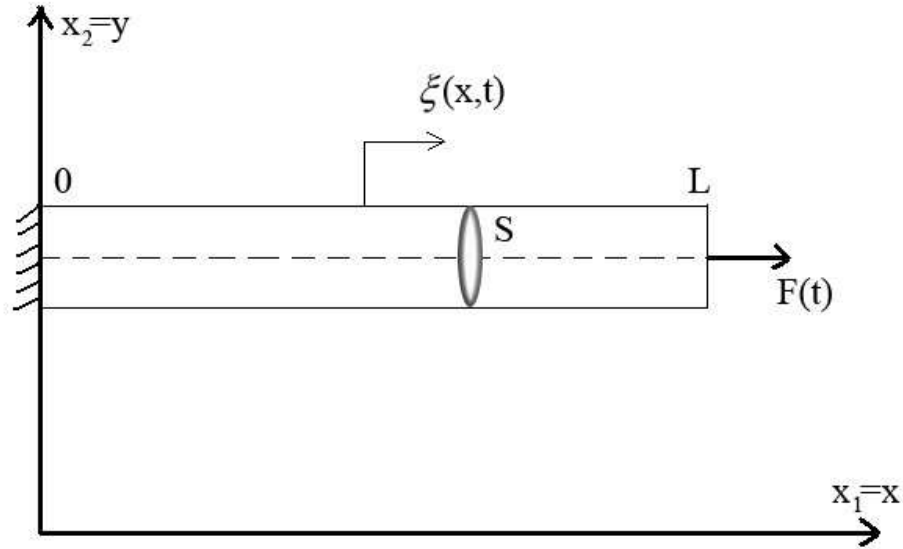


Fig.1.3. Fixed-forced bar

We begin by temporarily setting the force  $F(t)$  to zero, and assuming that  $\xi(x,t)$  can be separated into a product of the form:

$$\xi(x,t) = b(t)\phi(x) \quad (1.39)$$

Introducing (1.39) into (1.37) and applying the separation of variables principle, we obtain:

$$\frac{E}{\rho\phi} \frac{d^2\phi}{dx^2} = -\lambda^2 \quad (1.40)$$

with the result

$$\frac{d^2\phi}{dx^2} + \frac{\rho}{E} \lambda^2 \phi = 0 \quad (1.41)$$

The solution is:

$$\phi(x) = C \cos(kx) + D \sin(kx) \quad (1.42)$$

with

$$k^2 = \frac{\rho}{E} \lambda^2 \quad (1.43)$$

If we apply the boundary conditions (1.38) we obtain:

$$\xi(0, t) = b(t)\phi(0) = 0$$

or

$$\phi(0) = 0 \quad (1.44)$$

and

$$\frac{\partial \xi}{\partial x}(L, t) = \frac{d\phi}{dx}(L)b(t) = 0$$

or

$$\frac{d\xi}{dx}(L) = 0 \quad (1.45)$$

Applying (1.44) and (1.45) to (1.42) yields

$$C = 0 \quad (1.46)$$

and

$$Dk \cos kL = 0 \quad (1.47)$$

We let,

$$\cos kL = 0 \quad (1.48)$$

with the result

$$k_i L = (2i - 1) \frac{\pi}{2}, \quad i = 1, 2, 3, \dots \quad (1.49)$$

Then,

$$\phi_i(x) = D \sin \left( (2i - 1) \frac{\pi x}{2L} \right) \quad i = 1, 2, \dots, \infty \quad (1.50)$$

If we consider that the force is a point force acting in  $x=L$ , we can write eq. (1.36) as:

$$\begin{aligned} \rho S \langle \phi_i, \phi_i \rangle \frac{d^2 b_i(t)}{dt^2} + r S \langle \phi_i, \phi_i \rangle \frac{db_i(t)}{dt} + ES \langle \phi_i, \phi_i \rangle b_i(t) \\ - F(t) \delta(x-L) \phi_i(x) = 0 \end{aligned} \quad (1.51)$$

In expression (1.51) we can identify acceleration per length unit, friction force per length unit, stiffness force per length unit and external force per length unit and surface.

It is possible to write:

$$m_i \frac{d^2 b_i(t)}{dt^2} + r_i \frac{db_i(t)}{dt} + k_i b_i(t) - F(t) \phi_i(L) = 0 \quad (1.52)$$

where

$m_i = \rho S \langle \phi_i, \phi_i \rangle$  -the modal masses;

$r_i = r S \langle \phi_i, \phi_i \rangle$  -the modal dissipation;

$k_i = ES \langle \phi_i, \phi_i \rangle$  -the modal stiffness.

Due to mode orthogonality, eq. (1.52) is decoupled, and each  $b_i(t)$  can be solved separately, and then combined with the mode shapes  $\phi_i(x)$ .

Eq. (1.52) represents the energetically representation of one proper mode of the system.

Let define the modal momentum as

$$p_i = m_i \dot{b}_i \quad (1.53)$$

and the modal displacement as

$$q_i = b_i \quad (1.54)$$

Then, eq.(1.52) can be written as

$$\frac{d}{dt} p_i = -r_i p_i - k_i q_i + F(t) \phi_i(L) \quad (1.55)$$

and

$$\frac{dq_i}{dt} = \frac{p_i}{m_i} \tag{1.56}$$

For an  $i$ , we have an effort balance at the 1-junctions, and each external force is projected on the mode by its own proper function. The C, R and I correspond to the acceleration, friction and stiffness phenomena.

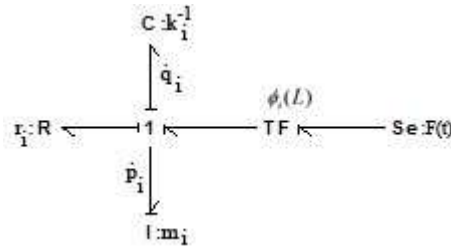


Fig.1.4. One proper mode representation

Fig. 1.5. shows a bond graph that would duplicate these modal equations for  $i=1,2,\dots$ . Each external force is projected on the mode through the corresponding proper function (TF-modulus  $\phi_i^{-1}$ ).

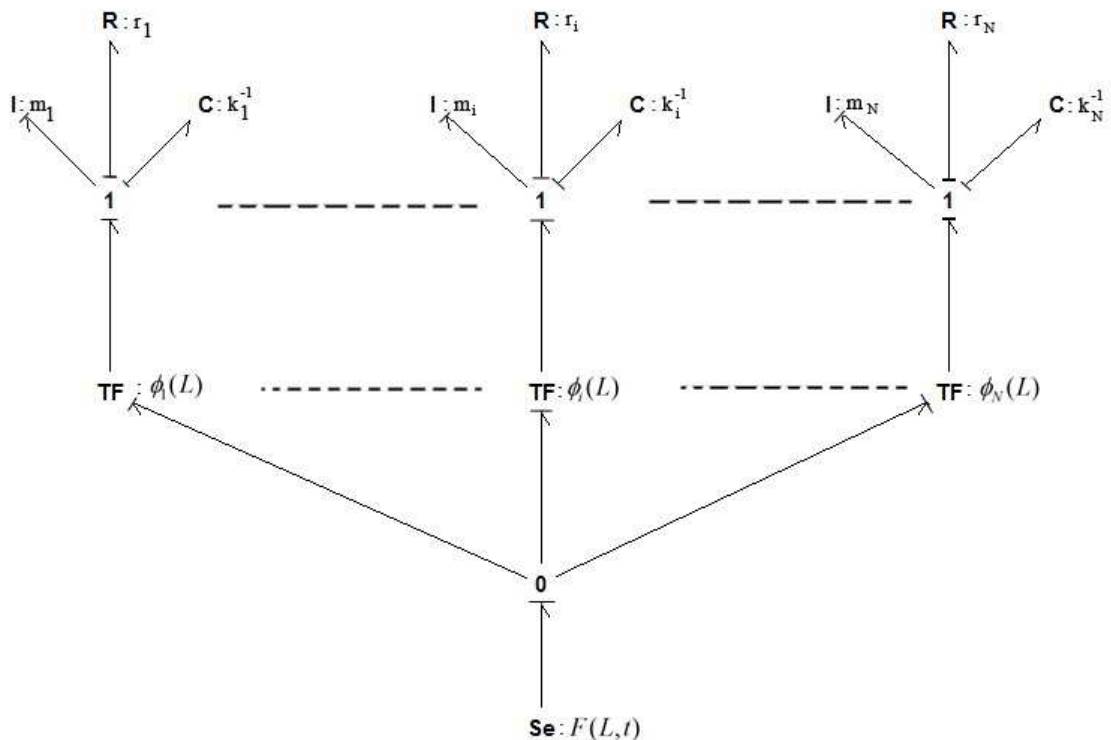


Fig.1.5. Compressed bar Bond Graph representation

### 1.3.3. Spectral methods

#### 1.3.3.1. Principle

These methods are based on the approximation of the solution under the form:

$$u_N = \sum_i b_i \phi_i(x) \quad (1.57)$$

The problem with this type of methods is to find the good choice of the base functions  $\phi_i$  in the domain  $\Omega$ . It is interesting to have a orthogonality property between the base functions  $\phi_i$  and the test functions  $w_i$ . This property is then used in simplification of the problem.

It is obvious that we would like our basis sets to have a number of properties: easy to compute, rapid convergence and completeness, which means that any solution can be represented to arbitrarily high accuracy by taking the truncation  $N$  to be sufficiently large.

Depending on the choice of the test function we have:

- the Tau method where the test functions are the same as the base functions, but they do not satisfy the boundary conditions as in the Galerkin method;

- the collocation method, where the test functions are equal to delta functions at special points, called collocation points. This method is developed hereafter.

The collocation method is also a weighted residual method, used to solve PDEs. Consider a function  $u(x,t)$  defined over a spatial domain  $\Omega$ , and the space and time evolution of  $u(x,t)$  governed by a PDE:

$$Au(x,t) = 0 \quad (1.58)$$

where  $A$  is a differential operator.

We seek to approximate the solution of eq. (1.58) by:

$$u_N(x,t) = \sum_{i=1}^N b_i(t)\phi_i(x) \quad (1.59)$$

We form the residual of  $A$ ,  $R(x,t)$ :

$$R(x,t) = Au_N(x,t) \quad (1.60)$$

$R(x,t)$  is a continuous function of  $x$  and  $t$ . The approximate solution is found for the average value of  $R(x,t)$  over  $\Omega$  to be zero. We perform this using the weighted function  $\psi(x)$ .

$$\int_{\Omega} \psi(x)R(x,t)dx = 0 \quad (1.61)$$

We can evaluate the average by using a discrete set of  $p$  points,  $x_j, j = 1..p$ , called collocation points:

$$\sum_{i=1}^p \psi(x_i)R(x_i,t) = 0 \quad (1.62)$$

We choose  $\psi(x_i)$  to be Dirac delta functions at this particular set of points.

$$\sum_{i=1}^p \delta(x_i - x_j)R(x_i,t) = 0, \quad j = 1..p \quad (1.63)$$

or

$$R(x_j,t) = 0, \quad j = 1..p \quad (1.64)$$

### 1.3.3.2. Bond Graph representation

For the compressed bar,

$$\rho S \frac{\partial^2 \zeta}{\partial t^2} + rS \frac{\partial \zeta}{\partial t} + ES \frac{\partial^2 \zeta}{\partial x^2} - F(t,L)S = 0 \quad (1.65)$$

if we assume that there are  $N$  points  $x_1, x_2, \dots, x_N$  in  $\Omega$  where we calculate the value of  $\zeta$ , using the collocation method, the approximation

$\hat{\zeta}$  is written as:

$$\hat{\xi} = \sum_{i=1}^N b_i(t) \phi_i(x) \quad (1.66)$$

where  $b_i$  are the solutions of equations:

$$\sum_{i=1}^N b_i(t) \phi_i(x_k) = \xi(x_k), \quad \forall k = 1, \dots, N \quad (1.67)$$

or in matrix form:

$$\mathbf{\Phi} \cdot \mathbf{b} = \boldsymbol{\zeta} \quad (1.68)$$

where  $\mathbf{\Phi} = (\phi_i(x_j))_{i,j=1,\dots,N}$ ;  $\mathbf{b} = (b_1, b_2, \dots, b_N)^T$ ;

$\boldsymbol{\zeta} = (\zeta(x_1), \zeta(x_2), \dots, \zeta(x_N))^T$ .

From here we have:

$$b_i = \sum \eta_{ij} \zeta(x_j), \quad i = 1, \dots, N \quad (1.69)$$

where  $\eta_{ij}$  are elements of  $\mathbf{\Phi}^{-1}$ .

Thus, the approximation is:

$$\hat{\zeta}(x, t) = \sum_{i=1}^N \left[ \phi_i(x) \left( \sum_{j=1}^N \eta_{ij} \zeta(x_j) \right) \right] \quad (1.70)$$

Introducing the approximation in eq.(1.65), we obtain:

$$\begin{aligned} & \sum_{i=1}^N \left[ \phi_i(x) \left( \sum_{j=1}^N \eta_{ij} \frac{\partial^2 \zeta(x_j)}{\partial t^2} \right) \rho S \right] + \sum_{i=1}^N \left[ \phi_i(x) \left( \sum_{j=1}^N \eta_{ij} \frac{\partial \zeta(x_j)}{\partial t} \right) r S \right] \\ & + \sum_{i=1}^N \left[ \frac{\partial^2 \phi_i(x)}{\partial x^2} \left( \sum_{j=1}^N \eta_{ij} \zeta(x_j) \right) E S \right] = F(x, t) S \end{aligned} \quad (1.71)$$

Multiplying (1.71) by  $\phi_p(x)$ , we obtain:

$$\begin{aligned} & \sum_{i=1}^N \left[ \langle \phi_i, \phi_p \rangle \left( \sum_{j=1}^N \eta_{ij} \frac{\partial^2 \zeta(x_j)}{\partial t^2} \right) \rho S \right] + \sum_{i=1}^N \left[ \langle \phi_i, \phi_p \rangle \left( \sum_{j=1}^N \eta_{ij} \frac{\partial \zeta(x_j)}{\partial t} \right) r S \right] \\ & + \sum_{i=1}^N \left[ \left\langle \frac{\partial^2 \phi_i}{\partial x^2}, \phi_p \right\rangle \left( \sum_{j=1}^N \eta_{ij} \zeta(x_j) \right) E S \right] = \langle F(L, t) S, \phi_m \rangle \end{aligned} \quad (1.72)$$

Because of orthogonality of  $\phi_i$ , we can write:

$$\sum_{j=1}^N \left[ \eta_{pj} \left( \frac{\partial^2 \zeta(x_j)}{\partial t^2} m_p + \frac{\partial \zeta(x_j)}{\partial t} r_p + \zeta(x_j) k_p \right) \right] = F(t) \cdot \phi_m(L) \quad (1.73)$$

where

$$\begin{aligned} m_p &= \rho S \langle \phi_p(x), \phi_p(x) \rangle \\ r_p &= r S \langle \phi_p(x), \phi_p(x) \rangle \\ k_p &= ES \gamma_m \langle \phi_p(x), \phi_p(x) \rangle \end{aligned} \quad (1.74)$$

Eq. (1.73) describes the projection of effort applied at point  $L$  on a mode.

The values  $m_p, r_p, k_p$  represent the mass, the friction and stiffness coefficients.

The bond graph figure 1.6. represents the projection of effort  $F(L)$  on different modes in collocation points.

For the construction of the bond graph we use the same concept as for the separation of variable method with the difference that here we have a sum of  $p$  modes.

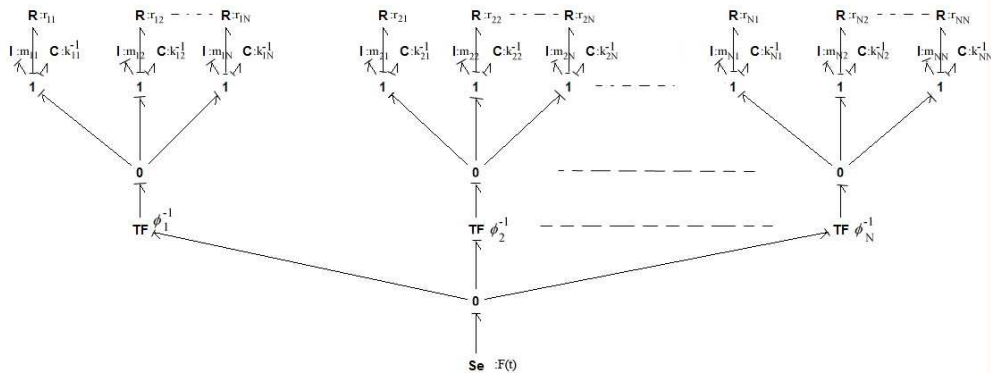


Fig.1.6. The bond graph representation for collocation method

### 1.3.4. Finite element method

#### 1.3.4.1. Principle

The finite element method is a method where the domain is represented as a collection of simple domains, called finite elements, so the approximation functions needed for the approximation of the solution are constructed over each element. The finite element method is not the only method that uses the discretization of the domain; there are also the finite difference method and finite volume method. The finite element method differs from other methods by the manner in which the approximation functions are constructed.

Finite element method has three basic features:

1) Division of the domain into parts, which allows the representation of the complex domains as a collection of geometrically simple domains that enables a systematic derivation of the approximation functions.

2) Derivation of approximation functions over each element; the approximation function are polynomials that are derived using interpolation.

3) Assembly of elements; the assembly of elements represents a discrete analog of the original domain, and the set of equations a numerical analog of the mathematical model of the problem.

These features are closely related: the geometry of the element must be chosen such that the approximation functions can be uniquely derived. The approximation functions depend on the geometry and on the number and location of points, called nodes, in the element and quantities to be interpolated. In finite element method is used the weak formulation instead of weighted formulation; in this case we have a relaxation of the conditions on the approximations. With the weak

formulation we pass from a punctual formulation, where the dependent variable is an application defined on the space of continuum derivable functions, named classical formulation, to a formulation where we rewrite the relations between functions through integrals.

Once the approximation functions have been derived, the procedure to obtain algebraic relations among the unknown coefficients is exactly the same as that used in the weighted-residual method.

The domain of the problem consists in all points between  $x = 0$  and  $x = L : \Omega = (0, L)$ . The domain  $\Omega$  is divided into a set of elements, each element having a specific length and being located between the borders of the domain. The collection of these elements forms the finite element mesh of the domain. The division of the domain is made for two reasons: to represent the geometry of the domain, and to approximate over each element the solution in order to obtain a better representation of the solution over the entire domain.

The approximation over each element is simpler than the approximation over the entire domain.

Because the solution must satisfy the boundary conditions of the problem, the choice of the approximation functions, especially when there are discontinuities in the geometry of the problem, is under severe restrictions.

To connect the elements at the common nodes and impose continuity of the solution there, the endpoints of each element is identified and called element nodes. Depending on the degree of the approximation polynomial used to represent the solution, additional nodes inside the element may be identified.

The number of elements depends mainly on the element type (cf. figure 1.7.) and accuracy desired. When the finite element method is used to solve a problem, it is necessary to investigate the convergence of the solution by gradually refining the mesh and comparing the solution with those obtained by higher order elements. The order of an element

refers to the degree of the polynomial used to represent the solution over the element.

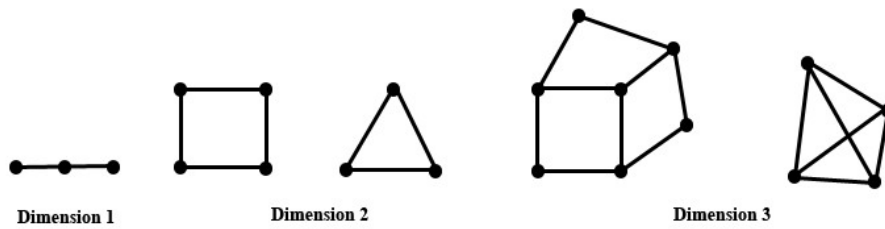


Fig.1.7. Types of finite element

We consider an element  $\Omega^e = (x_A, x_B)$  whose endpoints have the coordinates  $x = x_A$  and  $x = x_B$ .

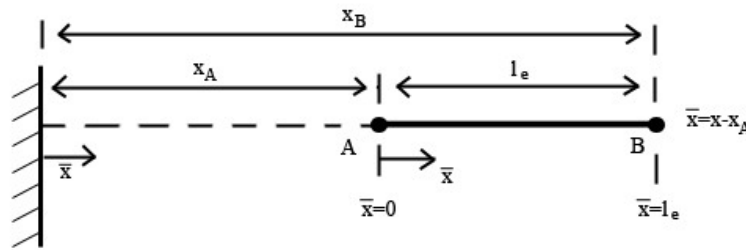


Fig.1.8. A finite element in 1 dimensional

The polynomial approximation of the solution on element  $\Omega^e$  is of the form:

$$U^e = \sum_{j=1}^n u_j^e \psi_j^e(x) \quad (1.75)$$

where  $u_j^e$  are the values of the solution at the nodes of the finite element and  $\psi_j^e$  are the approximation functions over the element.

In order to be convergent to the actual solution  $u$  as the number of elements is increased, the approximation solution  $U^e$  must fulfill certain requirements:

1) to be continuous over the element, and differentiable, as required by the weak form. 2) to be a complete polynomial, i.e., to include all lower

order terms up to the highest order used. This is required in order to capture all possible states, i.e. constant, linear and so on.

3) to be an interpolant of the primary variables at the nodes of the finite element. This is necessary in order to satisfy the essential boundary conditions of the element.

The simplest polynomial that can be chosen as approximation is:

$$U^e = a + bx \quad (1.76)$$

where  $a$  and  $b$  are constants.

This expression satisfies the first two requirements. To satisfy the third one:

$$U^e(x_A) = u_1^e \quad U^e(x_B) = u_2^e \quad (1.77)$$

Introducing this in equation (1.76) we obtain:

$$U^e(x) = \frac{1}{l_e}(\alpha_1^e + \beta_1^e x)u_1^e + \frac{1}{l_e}(\alpha_2^e + \beta_2^e x)u_2^e \quad (1.78)$$

where

$$l_e = x_B - x_A; \alpha_i^e = (-1)^i x_i^e; \beta_i^e = (-1)^i; x_1^e = x_A; x_2^e = x_B.$$

That is,

$$U^e(x) = \psi_1^e(x)u_1^e + \psi_2^e(x)u_2^e = \sum_{j=1}^2 \psi_j^e(x)u_j^e \quad (1.79)$$

where

$$\psi_1^e(x) = \frac{x_B - x}{x_B - x_A} \quad \psi_2^e(x) = \frac{x - x_A}{x_B - x_A} \quad (1.80)$$

This is a representation in terms of the global coordinates  $x$  (i.e., the coordinate of the problem) and only for an element domain  $\Omega^e$ . If we want to express them in terms of a coordinate  $\bar{x}$  with origin fixed at node 1 of the element,  $\psi_i^e, i = 1, 2$  of (1.80) take the forms:

$$\psi_1^e(\bar{x}) = 1 - \frac{\bar{x}}{l_e} \quad \psi_2^e(\bar{x}) = \frac{\bar{x}}{l_e} \quad (1.81)$$

where  $\bar{x}$  represents the local or element coordinate (figure 1.9).

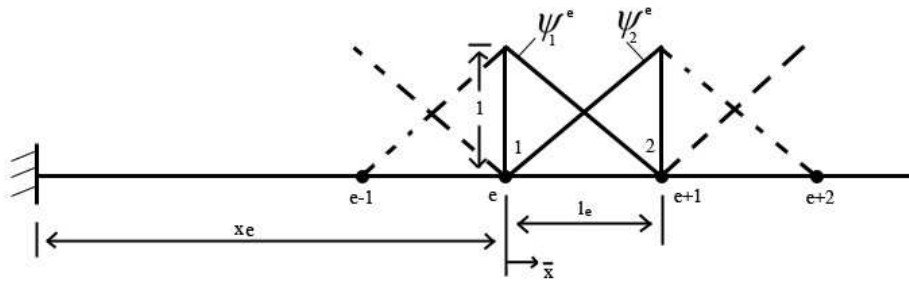
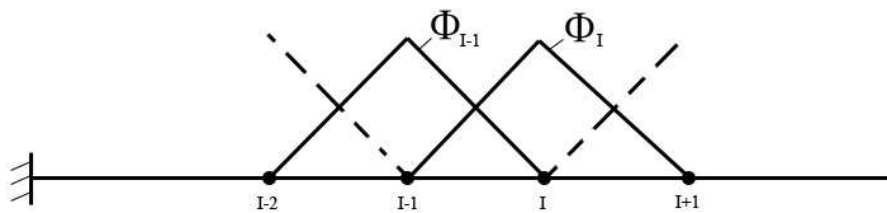


Fig.1.9. Local interpolation function

$\psi_1^e$  is equal to 1 at node 1 and zero at node 2, and  $\psi_2^e$  is equal to 1 at node 2 and equal to zero at node 1.

The global interpolation function  $\Phi_I$  (figure 1.10.) can be defined in terms of the element interpolation functions according to the global node  $I$ .



$$\Phi_I = \begin{cases} \psi_2^{I-1} & \text{for } x_{I-1} \leq x \leq x_I \\ \psi_1^I & \text{for } x_I \leq x \leq x_{I+1} \end{cases}$$

Fig. 1.10. Global interpolation function

This type of interpolation functions derived using the dependent unknown- not its derivatives- at the nodes are called the Lagrange family of interpolation functions.

To have a better approximation instead of using a linear polynomial we can use a quadratic one:

$$U^e(x) = a + bx + cx^2 \quad (1.82)$$

which requires to have three nodes on element in order to evaluate  $u(x)$  at the nodes. Two nodes as endpoints and another one placed at any interior point (figure 1.11.).

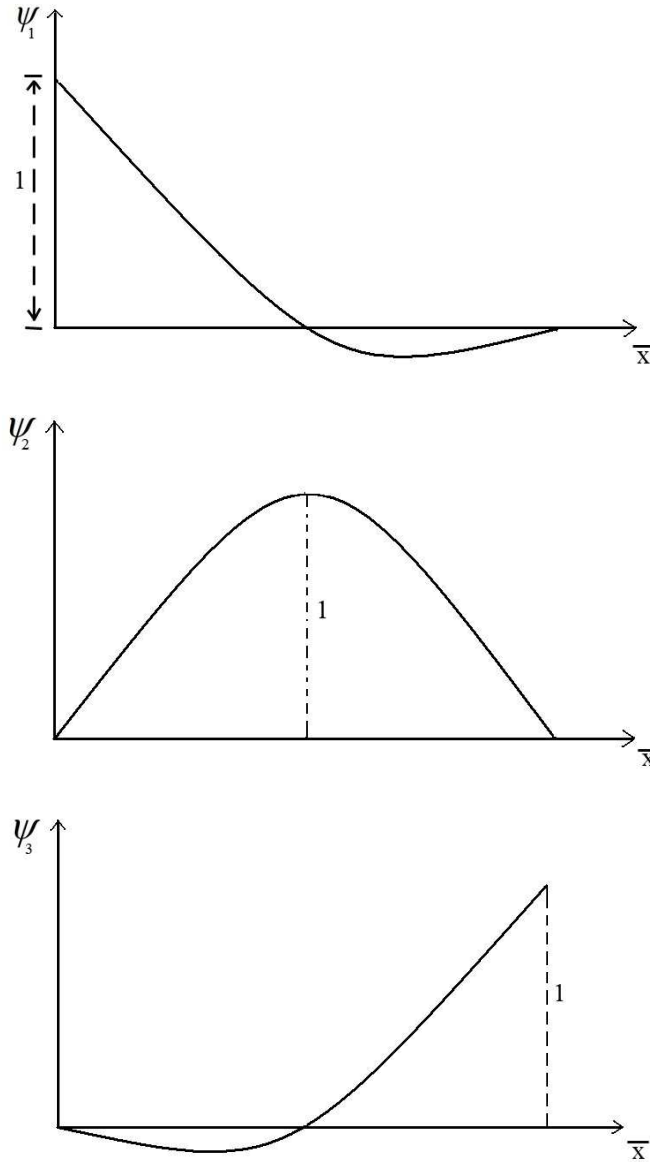


Fig. 1.11. One dimensional Lagrange quadratic element and its interpolation function

$$U^e(x) = \psi_1^e(x)u_1^e + \psi_2^e(x)u_2^e + \psi_3^e(x)u_3^e = \sum_{j=1}^n \psi_j^e(x)u_j^e \quad (1.83)$$

with

$$\begin{aligned} \psi_1^e(\bar{x}) &= \left(1 - \frac{\bar{x}}{h}\right) \left(1 - \frac{2\bar{x}}{h}\right) \\ \psi_2^e(\bar{x}) &= 4 \frac{\bar{x}}{h} \left(1 - \frac{\bar{x}}{h}\right) \\ \psi_3^e(\bar{x}) &= -\frac{\bar{x}}{h} \left(1 - \frac{2\bar{x}}{h}\right) \end{aligned} \quad (1.84)$$

All Lagrange family of interpolation functions satisfies the following properties:

$$\psi_j^e(x_i) = \delta_{ij} = \begin{cases} 0 & \text{if } i \neq j \\ 1 & \text{if } i = j \end{cases} \quad (1.85)$$

$$\sum_{j=1}^n \psi_j^e(x) = 1 \quad \text{hence} \quad \sum_{j=1}^n \frac{d\psi_j^e}{dx} = 0$$

For two dimensional problems we have the same basic step as in one dimensional case. The analysis is more complicated because now we have partial differential equations over geometrically complex region. The boundary of two-dimensional domain is, in general, a curve. We seek not only to approximate the solution on the domain but also to approximate the domain itself. The finite elements consist in triangles, rectangles, quadrilaterals, that allow unique derivation of the interpolation functions.

We introduce the approximation solution in equation and obtain the system of equations:

$$[K^e] \{u^e\} = \{f^e\} + \{Q^e\} \quad (1.86)$$

where the matrix  $[K^e]$  is called the coefficient matrix. The vector  $\{f^e\}$  is the source vector. Equation (1.86) contains  $2n$  unknowns:  $(u_1^e, u_2^e, \dots, u_n^e)$  and  $(Q_1^e, Q_2^e, \dots, Q_n^e)$  called primary and secondary element nodal degrees of freedom; hence it cannot be solved without having  $n$  additional conditions.

These are provided by the boundary conditions and by balance of the secondary variable  $Q_i^e$  at nodes common to several elements.

The finite element methods are the most used for numerical approximation. These methods, from a mathematical point of view, are very easy to handle, easy to adapt to any type of geometry of the domain and to changes in boundary conditions, and from a physical point of

view, facilitate the results interpretation. This method is not suitable for solving non linear equations.

### 1.3.4.2. Bond Graph representation

Let's consider the Bernoulli beam flexion problem where dissipative energy is neglected [DER 05].

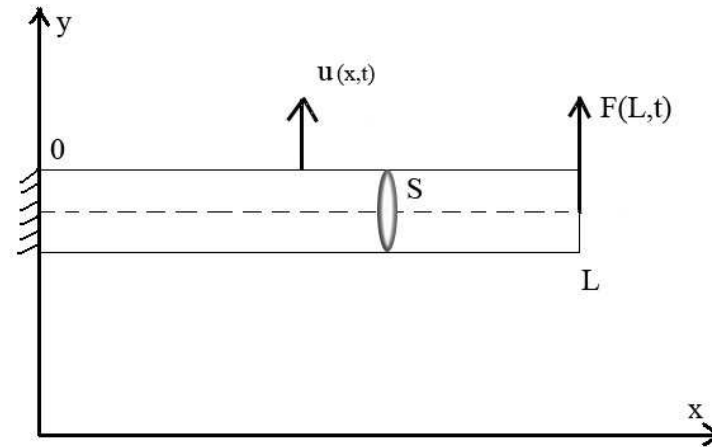


Fig.1.12. Fixed-forced Bernoulli beam flexion

The equation of the problem is:

$$EI(x) \frac{\partial^4 u(x,t)}{\partial x^4} + \rho S \frac{\partial^2 u(x,t)}{\partial t^2} = F(x,t) \quad (1.87)$$

The boundary conditions are:

$$\begin{cases} \frac{\partial u}{\partial x}(0,t) = 0 \\ M(L,t) = EI \frac{\partial^2 u}{\partial x^2}(L,t) = 0 \\ T(L,t) = EI \frac{\partial^3 u}{\partial x^3}(L,t) = F(t) \end{cases} \quad (1.88)$$

where:  $S$ -represents the uniform cross-sectional area,  $\rho$ -is the mass density;  $E$  is the Young's modulus,  $I$ - is the area moment of inertia and  $L$  the length.

On each element using a shape function we approximate the solution  $u(x,t)$ .

$$f(x, q) = f(x, u_1, \theta_1, \dots, u_{n+1}, \theta_{n+1}) \quad (1.89)$$

where  $q = [u_1, \theta_1, \dots, u_{n+1}, \theta_{n+1}]^T$  is the vector of nodal variables of the element,  $u$  is the transverse displacement vector,  $\theta$  is the angular displacement vector.

The velocity is approximated as:

$$v(x, t) = \frac{\partial f}{\partial q} \dot{q} \quad (1.90)$$

In each element we calculate the kinetic and potential energies.

The kinetic energy is:

$$E_c = \frac{1}{2} \int_0^l \rho S(x) v v dx = \frac{1}{2} \dot{q}^T M(x, q) \dot{q} \quad (1.91)$$

with  $M = \frac{1}{2} \int_0^l \rho S(x) \left( \frac{\partial f}{\partial q} \right)^T \frac{\partial f}{\partial q} dx$ .

The deformation energy is:

$$E_d = \frac{1}{2} \int_0^l EI(x) \frac{\partial^2 u}{\partial x^2} \frac{\partial^2 u}{\partial x^2} dx = \frac{1}{2} q^T K(x, q) q \quad (1.92)$$

with  $K = \int_0^l EI(x) \left( \frac{\partial^2 f}{\partial x^2} \right)^T \frac{\partial^2 f}{\partial x^2} dx$ .

The virtual work done when considering the mass forces and forces applied on the beam being reduced to a force  $F dx$  per length element  $dx$ , is:

$$\delta \tau = \int_0^l F^T \delta u dx = \left( \int_0^l F^T \frac{\partial f}{\partial q} dx \right) \delta \dot{q} = \Psi^T \delta \dot{q} \quad (1.93)$$

where  $\delta u$  is the virtual displacement field, and  $\Psi$  the generalized forces.

Considering an interpolation polynomial base  $N$  the element approximation can be written as:

$$f(x, q) = \mathbf{N}^T \mathbf{q} \quad (1.94)$$

Introducing in the kinetic energy equation we obtain:

$$E_c = \frac{1}{2} \int_0^l \rho S(x) v v dx = \frac{1}{2} \dot{q}^T M \dot{q} \quad (1.95)$$

where  $M = \int_0^l \rho S(x) N^T N dx = [M_{ij}]$  is the mass matrix.

After integration in a case with 2 elements we obtain:

$$M_e = \frac{\rho S l}{420} \begin{bmatrix} 156 & 22l & 54 & -13l \\ 22l & 4l^2 & 13l & -3l^2 \\ 54 & 13l & 156 & -22l \\ -13l & -3l^2 & -22l & 4l^2 \end{bmatrix} \quad (1.96)$$

Similarly the stiffness matrix is obtained:

$$E_d = \frac{1}{2} \int_0^l EI \frac{\partial^2 u}{\partial x^2} \frac{\partial^2 u}{\partial x^2} dx = \frac{1}{2} q^T K q \quad (1.97)$$

where  $K = \int_0^l EI \frac{\partial^2 N^T}{\partial x^2} \frac{\partial^2 N}{\partial x^2} dx = [K_{ij}]$ .

$$K_e = \frac{EI}{l^3} \begin{bmatrix} 12 & 6l & -12 & 6l \\ 6l & 4l^2 & -6l & 2l^2 \\ -12 & -6l & 12 & -6l \\ 6l & 2l^2 & -6l & 4l^2 \end{bmatrix} \quad (1.98)$$

The virtual work of the external forces is:

$$\delta \tau = \int_0^l F^T \delta u dx = \left( \int_0^l F^T N dx \right) \delta \dot{q} = \Psi^T \delta \dot{q} \quad (1.99)$$

where  $\delta u$  is the virtual displacement field, and  $\Psi$  the generalized forces:

$$\Psi = \int_0^l F^T N dx = \begin{bmatrix} F_1 \\ \Pi_1 \\ \cdot \\ \cdot \\ F_{n+1} \\ \Pi_{n+1} \end{bmatrix} \quad (1.100)$$

where  $F_i, \Pi_i$  are the nodal equivalent forces and torque.

Using the Lagrange equations in the nodal basis where  $q_i$  is a generalized coordinate,  $\Psi_i$  the generalized forces in  $u_i$  configuration:

$$\frac{d}{dt} \left( \frac{\partial L}{\partial \dot{q}_i} \right) - \frac{\partial L}{\partial q_i} = Q_i \quad \text{with} \quad L = E_c - E_d \quad (1.101)$$

we obtain:

$$M \frac{d^2 q}{dt^2} + Kq = \Psi \tag{1.102}$$

The Bond Graph representation of eq (1.102) is presented in the figure 1.13. Because we have a second order derivative it means that we have a kinetic energy thus an *I* element, and because we have an algebraic expression, it means that we have a potential energy thus a *C* element. The matrices *M* and *K* are full matrices.

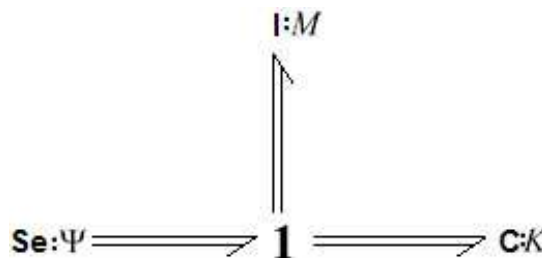


Fig.1.13. Representation multi bond graph

As example we have the representation for 2 elements using the Hermite polynomial as shape function, in figure 1.14.:

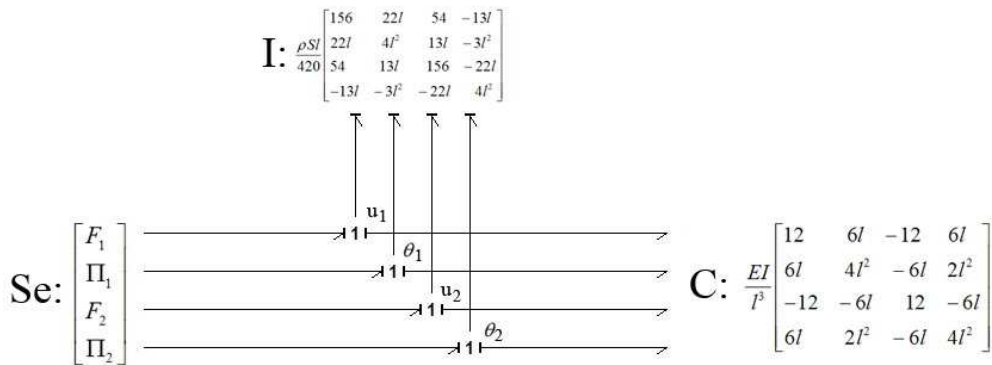


Fig.1.14. Bond graph representation of the entire beam

The representation of the entire beam is obtained by assembling the elementary mass and stiffness matrices using the implicit continuity conditions and energy balance at all nodes to obtain the final matrices before expressing the bond graph representation, as in figure 1.15.

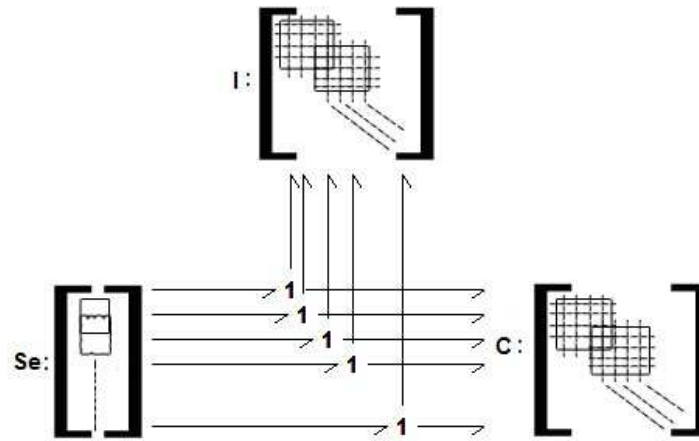


Fig.1.15. Bond graph with assembled matrix

When the number of elements changes, the whole matrices must be again evaluated.

### 1.3.5. Finite difference method

#### 1.3.5.1. Principle

The finite difference techniques [STR 04], [GUE 63] are based upon the approximations that permit replacing partial differential equations by finite difference equations. These finite difference approximations are algebraic in form, and the solutions are related to grid points.

Consider the prototype for all hyperbolic partial differential equations in the one way wave equation:

$$\frac{\partial u}{\partial t} + a \frac{\partial u}{\partial x} = 0 \quad (1.103)$$

where  $a$  is a constant,  $t$  represents time, and  $x$  represents the spatial variable.

If we impose the initial value at  $t = 0$ :

$$u(0, x) = u_0(x) \quad (1.104)$$

the solution of (1.103) will be:

$$u(t, x) = u_0(x - at) \quad (1.105)$$

We consider a grid of points in the  $(t, x)$  plane. Let consider  $h$  and  $k$  be positive numbers and the point  $(t_n, x_m) = (nk, mh)$  for arbitrary  $n$  and  $m$ . For a function  $v$  defined on the grid we write  $v_m^n$  for the value of  $v$  at point  $(t_n, x_m)$ . We are interested in grids with small values of  $h$  and  $k$  (figure 1.16.).

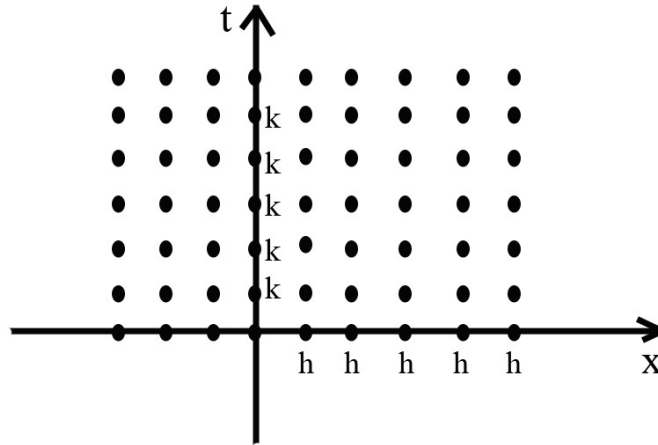


Fig.1.16. Grid points

The basic idea of the finite difference method is to replace derivatives by finite differences.

This can be done in many ways. As example:

$$\frac{\partial u}{\partial t}(t_n, x_m) \approx \frac{u(t_n + k, x_m) - u(t_n, x_m)}{k} \approx \frac{u(t_n + k, x_m) - u(t_n - k, x_m)}{2k} \quad (1.106)$$

Using this approximation we obtain the following finite difference schemes for equation (1.103) [STR 04]:

1) Implicit scheme

$$\frac{v_m^{n+1} - v_m^n}{k} + a \frac{v_{m+1}^{n+1} - v_m^{n+1}}{h} = 0 \quad (1.107)$$

2) Explicit scheme

Forward-time forward-space: 
$$\frac{v_m^{n+1} - v_m^n}{k} + a \frac{v_{m+1}^n - v_m^n}{h} = 0 \quad (1.108)$$

Forward-time backward-space: 
$$\frac{v_m^{n+1} - v_m^n}{k} + a \frac{v_m^n - v_{m-1}^n}{h} = 0 \quad (1.109)$$

$$\text{Forward-time central-space scheme: } \frac{v_m^{n+1} - v_m^n}{k} + a \frac{v_{m+1}^n - v_{m-1}^n}{2h} = 0 \quad (1.110)$$

$$\text{Leapfrog scheme: } \frac{v_m^{n+1} - v_m^{n-1}}{2k} + a \frac{v_{m+1}^n - v_{m-1}^n}{2h} = 0 \quad (1.111)$$

$$\text{Lax-Friedrichs scheme: } \frac{v_m^{n+1} - \frac{1}{2}(v_{m+1}^n + v_{m-1}^n)}{k} + a \frac{v_{m+1}^n - v_{m-1}^n}{2h} = 0 \quad (1.112)$$

Another used scheme is the Lax-Wendroff scheme. To obtain the Lax-Wendroff scheme for the wave equation we start with the Taylor series in time for  $u(t+k, x)$  where  $u$  is a solution to the inhomogeneous one way wave equation (1.103) :

$$u(t+k, x) = u(t, x) + k \frac{\partial u}{\partial t}(t, x) + \frac{k^2}{2} \frac{\partial^2 u}{\partial t^2}(t, x) + O(k^3) \quad (1.113)$$

We use:

$$\frac{\partial u}{\partial t} = -a \frac{\partial u}{\partial x} + f \quad (1.114)$$

and

$$\frac{\partial^2 u}{\partial t^2} = -a \frac{\partial^2 u}{\partial t \partial x} + \frac{\partial f}{\partial t} = a^2 \frac{\partial^2 u}{\partial x^2} - a \frac{\partial f}{\partial x} + \frac{\partial f}{\partial t} \quad (1.115)$$

to obtain

$$\begin{aligned} u(t+k, x) = & u(t, x) - ak \frac{\partial u}{\partial x}(t, x) + \frac{a^2 k^2}{2} \frac{\partial^2 u}{\partial x^2}(t, x) \\ & + kf - \frac{ak^2}{2} \frac{\partial f}{\partial x} + \frac{k^2}{2} \frac{\partial f}{\partial t} + O(k^3) \end{aligned} \quad (1.116)$$

Replacing the derivatives in  $x$  by second-order accurate differences and  $\partial f / \partial t$  by a forward difference, we obtain:

$$\begin{aligned}
u(t+k, x) = & u(t, x) - ak \frac{u(t, x+h) - u(t, x-h)}{2h} \\
& + \frac{a^2 k^2}{2} \frac{u(t, x+h) - 2u(t, x) + u(t, x-h)}{h^2} + \\
& + \frac{k}{2} [f(t+k, x) + f(t, x)] \quad (1.117) \\
& - \frac{ak^2}{2} \frac{[f(t, x+h) - f(t, x-h)]}{2h} \\
& + O(kh^2) + O(k^3)
\end{aligned}$$

The Lax-Wendroff scheme is:

$$\begin{aligned}
v_m^{n+1} = & v_m^n - \frac{a\lambda}{2} (v_{m+1}^n - v_{m-1}^n) + \frac{a^2 \lambda^2}{2} (v_{m+1}^n - 2v_m^n + v_{m-1}^n) + \\
& + \frac{k}{2} (f_m^{n+1} + f_m^n) - \frac{ak\lambda}{4} (f_{m+1}^n - f_{m-1}^n) \quad (1.118)
\end{aligned}$$

or, equivalently

$$\begin{aligned}
\frac{v_m^{n+1} - v_m^n}{k} + a \frac{v_{m+1}^n - v_{m-1}^n}{2h} - \frac{a^2 k}{2} \frac{v_{m+1}^n - 2v_m^n + v_{m-1}^n}{h^2} = \\
= \frac{1}{2} (f_m^{n+1} + f_m^n) - \frac{ak}{4h} (f_{m+1}^n - f_{m-1}^n) \quad (1.119)
\end{aligned}$$

where  $\lambda = k/h$  must satisfy the Courant-Friedrichs-Lewy (CFL) condition in order to be stable:

$$|a\lambda| \leq 1 \quad (1.120)$$

The CFL condition can be rewritten as

$$\lambda^{-1} \geq |a| \quad (1.121)$$

which can be interpreted as stating that the numerical speed of propagation must be greater than or equal to the speed of propagation of the partial differential equation.

When we have to solve an initial boundary value problem we must use the boundary conditions required by the partial differential equations in order to determine the finite difference solution.

When, for example we use the Lax-Wendorff scheme, the scheme can be applied only at the interior grid points and not at the boundary points. This is because the scheme requires grid points to the left and

right of  $(t_n, x_m)$  when computing  $v_m^{n+1}$  and at the boundaries either  $x_{m-1}$  or  $x_{m+1}$  is not a grid point. Assuming that  $a$  is positive, the value of  $v_0^n$  is supplied by the boundary data as required by the partial differential equation. At  $x_M$ , where  $x_M$  is the last grid point, we must use some means other than the scheme to compute  $v_M^{n+1}$ .

For example:

$$\begin{aligned} v_M^{n+1} &= v_{M-1}^{n+1} \\ v_M^{n+1} &= 2v_{M-1}^{n+1} - v_{M-2}^{n+1} \\ v_M^{n+1} &= v_{M-1}^n \end{aligned} \quad (1.122)$$

The finite difference method is the first numerical method used in numerical approximation. This method allows modifying the number and the form of the grid used in spatial decomposition. It is very useful in numerical approximation.

### 1.3.5.2. Bond Graph representation

Consider the compressing bar equation with the boundary conditions [Der 05]:

$$\begin{aligned} \rho S \frac{\partial^2 \xi}{\partial t^2} + r S \frac{\partial \xi}{\partial t} + ES \frac{\partial^2 \xi}{\partial x^2} - F(t, L) S &= 0 \\ \xi(t, 0) = 0 \quad \frac{\partial \xi}{\partial t}(t, L) &= 0 \end{aligned} \quad (1.123)$$

We make the following approximation using the backward difference for the second derivative, considering that the space is represented through a uniform grid with the fixed length  $\Delta x$  :

$$\left( \frac{d^2 \xi}{dx^2} \right)_i \approx \frac{1}{(\Delta x)^2} (\xi_{i+1} - 2\xi_i + \xi_{i-1}) \quad (1.124)$$

Equation (1.123) becomes:

$$\rho S \Delta x \frac{\partial^2 \xi_i}{\partial t^2} + r S \Delta x \frac{\partial \xi_i}{\partial t} + \frac{ES}{\Delta x} (\xi_{i+1} - 2\xi_i + \xi_{i-1}) = F_i(t) S \Delta x \quad (1.125)$$

$$m \frac{\partial^2 \xi_i}{\partial t^2} + r \frac{\partial \xi_i}{\partial t} + k (\xi_{i+1} - 2\xi_i + \xi_{i-1}) = F_i(t) S \Delta x \quad (1.126)$$

Writing the Newton's law for an element:

$$S\sigma(x+\Delta x) - S\sigma(x) = \rho S \Delta x \frac{\partial^2 \xi}{\partial t^2} \quad (1.127)$$

and

$$\sigma(x) = \frac{E [\xi(x) - \xi(x-\Delta x)]}{\Delta x} \quad (1.128)$$

When  $\Delta x \rightarrow 0$ , considering  $S\sigma = F$  we can write:

$$F_{i+1} - F_i = \frac{d}{dt} p_i \quad (1.129)$$

and

$$F_i = \frac{ES}{\Delta x} q_i \quad (1.130)$$

where

$$p_i = \rho S \Delta x \dot{\xi}_i \quad (1.131)$$

is the momentum of the  $i$  element, and

$$q_i = \xi_i - \xi_{i-1} \quad (1.132)$$

is the relative displacement between the  $i$ th and the  $(i-1)$ th element.

Equation (1.126) becomes:

$$k(q_i - q_{i-1}) + r \frac{\partial \xi_i}{\partial t} + m \frac{\partial^2 \xi_i}{\partial t^2} = 0 \quad (1.133)$$

For  $i$  fixed we have the following representation (figure 1.17.) for one element:

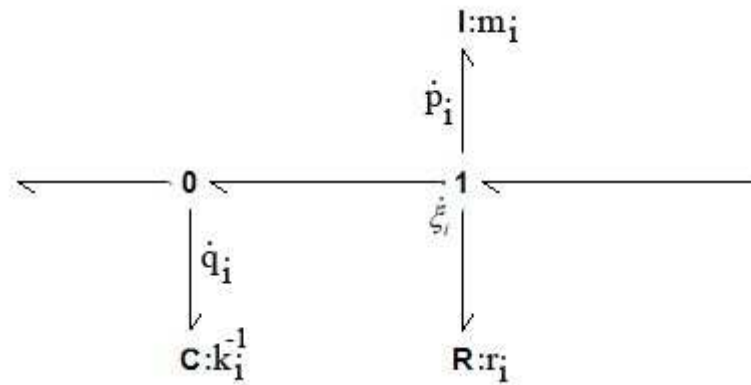


Fig.1.17. One element representation

The corresponding bond graph for the entire bar is in figure 1.18.

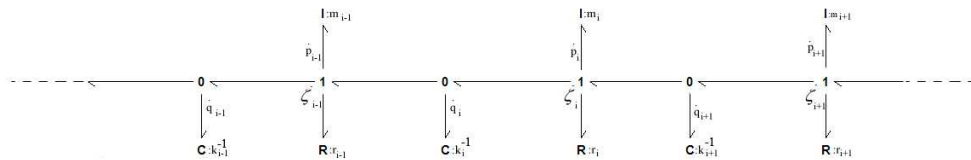


Fig.1.18. Bond Graph representation for difference finite

The generalized momentum corresponding to inertial part can be expressed in function of generalized displacement at each point. In the one dimensional linear case it gives:

$$\frac{dp_i}{dt} = k_{i+1}(q_{i+1}) - k_i(q_i) - \frac{r_i p_i}{m_i} \quad (1.134)$$

The same representation for the potential part is:

$$\frac{dq_i}{dt} = \frac{p_i}{m_i} - \frac{p_{i-1}}{m_{i-1}} \quad (1.135)$$

### 1.3.6. Finite volume method

#### 1.3.6.1. Principe

The finite volume method approximates the partial differential equation over a control volume surrounding the grid node, rather than at

the node itself as finite difference method. The discretization equations are obtained by integrating the partial differential equation over control volumes surrounding the grid nodes, after introducing necessary simplifications and assumptions. It often leads to the same discretization equations as the Taylor series method, however it is more flexible. It bears much commonality with the Galerkin Finite-element method but is easier to implement. In the finite volume method the integration domain is covered by control volumes; each control volume engulfs one grid node, which lies on a grid mesh. With gradient type boundary conditions, we need to solve over a control volume surrounding boundary point, but there is no need to introduce external imaginary nodes.

Let consider the case of heat conduction:

$$\frac{\partial}{\partial x} \left( k \frac{\partial T}{\partial x} \right) + \frac{\partial}{\partial y} \left( k \frac{\partial T}{\partial y} \right) = 0 \quad (1.136)$$

which for  $k \in \mathbb{R}$  reduces to:

$$k \left( \frac{\partial^2 T}{\partial x^2} + \frac{\partial^2 T}{\partial y^2} \right) = 0 \quad (1.137)$$

Integrating over a regular control-volume:

$$\begin{aligned} \int_y^{y+\Delta y} \int_x^{x+\Delta x} k \left( \frac{\partial^2 T}{\partial x^2} + \frac{\partial^2 T}{\partial y^2} \right) dx dy &= \int_y^{y+\Delta y} \int_x^{x+\Delta x} k \left( \frac{\partial^2 T}{\partial x^2} \right) dx dy \\ &+ \int_y^{y+\Delta y} \int_x^{x+\Delta x} k \left( \frac{\partial^2 T}{\partial y^2} \right) dx dy = 0 \end{aligned} \quad (1.138)$$

The first term may be integrated in x-direction as follows:

$$\int_y^{y+\Delta y} \int_x^{x+\Delta x} k \left( \frac{\partial^2 T}{\partial x^2} \right) dx dy = \int_y^{y+\Delta y} \left[ \left( k \frac{\partial T}{\partial x} \right)_{x+\Delta x} - \left( k \frac{\partial T}{\partial x} \right)_x \right] dy \quad (1.139)$$

To continue with integration we will assume that the quantities between brackets do not vary with y. We have:

$$\int_y^{y+\Delta y} \int_x^{x+\Delta x} k \left( \frac{\partial^2 T}{\partial x^2} \right) dx dy = \left[ \left( k \frac{\partial T}{\partial x} \right)_{x+\Delta x} \Delta y - \left( k \frac{\partial T}{\partial x} \right)_x \Delta y \right] \quad (1.140)$$

Then we use a central-difference formula to evaluate the gradient at the control volume, giving:

$$\int_y^{y+\Delta y} \int_x^{x+\Delta x} k \left( \frac{\partial^2 T}{\partial x^2} \right) dx dy = \left[ \left( k \frac{T_{i+1,j} - T_{i,j}}{\Delta x} \right) \Delta y - \left( k \frac{T_{i,j} - T_{i-1,j}}{\Delta x} \right) \Delta y \right] \quad (1.141)$$

We follow the same step for the second member of the equation (1.138) assuming no variation of the partial derivative in x-direction:

$$\int_y^{y+\Delta y} \int_x^{x+\Delta x} k \left( \frac{\partial^2 T}{\partial y^2} \right) dx dy = \left[ \left( k \frac{T_{i,j+1} - T_{i,j}}{\Delta y} \right) \Delta x - \left( k \frac{T_{i,j} - T_{i,j-1}}{\Delta y} \right) \Delta x \right] \quad (1.142)$$

Substituting (1.141) and (1.142) in (1.138) we have:

$$\begin{aligned} & \left[ \left( k \frac{T_{i+1,j} - T_{i,j}}{\Delta x} \right) \Delta y - \left( k \frac{T_{i,j} - T_{i-1,j}}{\Delta x} \right) \Delta y \right] \\ & + \left[ \left( k \frac{T_{i,j+1} - T_{i,j}}{\Delta y} \right) \Delta x - \left( k \frac{T_{i,j} - T_{i,j-1}}{\Delta y} \right) \Delta x \right] = 0 \end{aligned} \quad (1.143)$$

### 1.3.6.2. Bond Graph representation

Consider the bar equation with boundary conditions:

$$\begin{aligned} \rho S \frac{\partial^2 \xi}{\partial t^2} + r S \frac{\partial \xi}{\partial t} + E S \frac{\partial^2 \xi}{\partial x^2} - F(x,t) S &= 0 \\ \xi(0,t) = 0 \quad \frac{\partial \xi}{\partial t}(L,t) &= 0 \end{aligned} \quad (1.144)$$

Let consider the case where  $F(x,t)=0$ . We define a volume control like in the figure 1.19.

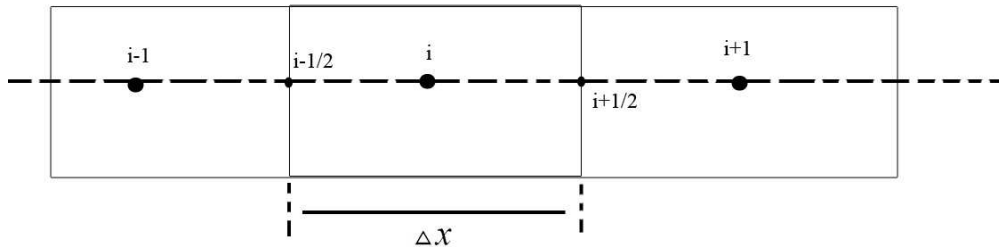


Fig.1.19. Volume control

Equation (1.144) becomes:

$$\int_{\Delta V} \rho S \frac{\partial^2 \xi}{\partial t^2} + \int_{\Delta V} r S \frac{\partial \xi}{\partial t} + \int_{\Delta V} E S \frac{\partial^2 \xi}{\partial x^2} = 0 \quad (1.145)$$

Eq. (1.145) becomes:

$$\left( ES \frac{\partial \xi}{\partial x} \right)_{i+1/2} - \left( ES \frac{\partial \xi}{\partial x} \right)_{i-1/2} + \left[ \rho S \left( \frac{\partial^2 \xi}{\partial t^2} \right)^* + rS \left( \frac{\partial \xi}{\partial t} \right)^* \right]_{\Delta V} = 0 \quad (1.146)$$

$\left( \frac{\partial \xi}{\partial t} \right)^*$  and  $\left( \frac{\partial^2 \xi}{\partial t^2} \right)^*$  are the average values of the first and second

derivative inside the control volume. We can consider several approximations of them:

$$\left( \frac{\partial \xi}{\partial t} \right)^* = \frac{\partial \xi_i}{\partial t} \quad \left( \frac{\partial^2 \xi}{\partial t^2} \right)^* = \frac{\partial^2 \xi_i}{\partial t^2} \quad (1.147)$$

or

$$\left( \frac{\partial \xi}{\partial t} \right)^* = \frac{1}{2} \left( \frac{\partial \xi_{i-1/2}}{\partial t} + \frac{\partial \xi_{i+1/2}}{\partial t} \right) \quad \left( \frac{\partial^2 \xi}{\partial t^2} \right)^* = \frac{1}{2} \left( \frac{\partial^2 \xi_{i-1/2}}{\partial t^2} + \frac{\partial^2 \xi_{i+1/2}}{\partial t^2} \right) \quad (1.148)$$

It is also necessary to approximate the value of  $\xi$  at face  $i-1/2$  and  $i+1/2$ . We chose a linear approximation. The central difference approximation:

$$\left( ES \frac{\partial \xi}{\partial x} \right)_{i-1/2} = ES \frac{\xi_i - \xi_{i-1}}{\Delta x} \quad (1.149)$$

and

$$\left( ES \frac{\partial \xi}{\partial x} \right)_{i+1/2} = ES \frac{\xi_{i+1} - \xi_i}{\Delta x} \quad (1.150)$$

Using the approximations (1.147), (1.149) and (1.150), eq. (1.146) becomes:

$$ES \left( \frac{\xi_{i+1} - \xi_i}{\Delta x} - \frac{\xi_i - \xi_{i-1}}{\Delta x} \right) + \left[ \rho S \frac{\partial^2 \xi_i}{\partial t^2} + rS \frac{\partial \xi_i}{\partial t} \right] S_{\Delta x} = 0 \quad (1.151)$$

or

$$\frac{ES}{\Delta x} (\xi_{i+1} - 2\xi_i + \xi_{i-1}) + \rho S^2_{\Delta x} \frac{\partial^2 \xi_i}{\partial t^2} + rS^2_{\Delta x} \frac{\partial \xi_i}{\partial t} = 0 \quad (1.152)$$

The displacement between the  $i$ th and the  $(i-1)$ th element:

$$q_i = \xi_i - \xi_{i-1} \quad (1.153)$$

and the momentum of the  $i$  element:

$$p_i = \rho S_{\Delta x} \dot{\xi}_i \quad (1.154)$$

Equation (1.152) becomes:

$$k(q_i - q_{i-1}) + r \frac{\partial \xi_i}{\partial t} + m \frac{\partial^2 \xi_i}{\partial t^2} = 0 \quad (1.155)$$

The corresponding bond graph is in figure 1.20.

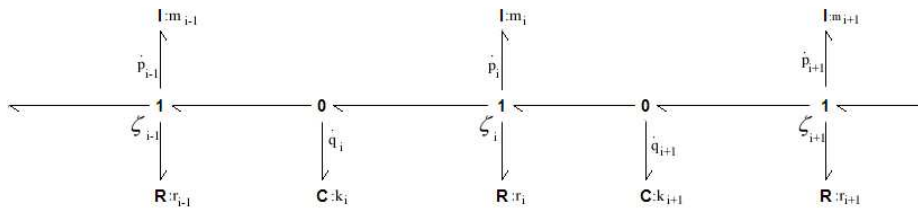


Fig.1.20. Bond Graph representation for difference finite

The finite volumes method is a method used to solve the nonlinear conservation equations. Finite volume methods are very robust and efficient for practical computation when applied to the direct simulation of complex physics. This is particularly the case in computational fluid dynamics.

#### 1.4. Conclusion

The spectral methods use a weighted-integral statement in order to calculate  $b_j$ . They produce a sufficient and necessary number of algebraic equations that are equivalent to minimizing the error introduced in the approximation of the differential equation in a weighted-integral sense.

The main disadvantage, from the practical point of view, is the difficulty encountered in selecting the approximation functions. There is not a unique procedure for constructing them and it becomes more

difficult when the domain is geometrically complex and the boundary conditions complicated.

To solve a problem with the variable separation method, Karnopp and all [KAR 90], proposed to split the domain into a sufficient number of modes and to replace the neglected others with an equivalent stiffness not to lose the static comportment of the system. Doing that the solution is no more an exact one and the method enters in the spectral method group of approximation problem.

Finite element methods are similar in philosophy to spectral algorithms; the major difference is that finite elements chop the interval in  $x$  into a number of sub-intervals, and choose the  $\phi_i(x)$  to be *local* functions which are polynomials of *fixed* degree which are non-zero only over a couple of sub-intervals. In contrast, spectral methods use *global* basis functions in which  $\phi_i(x)$  is a polynomial (or trigonometric polynomial) of *high* degree which is non-zero, except at isolated points, over the entire computational domain.

When more accuracy is needed, the finite element method has three different strategies: to subdivide each element so as to improve resolution uniformly over the whole domain; to subdivide only in regions of steep gradients where high resolution is needed; to keep the subdomains fixed while increasing  $p$ , the degree of the polynomials in each subdomain.

Finite elements have two advantages: they convert differential equations into matrix equations that are *sparse* because only a handful of basis functions are non-zero in a given sub-interval; in multi-dimensional problems, the little sub-intervals become little triangles or tetrahedra which can be fitted to irregularly-shaped bodies like the shell of an automobile. Their disadvantage is low accuracy (for a given number of degrees of freedom  $N$ ) because each basis function is a polynomial of low degree.

Spectral methods generate algebraic equations with full matrices, but in compensation, the high order of the basis functions gives high accuracy for a given  $N$ . When fast iterative matrix-solvers are used, spectral methods can be much more efficient than finite element or finite difference methods for many classes of problems. However, they are most useful when the *geometry* of the problem is fairly smooth and regular.

# **Chapter 2.**

## **Port-Hamiltonian systems**



## Contents

<b>Chapter 2. Port-Hamiltonian systems</b> .....	55
2.1. Introduction.....	59
2.2. The principle of least action.....	60
2.3. Hamiltonian formalism .....	61
2.3.1. Port Hamiltonian representation.....	63
2.4. Transmission line application .....	76
2.4.1. Without dissipation .....	76
2.4.2. With dissipation.....	77
2.4.3. Spatial discretization.....	81
2.4.4. Constitutive equations.....	87
2.5. Conclusion.....	90



## Chapter 2. Port-Hamiltonian systems

### 2.1. Introduction

Usually, distributed parameter systems are complex systems which raise problems in simulation and control. The most important problem consists due to their infinite dimension model. Another problem is a numerical one and proceeds from the fact that the numerical methods for partial differential equations usually assume the boundary conditions to be given, while more often the interactions of distributed components take place through the boundary.

Starting from these problems and trying to solve them, an approach that uses the same principles as in bond graph formalism was developed. This approach assumes that the system can be represented as the result of interaction between elements which are characterized by an energetic behavior. The elements interact with the environment through *ports* and the product between the input and output signals are represented by the instantaneous *power*. The exchange of power between components and between the system and his environment can be mathematical represented by a Dirac structure in finite dimensional case or by a Stokes-Dirac structure in infinite dimensional one, whose the most important properties is its conservativity. The dynamics of the model are specified when an energy function (Hamiltonian) and the space of energy variables are defined. The Dirac structure together with

the energy function and the energy variables are the base of port Hamiltonian formalism [Sch 02], [Sch 05].

In this chapter we will make a presentation of the formalism, and then we will present through an application the extension of telegrapher's equations in the infinite dimensional case with dissipation [Che 07], [Che 09].

## 2.2. *The principle of least action*

The most natural representation of dynamic systems is in terms of energy.

In 1744, Maupertius presented the fact that all the physical phenomena are governed by the same fundamental principle: nature always chooses the way which needs the "least effort"; it is called "the least action principle".

One domain in which this principle is applied is classical mechanics with the equation of motion for particles. Let consider a particle with  $q$  the coordinate,  $t$  the time and  $q(t)$  is the trajectory. Suppose that we know the particle's position at time  $t_1$  and  $t_2$  :

$$\begin{aligned} q(t_1) &= q_1 \\ q(t_2) &= q_2 \end{aligned} \tag{2.1}$$

i.e.,  $q(t)$  is subjected to essential boundary conditions. The question is: which trajectory  $q(t)$  would the particle take to go through points  $q_1$  and  $q_2$  exactly at times  $t_1$  and  $t_2$  ?

The principle of least action states that the real trajectory of the particle is the one that minimizes (or maximizes) the action functional,

$$S[q(t)] = \int_{t_1}^{t_2} L(t, q(t), \dot{q}(t)) dt \tag{2.2}$$

where  $L(t, q(t), \dot{q}(t))$  is the Lagrangian of the system,

$$L(q, \dot{q}) = \frac{1}{2}m(\dot{q}(t))^2 - V(q) \quad (2.3)$$

where:  $m$  is the mass,  $\dot{q}(t)$  is the velocity and  $V(q)$  is the potential energy.

The real trajectory of the particle must have  $\delta S = 0$  (Annex 1), and hence satisfies the Euler-Lagrange equations,

$$\frac{d}{dt} \left( \frac{\partial L}{\partial \dot{q}} \right) - \frac{\partial L}{\partial q} = 0 \quad (2.4)$$

When the Lagrangian takes the form of eq. (2.3), this leads to the following equation of motion,

$$m\ddot{q}(t) = -\frac{\partial V}{\partial q} \quad (2.5)$$

which is identical to the Newton's equation of motion. In general, if the system has  $n$  degrees of freedom,  $q_1, \dots, q_n$ , the Lagrange's equations of motion are

$$\frac{d}{dt} \left( \frac{\partial L}{\partial \dot{q}_i} \right) - \frac{\partial L}{\partial q_i} = 0 \quad \text{for all } i = 1, 2, \dots, n. \quad (2.6)$$

### 2.3. Hamiltonian formalism

Hamiltonian formulation gives us not  $n$  second order equations as in (2.6), but  $2n$  first order equations.

From Euler-Lagrange equations:

$$\frac{d}{dt} \left( \frac{\partial L}{\partial \dot{q}}(q(t), \dot{q}(t), t) \right) - \frac{\partial L}{\partial q}(q(t), \dot{q}(t), t) = 0 \quad (2.7)$$

we consider

$$p(t) = \frac{\partial L}{\partial \dot{q}} \Rightarrow \dot{p}(t) = \frac{\partial L}{\partial q} \quad (2.8)$$

where  $p(t)$  represents the momentum or the impulse of a mass.

To express these equations in function of  $q$  and  $p$  instead of  $q$  and  $\dot{q}$ , we introduce the Hamiltonian

$$H(q, p) = p\dot{q} - L(q, \dot{q}) \quad (2.9)$$

for one degree of freedom, and

$$H(q, p) = \sum_{i=1}^n p_i \dot{q}_i - L(q, \dot{q}) \quad (2.10)$$

for  $n$  degrees of freedom.

$H(q, p)$  is the Legendre transformation of  $L(q, \dot{q})$ .

Hereafter are recalled the Hamiltonian equations of motion:

$$\begin{cases} \dot{p} = -\frac{\partial H}{\partial q} \\ \dot{q} = \frac{\partial H}{\partial p} \end{cases} \quad (2.11)$$

In general,  $H$  represents the total energy stored in the model.

This representation can be found from the Poisson bracket. This is defined for two functions  $F$  and  $G$  in the phase space like:

$$\{F, G\} = \frac{\partial F}{\partial q} \frac{\partial G}{\partial p} - \frac{\partial F}{\partial p} \frac{\partial G}{\partial q} \quad (2.12)$$

The properties of the Poisson bracket are:

- 1) it is skew-symmetric  $\{F, G\} = -\{G, F\}$
- 2) it satisfies the Jacobi identity:

$$\{F, \{G, H\}\} + \{G, \{H, F\}\} + \{H, \{F, G\}\} = 0$$

The canonical equations of mechanics are [Arn 89] :

$$\begin{cases} \dot{p} = \{p, H\} = -\frac{\partial H}{\partial q} \\ \dot{q} = \{q, H\} = \frac{\partial H}{\partial p} \end{cases} \quad (2.13)$$

### 2.3.1. Port Hamiltonian representation

In engineering a fundamental concept is the notion of “open system” [Ort 01], which is a system with a direct interface with its environment. This concept is used in the representation of the system as a grid interconnecting components [Sch 02]. The network modeling assumes that the system has external variables, which can be interconnected to other open systems. In order to have this property, the canonical equations are modified and an exterior force is added [Sch 95].

#### 2.3.1.1. Finite dimension

##### a) Without dissipation

When there are external forces  $F$ , the canonical equations become:

$$\begin{cases} \dot{p} = \{p, H\} = -\frac{\partial H}{\partial q} + F \\ \dot{q} = \{q, H\} = \frac{\partial H}{\partial p} \end{cases} \quad (2.14)$$

By calculating the power balance it leads to:

$$\begin{aligned}
 \frac{dH(q, p)}{dt} &= \left( \frac{\partial H}{\partial p} \right)^T \dot{p} + \left( \frac{\partial H}{\partial q} \right)^T \dot{q} \\
 &= \left( \frac{\partial H}{\partial p} \right)^T \left( - \left( \frac{\partial H}{\partial q} \right) + F \right) + \left( \frac{\partial H}{\partial q} \right)^T \dot{q} \\
 &= - \left( \frac{\partial H}{\partial p} \right)^T \left( \frac{\partial H}{\partial q} \right) + \left( \frac{\partial H}{\partial p} \right)^T F + \left( \frac{\partial H}{\partial q} \right)^T \dot{q} \\
 &= \dot{q}^T F
 \end{aligned} \tag{2.15}$$

All these equations are suitable for representing mechanical systems.

For control design purpose,  $F$  can be considered as inputs (the forces that act on the system). We consider a system with inputs and outputs and we choose  $y$  as outputs, in such manner that the product  $y^T F$  is a power. With these, we can work using the concept of energy and we can use by analogy this concept in other domains.

We take:

$$y = \frac{\partial H}{\partial p} \tag{2.16}$$

**Note** :the variation of energy versus time in a conservative Hamiltonian system is equal to the supplied power.

The representation with collocated inputs and outputs is:

$$\begin{aligned}
 \dot{q} &= \frac{\partial H}{\partial p}(q, p), \quad q \in \mathbb{R}^n, p \in \mathbb{R}^n \\
 \dot{p} &= - \frac{\partial H}{\partial q}(q, p) + B(q)u, \quad u \in \mathbb{R}^m \\
 y &= B^T(q) \frac{\partial H}{\partial p}(q, p) \quad (= B^T(q)\dot{q}), \quad y \in \mathbb{R}^m
 \end{aligned} \tag{2.17}$$

where  $B$  is the input matrix,  $Bu$  is the set of generalized forces obtained from inputs  $u=F$ . This representation is called the port-Hamiltonian system.

The power consumed in the system is  $\frac{dH}{dt}$  and is equal to the power supplied to the system as shown in the following equations:

$$\frac{dH(q, p)}{dt} = y^T u \quad (2.18)$$

The system is power conservative.

**Note:**  $y$  being chosen in order to have as the product between it and the vector of inputs an instantaneous power, thus we have a similarity with the bond graph representation.

The work space is of dimension  $(2 \cdot n)$  and is the phase space.

Another modality to write the eq. (2.17) can be obtained if we consider a vector  $x = (x_1, \dots, x_n)$  of local coordinates for a  $n$ -dimensional state space manifold on  $\mathbb{R}^2$ :

$$\dot{x} = \begin{bmatrix} \dot{q} \\ \dot{p} \end{bmatrix} \quad \frac{\partial H}{\partial x} = \begin{bmatrix} \frac{\partial H}{\partial q} \\ \frac{\partial H}{\partial p} \end{bmatrix} \quad (2.19)$$

$$\begin{cases} \dot{x} = J(x) \frac{\partial H}{\partial x}(x) + g(x)u, & x \in \mathbb{R}^{2n}, u \in \mathbb{R}^m \\ y = g^T(x) \frac{\partial H}{\partial x}(x), & y \in \mathbb{R}^m \end{cases} \quad (2.20)$$

where  $J(x)$  is a  $(2n \times 2n)$  skew-symmetric matrix

$$J(x) = -J^T(x) \quad (2.21)$$

$$J(x) = \begin{bmatrix} 0 & I_n \\ -I_n & 0_n \end{bmatrix} \quad g(x) = \begin{bmatrix} 0_n \\ B \end{bmatrix}$$

The system represented by eq. (2.20) having the matrix  $J$  satisfying eq. (2.21), is called a “port-Hamiltonian system” and is represented in figure 2.1.

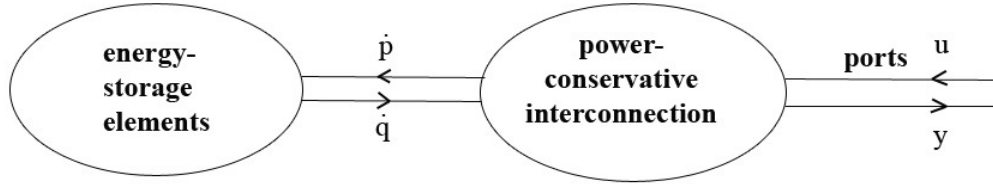


Fig.2.1. Port-Hamiltonian system without dissipation

### b) Dissipative systems

To take into account the energy dissipation phenomena (resistance, etc..) we introduce the variables  $u_R$  to define a new input

vector as  $\begin{bmatrix} u \\ u_R \end{bmatrix}$ . To keep the same number of inputs and outputs, we

introduce the variables  $y_R$  in the output vector as

$$\begin{bmatrix} y \\ y_R \end{bmatrix} = \begin{bmatrix} g^T(x) \frac{\partial H}{\partial x}(x) \\ g_R^T(x) \frac{\partial H}{\partial x}(x) \end{bmatrix} \quad (2.22)$$

The model (2.20) becomes:

$$\begin{aligned} \dot{x} &= J(x) \frac{\partial H}{\partial x}(x) + g(x)u + g_R(x)u_R \\ y &= g^T(x) \frac{\partial H}{\partial x}(x) \\ y_R &= g_R^T(x) \frac{\partial H}{\partial x}(x) \end{aligned} \quad (2.23)$$

where  $u_R, y_R$  represent the connections with the dissipative part. If we do not have any energy storage, the component is of algebraic type:  $u_R = -F(y_R)$ , where the (-) sign is due to convention for dissipative phenomena.

The power which will be transformed into stored energy is thus:

$$\begin{aligned} \frac{dH}{dt} &= \left( \frac{\partial H}{\partial x} \right)^T \dot{x} = \left( \frac{\partial H}{\partial x} \right)^T \left( J(x) \frac{\partial H}{\partial x} + g(x)u + g_R(x)u_R \right) \\ &= \underbrace{\left( \frac{\partial H}{\partial x} \right)^T J(x) \frac{\partial H}{\partial x}}_{=0} + \underbrace{\left( \frac{\partial H}{\partial x} \right)^T g(x)u}_{=y^T u} + \underbrace{\left( \frac{\partial H}{\partial x} \right)^T g_R(x)u_R}_{=y_R^T u_R} \end{aligned} \quad (2.24)$$

But,  $u_R = -F(y_R)$ , so we have:

$$\frac{dH}{dt} = y^T u - y_R^T F(y_R) \quad (2.25)$$

with  $y_R^T F(y_R) \geq 0$ .

In the linear case, we can write the relation  $u_R = -Sy_R$ , for some semi-positive symmetric matrix  $S = S^T \geq 0$ .

$$\begin{aligned} \dot{x} &= J(x) \frac{\partial H}{\partial x}(x) + g(x)u - g_R(x)Sy_R \\ y &= g^T(x) \frac{\partial H}{\partial x}(x) \end{aligned} \quad (2.26)$$

Using  $y_R = g_R^T(x) \frac{\partial H}{\partial x}(x)$ , it leads to:

$$\begin{aligned} \dot{x} &= J(x) \frac{\partial H}{\partial x}(x) + g(x)u - g_R(x)Sg_R^T(x) \frac{\partial H}{\partial x}(x) \\ y &= g^T(x) \frac{\partial H}{\partial x}(x) \end{aligned} \quad (2.27)$$

Finally, it leads to:

$$\begin{aligned} \dot{x} &= [J(x) - R(x)] \frac{\partial H}{\partial x}(x) + g(x)u \\ y &= g^T(x) \frac{\partial H}{\partial x}(x) \end{aligned} \quad (2.28)$$

with  $R(x) = g_R(x)Sg_R^T(x)$ .

This is the representation of a port-Hamiltonian system with dissipation.

The power-balance has the form:

$$\frac{dH}{dt}(x(t)) = y^T u - \left( \frac{\partial H}{\partial x} \right)^T R(x(t)) \frac{\partial H}{\partial x} \leq y^T u \quad (2.29)$$

We can see the system from a network modelling perspective like being constituted by a set of energy-storage elements, a set of energy-dissipating or resistive elements, and a set of ports, interconnected to each other by a power-conservative interconnection (see figure 2.2).

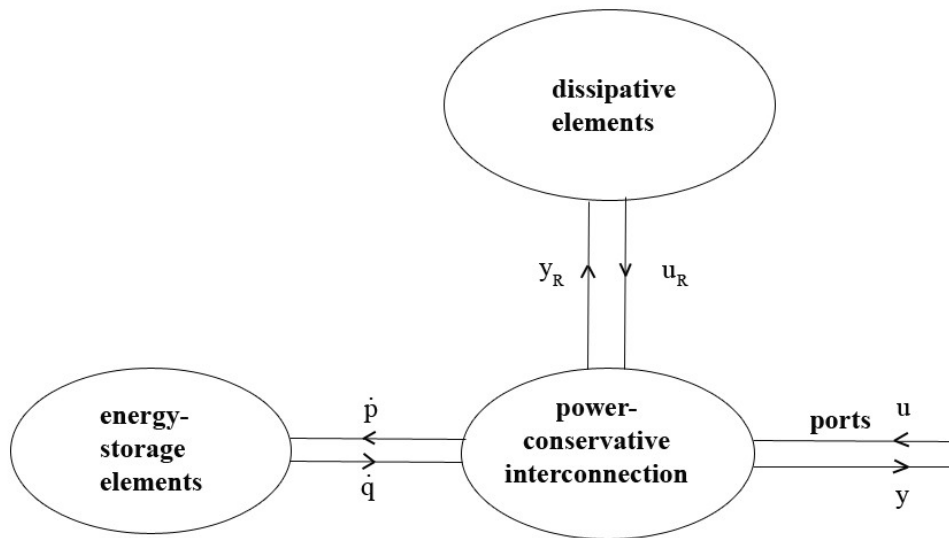


Fig.2.2. Port-Hamiltonian system with dissipation

### c) Effort-flow representation

Let us consider a state space  $n$ -dimensional ( $\mathfrak{X}$ ) where the energy variables are  $x_1, x_2, \dots, x_n$ , and the total energy  $H : \mathfrak{X} \rightarrow \mathbb{R}$ . The representation of power-conservative interconnection can be done by a constant Dirac structure  $D$  (Appendices B) defined on a finite-dimensional linear space  $F$  or more often by a Dirac structure modulated by the state variables  $x$ .

In the first case the linear space  $F$  contains the space of flows  $f_S$  linked to the energy-storage elements ( $F_S$ ), the space of flows  $f_R$  linked to the dissipative elements ( $F_R$ ), and the space of external flows  $f_P$  linked to the environment ( $F_P$ ). We have the dual space  $F^*$ , with the corresponding space of efforts  $e_S$  connected to the energy-storage elements ( $F_S^*$ ), the space of efforts  $e_R$  connected to the resistive elements ( $F_R^*$ ), and the space of efforts  $e_P$  connected to the environment of the system ( $F_P^*$ ).

For the energy-storage element, the flow variables are given by:

$$f_S = -\dot{x} \quad (2.30)$$

and the effort variables by:

$$e_S = \frac{\partial H}{\partial x}(x) \quad (2.31)$$

The minus sign is introduced in order to have a consistent sign convention.

For the resistive elements we consider here only the linear case, so the variables effort and flow are related as

$$f_R = -\mathbf{R}e_R \quad (2.32)$$

for some matrix  $\mathbf{R} = \mathbf{R}^T \geq 0$ . It results in what it is called an implicit port-Hamiltonian system (with dissipation) related to a constant Dirac structure:

$$\left( f_S = -\dot{x}, f_R = -\mathbf{R}e_R, f_P, e_S = \frac{\partial H}{\partial x}(x), e_R, e_P \right) \in D \quad (2.33)$$

In the finite dimensional case the Dirac structure can be used to formalize Hamiltonian systems as implicit Hamiltonian system.

Using the representation of energy accumulation [Baa 08] (figure 2.3.):

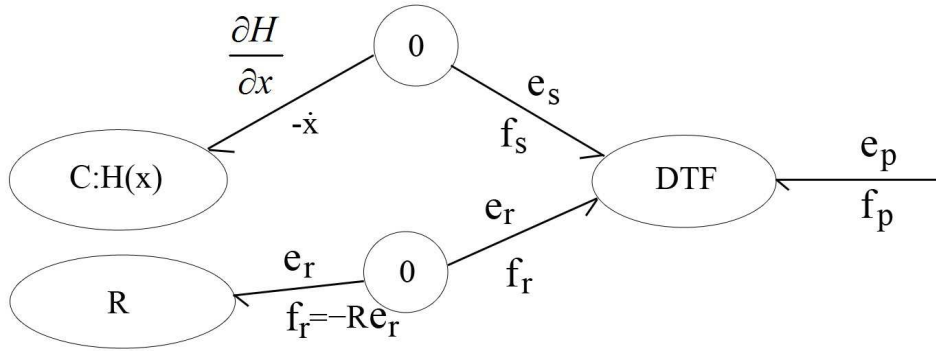


Fig.2.3. System representation

### 2.3.1.2. Infinite dimension

In the infinite-dimensional physical systems, the Dirac structure has a special form called Stokes-Dirac structure, and to represent the systems as a port-Hamiltonian one, the distributed parameter system is formulated as a system of conservation laws, coupled with a set of closure equations.

#### a) Port-based formulation for b-dimensional spatial domain

Consider a  $b$ -dimensional manifold  $\Omega$  with  $(b-1)$ -dimensional boundary  $\partial\Omega$ . Denote by  $\Lambda^k(\Omega)$  the vector space of  $k$ -forms on  $\Omega$  and by  $\Lambda^k(\partial\Omega)$  the vector space of  $k$ -forms on boundary. Be  $\Lambda = \bigoplus_{k \geq 0} \Lambda^k(\Omega)$  the algebra of differential forms over  $\Omega$  and recall that it is endowed with an exterior product  $\wedge$  and an exterior derivation  $d$  (Annex 1).

In [Sch 05] it has been shown that a *system of conservation laws* is defined by a set of *conserved quantities*  $y_i \in \Lambda^{k_i}(\Omega)$ ,  $i \in \{1, \dots, N\}$ ,  $N \in \mathbb{N}$ ,  $k_i \in \mathbb{N}$  defining the state space  $Y = \bigotimes_{i=1, \dots, N} \Lambda^{k_i}(\Omega)$ . They satisfy a set of *conservation laws*

$$\frac{\partial y_i}{\partial t} + d\beta_i = g_i \quad (2.34)$$

where  $\beta_i \in \Lambda^{k_i-1}(\Omega)$  denote the set of *fluxes* and  $g_i \in \Lambda^{k_i}(\Omega)$  denote the set of distributed *interaction forms*. Finally, the fluxes  $\beta_i$  are defined by the *closure equations* which appear from the description of the canonical interaction of two physical domains with  $x \in \Omega$ :

$$\beta_i = M(y_i, x), \quad i = 1, \dots, N \quad (2.35)$$

The integral form of the conservation laws yields the following *balance equations*

$$\frac{\partial}{\partial t} \int_{\Omega} y_i + \int_{\partial\Omega} \beta_i = \int_{\Omega} g_i \quad (2.36)$$

Let consider the conserved quantities  $y_q \in \Lambda^q(\Omega)$  and  $y_p \in \Lambda^p(\Omega)$ , part of a system of two conservation laws, which are differential forms with the degrees  $p$  and  $q$  on a  $b$ -dimensional spatial domain  $\Omega$  and  $p+q=b+1$ . The closure equations generated by a Hamilton density function  $\mathcal{H}f : \Lambda^p(\Omega) \times \Lambda^q(\Omega) \times \Omega \rightarrow \Lambda^b(\Omega)$  resulting in the total Hamiltonian  $H = \int_{\Omega} \mathcal{H}f \in \mathbb{R}$  are given by:

$$\begin{pmatrix} \beta_p \\ \beta_q \end{pmatrix} = \varepsilon \begin{pmatrix} 0 & (-1)^r \\ 1 & 0 \end{pmatrix} \begin{pmatrix} \frac{\delta H}{\delta y_p} \\ \frac{\delta H}{\delta y_q} \end{pmatrix} \quad (2.37)$$

with  $r = pq + 1, \varepsilon \in \{-1, +1\}$ . These form a system of *two conservation laws with canonical interdomain coupling*.

As in the one dimensional case we define the power variables. As we saw before the Hamiltonian is the total stored energy of the system. The state variables  $y_i, i = 1 \dots b$  are called the *energy variables* and the

variational derivatives  $\frac{\delta H}{\delta y_i}$  are called the *co-energy variables or power variables*.

We define the vector of effort variables

$$\begin{pmatrix} e_p \\ e_q \end{pmatrix} = \begin{pmatrix} \frac{\delta H}{\delta y_p} \\ \frac{\delta H}{\delta y_q} \end{pmatrix} \quad (2.38)$$

and the vector of flow variables

$$\begin{pmatrix} f_p \\ f_q \end{pmatrix} = \begin{pmatrix} \frac{\partial y_p}{\partial t} \\ \frac{\partial y_q}{\partial t} \end{pmatrix} \quad (2.39)$$

The flow and effort variables are *power-conjugated* as their product is the time-variation of the Hamiltonian function:

$$\frac{dH}{dt} = \int_{\Omega} \left( \frac{\delta H}{\delta y_p} \wedge \frac{\partial y_p}{\partial t} + \frac{\delta H}{\delta y_q} \wedge \frac{\partial y_q}{\partial t} \right) = \int_{\Omega} (e_p \wedge f_p + e_q \wedge f_q) \quad (2.40)$$

One may write the time-variation of the Hamiltonian using the conservation laws, the closure relations, the properties of the exterior derivative and Stokes' theorem (Appendices B):

$$\begin{aligned} \frac{dH}{dt} &= \int_{\Omega} (\varepsilon \beta_q \wedge (-d\beta_p) + (-1)^r \beta_p \wedge \varepsilon(-d\beta_q)) \\ &= -\varepsilon \int_{\Omega} (\beta_q \wedge d\beta_p + (-1)^{pq+1} (-1)^{(p-1)q} \beta_q \wedge d\beta_p) \\ &= -\varepsilon \int_{\Omega} (\beta_q \wedge d\beta_p + (-1)^q \beta_q \wedge d\beta_p) \\ &= -\varepsilon \int_{\partial\Omega} \beta_q \wedge \beta_p \end{aligned} \quad (2.41)$$

We define flow and effort variables on the boundary of the system as the *restriction* of the flux variables to the boundary  $\partial\Omega$  of the domain  $\Omega$ :

$$\begin{pmatrix} f_\partial \\ e_\partial \end{pmatrix} = \begin{pmatrix} \beta_q|_{\partial\Omega} \\ \beta_p|_{\partial\Omega} \end{pmatrix} \quad (2.42)$$

They are also power conjugated variables.

We can define an interconnection structure between two systems of conservation laws by the equations of differential forms defined on the boundary  $\partial\Omega$ , together with the conservation laws and closure equations.

$$\begin{pmatrix} f_p \\ f_q \end{pmatrix} = \varepsilon \begin{pmatrix} 0 & (-1)^r d \\ d & 0 \end{pmatrix} \begin{pmatrix} e_p \\ e_q \end{pmatrix} \quad (2.43)$$

The power-conjugated variables make this interconnection power continuous because the variables satisfy the power continuity relation from (2.40) and (2.41):

$$\int_Z (e_p \wedge f_p + e_q \wedge f_q) + \varepsilon \int_{\partial Z} f_\partial \wedge e_\partial = 0 \quad (2.44)$$

### b) Port Hamiltonian for distributed-parameter systems with boundary energy flow

This is the case where we are interested only by what happened at the boundary level.

In the case of a distributed-parameter system with boundary energy flow we present a definition with respect to a Stokes-Dirac structure (Annexes 1).

We consider a  $b$ -dimensional manifold  $Q$  with boundary  $\partial Q$ , and let  $D$  be a Stokes Dirac structure.

Let consider

$$\mathcal{H} : \Lambda^p(Q) \times \Lambda^q(Q) \times Q \rightarrow \Lambda^b(Q)$$

$$H := \int_\Omega \mathcal{H} \in \mathbb{R}$$

a Hamiltonian density with total energy  $H$ .

For

$$\delta_p H \in \Lambda^{b-p}(Q)$$

$$\delta_q H \in \Lambda^{b-q}(Q)$$

defined differential forms,  $(\delta_p H, \delta_q H) \in \Lambda^{b-p}(Q) \times \Lambda^{b-q}(Q)$  can be seen as variational derivatives of  $H$  at  $(u_p, u_q) \in \Lambda^p(Q) \times \Lambda^q(Q)$ .

The Hamiltonian time variation is:

$$\frac{dH}{dt} = \int_Z \left[ \delta_p H \wedge \frac{\partial u_p}{\partial t} + \delta_q H \wedge \frac{\partial u_q}{\partial t} \right] \quad (2.45)$$

The rates of the energy variables  $\frac{\partial u_p}{\partial t}, \frac{\partial u_q}{\partial t}$  are connected to  $D$  by:

$$\begin{aligned} f_p &= -\frac{\partial u_p}{\partial t} \\ f_q &= -\frac{\partial u_q}{\partial t} \end{aligned} \quad (2.46)$$

We set

$$\begin{aligned} e_p &= \delta_p H \\ e_q &= \delta_q H \end{aligned} \quad (2.47)$$

It results the definition of boundary port-Hamiltonian system defined on a  $n$ -dimensional manifold, with state space  $\Lambda^p(Q) \times \Lambda^q(Q)$ , with a Stokes-Dirac structure  $D$ , and a Hamilton  $H$ :

$$\begin{aligned} \begin{bmatrix} -\frac{\partial \alpha_p}{\partial t} \\ \frac{\partial \alpha_q}{\partial t} \end{bmatrix} &= \begin{bmatrix} 0 & (-1)^r d \\ d & 0 \end{bmatrix} \begin{bmatrix} \delta_p H \\ \delta_q H \end{bmatrix} \\ \begin{bmatrix} f_\partial \\ e_\partial \end{bmatrix} &= \begin{bmatrix} 1 & 0 \\ 0 & -(-1)^{n-q} \end{bmatrix} \begin{bmatrix} \delta_p H|_{\partial Z} \\ \delta_q H|_{\partial Z} \end{bmatrix} \end{aligned} \quad (2.48)$$

Because any Dirac structure is power-conservative, it results that in the Stokes-Dirac structure  $D$ , any  $(f_p, f_q, f_\partial, e_p, e_q, e_\partial)$  satisfies:

$$\int_{\Omega} [e_p \wedge f_p + e_q \wedge f_q] + \int_{\partial\Omega} e_\partial \wedge f_\partial = 0 \quad (2.49)$$

When the system interacts with its environment through dissipative components and inputs that affect the power balance of the system, the space is augmented for some  $m$ -manifolds  $S$  with the flows denoting the externally supplied distributed control flow  $f^d \in \Omega^d(S)$ , and the efforts corresponding to a power exchange  $e^d \in \Omega^{b-d}(S)$ .

The Stokes Dirac structure is now:

$$\begin{aligned} \begin{bmatrix} f_p \\ f_q \end{bmatrix} &= \begin{bmatrix} 0 & (-1)^r d \\ d & 0 \end{bmatrix} \begin{bmatrix} e_p \\ e_q \end{bmatrix} + G(f_d) \\ \begin{bmatrix} f_\partial \\ e_\partial \end{bmatrix} &= \begin{bmatrix} 1 & 0 \\ 0 & -(-1)^{b-q} \end{bmatrix} \begin{bmatrix} e_p|_{\partial Z} \\ e_q|_{\partial Z} \end{bmatrix} \\ e_d &= -G^* \begin{bmatrix} e_p \\ e_q \end{bmatrix} \end{aligned} \quad (2.50)$$

with  $G$  a linear map:

$$G = \begin{pmatrix} G_p \\ G_q \end{pmatrix} : \Lambda^d(S) \rightarrow \Lambda^p(Q) \times \Lambda^q(Q) \quad (2.51)$$

with dual map

$$G^* = (G_p^*, G_q^*) : \Lambda^{b-p}(Q) \times \Lambda^{b-q}(Q) \rightarrow \Lambda^{b-d}(S) \quad (2.52)$$

satisfying

$$\int_Z [e_p \wedge G_p(f_d) + e_q \wedge G_q(f_d)] = \int_S [G_p^*(e_p) + G_q^*(e_q)] \wedge f_d \quad (2.53)$$

The external variables are now:

$f_\partial, e_\partial$  - the boundary external variables

$f_d, e_d$  - the distributed external variables.

The power balance:

$$\frac{dH}{dt} = \int_{\partial\Omega} e_\partial \wedge f_\partial + \int_S e_d \wedge f_d \quad (2.54)$$

with the first term denoting the power flow through boundary, and the second the distributed power flow.

The energy dissipation can be incorporated by terminating some ports with resistive relation.

Let  $R : \Lambda^{b-d}(S) \rightarrow \Lambda^d(S)$  be a map satisfying:

$$\int_S e_d \wedge R(e_d) \geq 0, \quad \forall e_d \in \Lambda^{b-d}(S) \quad (2.55)$$

The port-Hamiltonian system with dissipation defined with respect to the Dirac structure satisfies the power inequality:

$$\frac{dH}{dt} = \int_{\partial\Omega} e_\partial \wedge f_\partial - \int_S e_d \wedge R(e_d) \leq \int_{\partial\Omega} e_\partial \wedge f_\partial \quad (2.56)$$

## 2.4. Transmission line application

### 2.4.1. Without dissipation

In the 1880s, Oliver Heaviside, developed the transmission line model. Starting from this model have been found the telegrapher's equations, a pair of linear differential equations, which describe on an electrical transmission line the voltage and current with distance and time.



Fig.2.4. Transmission line

This approach can be applied to high-frequency transmission lines and is important for designing high-voltage energy transmission lines. The model obtained shows up that the electromagnetic waves can be reflected on the wire, and that wave patterns can appear along the line.

If we consider a long transmission line, we can split the line into segments of small dimension  $dx$  and we can consider the currents being quasi-steady.

When the elements  $r$  (resistance) and  $g$  (conductance) are very small, their influence can be neglected, and we have the lossless transmission line model, where we have the dependence on  $l$  (inductance) and  $c$  (capacitance):

$$\begin{aligned}\frac{\partial}{\partial x}v(x,t) &= -l\frac{\partial}{\partial t}i(x,t) \\ \frac{\partial}{\partial x}i(x,t) &= -c\frac{\partial}{\partial t}v(x,t)\end{aligned}\tag{2.57}$$

When the effects of  $r$  and  $g$  are not negligible we have:

$$\begin{aligned}\frac{\partial}{\partial x}v(x,t) &= -l\frac{\partial}{\partial t}i(x,t) - ri(x,t) \\ \frac{\partial}{\partial x}i(x,t) &= -c\frac{\partial}{\partial t}v(x,t) - gv(x,t)\end{aligned}\tag{2.58}$$

### 2.4.2. With dissipation

Let us consider a transmission line with  $\Omega = [0,1] \subset \mathbb{R}$  and define the energy variables as the charge density  $q = q(t,x) \in \Lambda^1(\Omega)$  and the magnetic flux density  $\phi = \phi(t,x) \in \Lambda^1(\Omega)$  where  $\Lambda^1(\Omega)$  denotes the 1-forms space. The energy density (or the Hamiltonian density)  $H$  at time  $t$  in the homogeneous transmission line is given as:

$$H(q, \phi) = \frac{1}{2} \left[ q(t, x) \wedge * \frac{q(t, x)}{c} + \phi(t, x) \wedge * \frac{\phi(t, x)}{l} \right] \quad (2.59)$$

where  $l$  and  $c$  represent respectively inductance and capacitance density and where  $(\wedge)$  is the wedge product and  $(*)$  is the Hodge star operator, defined as

$$*(\mathcal{D}) : \Lambda^k(\mathcal{D}) \rightarrow \Lambda^{n-k}(\mathcal{D}) \quad (2.60)$$

where  $\mathcal{D}$  is an open in  $\Omega$  (a Riemannian manifold). In order to introduce the energy variables, we write the power balance of the transmission line starting with total energy

$$\frac{dH(q, \phi)}{dt} = \int_{\Omega} \frac{\delta H(q, \phi)}{\delta q} \wedge \frac{\partial q}{\partial t} + \frac{\delta H(q, \phi)}{\delta \phi} \wedge \frac{\partial \phi}{\partial t} \quad (2.61)$$

where variational derivatives are given by

$$\begin{aligned} \frac{\delta H(q, \phi)}{\delta q} &= * \frac{1}{c} q(t, x) \\ \frac{\delta H(q, \phi)}{\delta \phi} &= * \frac{1}{l} \phi(t, x) \end{aligned} \quad (2.62)$$

We introduce the conjugate energy variables flow (*1-form*) and effort (*0-forms*) as follows:

$$\begin{aligned} f_q(t, x) &= \frac{\partial q(t, x)}{\partial t} & f_\phi(t, x) &= \frac{\partial \phi(t, x)}{\partial t} \\ e_q(t, x) &= * \frac{\delta h(q, \phi)}{\delta q} & e_\phi(t, x) &= * \frac{\delta h(q, \phi)}{\delta \phi} \end{aligned} \quad (2.63)$$

The equation (2.61) becomes,

$$\frac{dH(q, \phi)}{dt} = \int_{\Omega} e_q \wedge f_q + e_\phi \wedge f_\phi \quad (2.64)$$

In addition, we have the telegraph equations written in terms of conjugate variables and differential forms.

We have two cases:

1) Without dissipation [Gol 02]:

$$\begin{cases} f_\phi = -de_q \\ f_q = -de_\phi \end{cases} \quad (2.65)$$

2) With dissipation

We propose in our paper [Che 09] to extend to dissipative systems the study made for undissipative ones:

$$\begin{cases} f_\phi = -de_q - r(*e_\phi) \\ f_q = -de_\phi - g(*e_q) \end{cases} \quad (2.66)$$

$r$  and  $g$  represent respectively resistance and conductance density and  $d$  is the usual exterior-derivative.

Substitution in the equation (2.61) gives:

1)

$$\begin{aligned} \frac{dH}{dt} &= \int_{\Omega} e_q \wedge (-de_\phi) + e_\phi \wedge (-de_q) \\ &= \int_{\Omega} [-e_q \wedge de_\phi - e_\phi \wedge de_q] \\ &= -\int_{\Omega} d(e_\phi \wedge e_q) \\ &= -\int_{\partial\Omega} e_q \wedge e_\phi \end{aligned} \quad (2.67)$$

2)

$$\begin{aligned} \frac{dH}{dt} &= \int_{\Omega} e_q \wedge (-de_\phi - g(*e_q)) + e_\phi \wedge (-de_q - r(*e_\phi)) \\ &= \int_{\Omega} [-e_q \wedge de_\phi - e_\phi \wedge de_q] - \int_{\Omega} [e_q \wedge g(*e_q) + e_\phi \wedge r(*e_\phi)] \\ &= -\int_{\Omega} d(e_\phi \wedge e_q) - \int_{\Omega} [e_q \wedge g(*e_q) + e_\phi \wedge r(*e_\phi)] \\ &= -\int_{\partial\Omega} e_q \wedge e_\phi - \int_{\Omega} (e_q \wedge g(*e_q) + e_\phi \wedge r(*e_\phi)) \end{aligned} \quad (2.68)$$

where  $\partial\Omega = \{0,1\}$  represents the boundary set of  $\Omega$ . We have the following structure:

1)

$$\int_{\Omega} e_q \wedge f_q + e_{\phi} \wedge f_{\phi} + \int_{\partial\Omega} e_b \wedge f_b = 0 \quad (2.69)$$

2)

$$\int_{\Omega} e_q \wedge f_q + e_{\phi} \wedge f_{\phi} + \int_{\partial\Omega} e_b \wedge f_b + \int_{\Omega} e_{dq} \wedge f_{dq} + e_{d\phi} \wedge f_{d\phi} = 0 \quad (2.70)$$

where  $e_b = e_q|_{\partial\Omega}$  and  $f_b = e_{\phi}|_{\partial\Omega}$  define the restriction of flow and effort on  $\partial\Omega$ ,

$$f_{d\phi} = r(*e_{\phi}) = \frac{r}{l}\phi(t, x) \in \Lambda^1(\Omega), \quad f_{dq} = g(*e_q) = \frac{g}{c}q(t, x) \in \Lambda^1(\Omega), \text{ and}$$

$$e_{dq} = e_q, \quad e_{d\phi} = e_{\phi}$$

The two last terms of the left side of equation (2.70) represent the power flow at the boundary and the dissipation power in a transmission line. In this way, equation (2.66) becomes

$$\begin{aligned} f_{\phi} &= -de_q - f_{dq} \\ f_q &= -de_{\phi} - f_{d\phi} \end{aligned} \quad (2.71)$$

The resulting port-Hamiltonian systems are:

1)

$$\begin{pmatrix} f_{\phi} \\ f_q \end{pmatrix} = \begin{pmatrix} 0 & -d \\ -d & 0 \end{pmatrix} \begin{pmatrix} e_q \\ e_{\phi} \end{pmatrix} \quad (2.72)$$

$$\begin{pmatrix} e_{b0} \\ e_{b1} \\ f_{b0} \\ f_{b1} \end{pmatrix} = \begin{pmatrix} 1 & 0 & 0 & 0 \\ 0 & 1 & 0 & 0 \\ 0 & 0 & 1 & 0 \\ 0 & 0 & 0 & 1 \end{pmatrix} \begin{pmatrix} e_q(t, 0) \\ e_q(t, 1) \\ e_{\phi}(t, 0) \\ e_{\phi}(t, 1) \end{pmatrix} \quad (2.73)$$

2)

$$\begin{pmatrix} f_{\phi} \\ f_q \end{pmatrix} = \begin{pmatrix} 0 & -d \\ -d & 0 \end{pmatrix} \begin{pmatrix} e_q \\ e_{\phi} \end{pmatrix} - \begin{pmatrix} 1 & 0 \\ 0 & 1 \end{pmatrix} \begin{pmatrix} f_{d\phi} \\ f_{dq} \end{pmatrix} \quad (2.74)$$

$$\begin{pmatrix} f_{d\phi} \\ f_{dq} \end{pmatrix} = \begin{pmatrix} r^* & 0 \\ 0 & g^* \end{pmatrix} \begin{pmatrix} e_{\phi} \\ e_q \end{pmatrix} \quad (2.75)$$

$$\begin{pmatrix} e_{b_0} \\ e_{b_1} \\ f_{b_0} \\ f_{b_1} \end{pmatrix} = \begin{pmatrix} 1 & 0 & 0 & 0 \\ 0 & 1 & 0 & 0 \\ 0 & 0 & 1 & 0 \\ 0 & 0 & 0 & 1 \end{pmatrix} \begin{pmatrix} e_q(t,0) \\ e_q(t,1) \\ e_\phi(t,0) \\ e_\phi(t,1) \end{pmatrix} \quad (2.76)$$

$b_0$  and  $b_1$  denote, respectively, the left and right boundary.

**Note :**

In terms of current and voltage, the transmission line with dissipation satisfies the following equation:

$$\frac{dH}{dt} = v(t,0)i(t,0) - v(t,1)i(t,1) - \int_{\Omega} [gv^2(t,x) + ri^2(t,x)] \quad (2.77)$$

where  $i(t,x) = * \frac{1}{l} \phi(t,x)$  and  $v(t,x) = * \frac{1}{c} q(t,x)$

### 2.4.3. Spatial discretization

For the dissipation case, we will carry out a separation of variables and we will use the Whitney forms which make it possible to preserve the properties of the p-forms at the time of a spatial discretization [Bos 91].

For linear interpolation of 0-forms to the whole space, we can use the linear interpolation basis. With each vertex  $v_i$  is associated a basis denoted as  $\varphi_i$ :

$$\varphi_i = 1 \quad \text{at } v_i, \quad \varphi_i = 0 \quad \text{at } v_j \neq v_i \quad (2.78)$$

while  $\varphi_i$  linearly goes to zero in the one-ring neighborhood of  $v_i$ . These functions are the *barycentric coordinates*, introduced by Möbius in 1827 as mass point to define a coordinate-free geometry.

If we denote a vertex  $v_j$  by  $\sigma_j$ , with this basis we have:

$$\int_{v_j} \varphi_{v_i} = \int_{\sigma_j} \varphi_{\sigma_i} = \int_{\sigma_j} \varphi_i = \begin{cases} 1 & \text{if } i = j \\ 0 & \text{if } i \neq j \end{cases} \quad (2.79)$$

For the 1-forms interpolation we use the *Whitney* 1-form associated with an edge  $\sigma_{ij}$  between  $v_i$  and  $v_j$ .

$$\varphi_{\sigma_{ij}} = \varphi_i d\varphi_j - \varphi_j d\varphi_i \quad (2.80)$$

We have:

$$\int_{\sigma_{kl}} \varphi_{\sigma_{ij}} = \begin{cases} 1 & \text{if } i = k \text{ and } j = l \\ -1 & \text{if } i = l \text{ and } j = k \\ 0 & \text{otherwise} \end{cases} \quad (2.81)$$

This is zero when at least one vertex is not on the edge. Along the edge  $\sigma_{ij}$ , we have  $\varphi_i + \varphi_j = 1$ . Thus:

$$\int_{\sigma_{ij}} \varphi_{\sigma_{ij}} = \int_{\varphi_i=1}^{\varphi_i=0} (\varphi_i d(1-\varphi_i) - (1-\varphi_i) d\varphi_i) = \int_{\varphi_i=1}^{\varphi_i=0} (-d\varphi_i) = 1 \quad (2.82)$$

Next we make the spatial discretization of the telegrapher's equations. The transmission line is split into  $m$  cells. Due to spatial compositionality (i.e. interconnection of two transmission lines via a common boundary once again gives a transmission line), we need to perform discretization to only one cell. That is to say the cell delimited by space  $\Omega_c = [\alpha, \beta]$ . One considers a cell (with the length  $(\beta-\alpha)$ ), and we denote the spatial manifold  $\Omega_c = [\alpha, \beta]$ .

We express the boundary variables as functions of the efforts:

$$\begin{aligned} e_{b\alpha}(t) &= e_q(t, \alpha) & e_{b\beta}(t) &= e_q(t, \beta) \\ f_{b\alpha}(t) &= e_\phi(t, \alpha) & f_{b\beta}(t) &= e_\phi(t, \beta) \end{aligned} \quad (2.83)$$

We consider the size of a sufficiently small cell, to be able to make the following approximations to represent flows inside the cell:

$$\begin{aligned} f_q(t, x) &\approx f_q^{\alpha\beta}(t) \cdot {}^1w_q(x) \\ f_\phi(t, x) &\approx f_\phi^{\alpha\beta}(t) \cdot {}^1w_\phi(x) \end{aligned} \quad (2.84)$$

where  ${}^1w_q, {}^1w_\phi \in \Lambda^1(\Omega_c)$  are the 1-form satisfying the conditions:

$$\int_{\Omega_c} {}^1w_q(x) = 1 \quad \text{and} \quad \int_{\Omega_c} {}^1w_\phi(x) = 1 \quad (2.85)$$

In the same way, the efforts  $e_q(t, x)$  and  $e_\phi(t, x)$ , inside the cell, are approximated by :

$$\begin{aligned} e_q(t, x) &= e_q^\alpha(t) \cdot w_q^\alpha(x) + e_q^\beta(t) \cdot w_q^\beta(x) \\ e_\phi(t, x) &= e_\phi^\alpha(t) \cdot w_\phi^\alpha(x) + e_\phi^\beta(t) \cdot w_\phi^\beta(x) \end{aligned} \quad (2.86)$$

where  $w_q^\alpha, w_q^\beta, w_\phi^\alpha, w_\phi^\beta \in \Lambda^0(\Omega_c)$  are the 0-forms satisfying the conditions:

$$\begin{aligned} w_q^\alpha(\alpha) &= 1 & w_q^\alpha(\beta) &= 0 & w_q^\beta(\alpha) &= 0 & w_q^\beta(\beta) &= 1 \\ w_\phi^\alpha(\alpha) &= 1 & w_\phi^\alpha(\beta) &= 0 & w_\phi^\beta(\alpha) &= 0 & w_\phi^\beta(\beta) &= 1 \end{aligned} \quad (2.87)$$

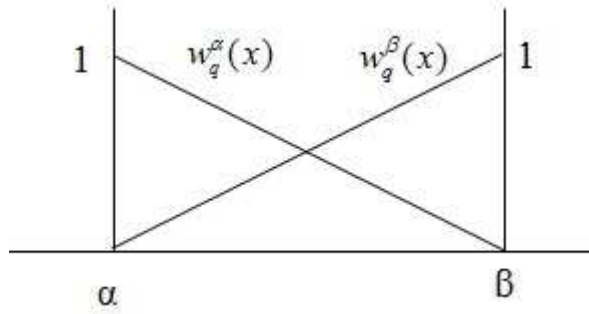


Fig. 2.5. A Whitney 0-form

This Whitney 0-form, as shown figure 2.5., makes it possible to have the following relations:

$$w_q^\alpha(x) + w_q^\beta(x) = 1 \quad \text{and} \quad w_\phi^\alpha(x) + w_\phi^\beta(x) = 1 \quad (2.88)$$

By substitution of (2.84) and (2.86) in (2.71) and by taking into account (2.75) we obtain:

$$\begin{aligned} f_\phi^{\alpha\beta}(t) \lrcorner w_\phi(x) &= -e_q^\alpha(t) dw_q^\alpha(x) - e_q^\beta(t) dw_q^\beta(x) \\ &\quad - r \left( e_\phi^\alpha(t) (*w_\phi^\alpha(x)) + e_\phi^\beta(t) (*w_\phi^\beta(x)) \right) \\ f_q^{\alpha\beta}(t) \lrcorner w_q(x) &= -e_\phi^\alpha(t) dw_\phi^\alpha(x) - e_\phi^\beta(t) dw_\phi^\beta(x) \\ &\quad - g \left( e_q^\alpha(t) (*w_q^\alpha(x)) + e_q^\beta(t) (*w_q^\beta(x)) \right) \end{aligned} \quad (2.89)$$

In order to determine the dynamic equations inside a cell, we integrate the equations above:

$$\begin{aligned}
f_\phi^{\alpha\beta}(t) \int_{\Omega_c} {}^1w_\phi(x) &= -e_q^\alpha(t) \int_{\Omega_c} dw_q^\alpha(x) - e_q^\beta(t) \int_{\Omega_c} dw_q^\beta(x) \\
&\quad - re_\phi^\alpha(t) \int_{\Omega_c} (*w_\phi^\alpha(x)) - re_\phi^\beta(t) \int_{\Omega_c} (*w_\phi^\beta(x)) \\
f_q^{\alpha\beta}(t) \int_{\Omega_c} {}^1w_q(x) &= -e_\phi^\alpha(t) \int_{\Omega_c} dw_\phi^\alpha(x) - e_\phi^\beta(t) \int_{\Omega_c} dw_\phi^\beta(x) \\
&\quad - ge_q^\alpha(t) \int_{\Omega_c} (*w_q^\alpha(x)) - ge_q^\beta(t) \int_{\Omega_c} (*w_q^\beta(x))
\end{aligned} \tag{2.90}$$

Using the relations (2.85) and the properties

$$\int_{\Omega} dw = \int_{\partial\Omega} w \quad \text{and} \quad (*w) = wdx \tag{2.91}$$

where  $w$  is a 0-form and  $(*w)$  is a 1-form,

$$w_\phi^\alpha = w_q^\alpha = \frac{x - \beta}{\alpha - \beta} \quad \text{and} \quad w_\phi^\beta = w_q^\beta = \frac{x - \alpha}{\beta - \alpha} \tag{2.92}$$

the Whitney 0-form leads to the following relations:

$$\begin{aligned}
f_\phi^{\alpha\beta}(t) &= e_q^\alpha(t) - e_q^\beta(t) - \frac{1}{2} r_{\alpha\beta} (e_\phi^\alpha(t) + e_\phi^\beta(t)) \\
f_q^{\alpha\beta}(t) &= e_\phi^\alpha(t) - e_\phi^\beta(t) - \frac{1}{2} g_{\alpha\beta} (e_q^\alpha(t) + e_q^\beta(t))
\end{aligned} \tag{2.93}$$

where  $r_{\alpha\beta} = r(\beta - \alpha)$  and  $g_{\alpha\beta} = g(\beta - \alpha)$ .

We arrive to the following spatial discretization representation of this typical cell:

$$\begin{pmatrix} f_{b\alpha}(t) \\ f_{b\beta}(t) \\ e_{b\alpha}(t) \\ e_{b\beta}(t) \\ f_\phi^{\alpha\beta}(t) \\ f_q^{\alpha\beta}(t) \end{pmatrix} = \begin{pmatrix} 1 & 0 & 0 & 0 \\ 0 & 1 & 0 & 0 \\ 0 & 0 & 1 & 0 \\ 0 & 0 & 0 & 1 \\ -.5r_{\alpha\beta} & -.5r_{\alpha\beta} & 1 & -1 \\ 1 & -1 & -.5g_{\alpha\beta} & -.5g_{\alpha\beta} \end{pmatrix} \begin{pmatrix} e_\phi^\alpha(t) \\ e_\phi^\beta(t) \\ e_q^\alpha(t) \\ e_q^\beta(t) \end{pmatrix} \tag{2.94}$$

It remains to check that this is a port Hamiltonian system corresponding to a cell which preserves the Dirac structure. This corresponds to an instantaneous conservation of the power (net power).

$$P_{\Omega_c} = \int_{\Omega_c} e_q \wedge f_q + \int_{\Omega_c} e_\phi \wedge f_\phi + \int_{\partial\Omega_c} e_b \wedge f_b \quad (2.95)$$

One replaces  $e_q(t, x)$ ,  $e_\phi(t, x)$ ,  $f_q(t, x)$  and  $f_\phi(t, x)$  by their approximations from (2.84) and (2.86) to obtain the following expression:

$$P_{\Omega_c} = \int_{\Omega_c} (e_q^\alpha w_q^\alpha + e_q^\beta w_q^\beta) f_q^{\alpha\beta} {}^1w_q + \int_{\Omega_c} (e_\phi^\alpha w_\phi^\alpha + e_\phi^\beta w_\phi^\beta) f_\phi^{\alpha\beta} {}^1w_\phi + e_{b\beta} f_{b\beta} - e_{b\alpha} f_{b\alpha} \quad (2.96)$$

or

$$P_{\Omega_c} = \left( e_q^\alpha \int_{\Omega_c} w_q^\alpha {}^1w_q + e_q^\beta \int_{\Omega_c} w_q^\beta {}^1w_q \right) f_q^{\alpha\beta} + \left( e_\phi^\alpha \int_{\Omega_c} w_\phi^\alpha {}^1w_\phi + e_\phi^\beta \int_{\Omega_c} w_\phi^\beta {}^1w_\phi \right) f_\phi^{\alpha\beta} + e_{b\beta} f_{b\beta} - e_{b\alpha} f_{b\alpha} \quad (2.97)$$

Before developing calculations, we establish initially some relations between the various 1-forms brought into play.

Combination of equations (2.89) and (2.93) gives :

$$\begin{aligned} (e_q^\alpha - e_q^\beta - \frac{1}{2} r_{\alpha\beta} (e_\phi^\alpha + e_\phi^\beta)) {}^1w_\phi &= -e_q^\alpha dw_q^\alpha - e_q^\beta dw_q^\beta - r (e_\phi^\alpha (*w_\phi^\alpha) + e_\phi^\beta (*w_\phi^\beta)) \\ (e_\phi^\alpha - e_\phi^\beta - \frac{1}{2} g_{\alpha\beta} (e_q^\alpha + e_q^\beta)) {}^1w_q &= -e_\phi^\alpha dw_\phi^\alpha - e_\phi^\beta dw_\phi^\beta - g (e_q^\alpha (*w_q^\alpha) + e_q^\beta (*w_q^\beta)) \end{aligned} \quad (2.98)$$

From them it results:

$$\begin{aligned} {}^1w_\phi &= -dw_q^\alpha = dw_q^\beta \\ {}^1w_q &= -dw_\phi^\alpha = dw_\phi^\beta \end{aligned} \quad (2.99)$$

In addition, the use of the Whitney forms enables us to have the following relation:

$${}^1w_q = w_q^\alpha dw_q^\beta - w_q^\beta dw_q^\alpha = w_q^\alpha {}^1w_\phi + w_q^\beta {}^1w_\phi = (w_q^\alpha + w_q^\beta) {}^1w_\phi = {}^1w_\phi \quad (2.100)$$

We take  $\gamma = \int_{\Omega_c} w_q^\alpha {}^1w_q$ , which leads to:

$$\begin{aligned}\int_{\Omega_c} w_q^{\beta 1} w_q &= 1 - \gamma \\ \int_{\Omega_c} w_\phi^{\alpha 1} w_\phi &= 1 - \gamma \\ \int_{\Omega_c} w_\phi^{\beta 1} w_\phi &= \gamma\end{aligned}\quad (2.101)$$

Indeed,

$$\begin{aligned}\int_{\Omega_c} w_q^{\alpha 1} w_q + \int_{\Omega_c} w_\phi^{\alpha 1} w_\phi &= -\int_{\Omega_c} w_q^\alpha dw_q^\alpha - \int_{\Omega_c} w_\phi^\alpha dw_\phi^\alpha = -\int_{\Omega_c} d(w_q^\alpha w_\phi^\alpha) \\ &= -(w_q^\alpha(\beta)w_\phi^\alpha(\beta) - w_q^\alpha(\alpha)w_\phi^\alpha(\alpha)) = 1\end{aligned}\quad (2.102)$$

The equation (2.97) becomes:

$$P_{\Omega_c} = (\gamma e_q^\alpha + (1 - \gamma)e_q^\beta) f_q^{\alpha\beta} + ((1 - \gamma)e_\phi^\alpha + \gamma e_\phi^\beta) f_\phi^{\alpha\beta} + e_{b\beta} f_{b\beta} - e_{b\alpha} f_{b\alpha} \quad (2.103)$$

We say that

$$\begin{aligned}e_{b\alpha} &= e_q^\alpha & e_{b\beta} &= e_q^\beta \\ f_{b\alpha} &= e_\phi^\alpha & f_{b\beta} &= e_\phi^\beta\end{aligned}\quad (2.104)$$

what makes it possible to write the equations (2.93) in the form:

$$\begin{aligned}f_\phi^{\alpha\beta}(t) &= e_{b\alpha} - e_{b\beta} - \frac{1}{2} r_{\alpha\beta} (f_{b\alpha} + f_{b\beta}) \\ f_q^{\alpha\beta}(t) &= f_{b\alpha} - f_{b\beta} - \frac{1}{2} g_{\alpha\beta} (e_{b\alpha} + e_{b\beta})\end{aligned}\quad (2.105)$$

For the efforts of the cell:

$$e_q^{\alpha\beta} = \gamma e_{b\alpha} + (1 - \gamma)e_{b\beta} \text{ et } e_\phi^{\alpha\beta} = (1 - \gamma)f_{b\alpha} + \gamma f_{b\beta} \quad (2.106)$$

the instantaneous power is written then:

$$P_{\Omega_c} = \langle e^{\alpha\beta} | f^{\alpha\beta} \rangle = e_q^{\alpha\beta} f_q^{\alpha\beta} + e_\phi^{\alpha\beta} f_\phi^{\alpha\beta} + e_{b\beta} f_{b\beta} - e_{b\alpha} f_{b\alpha} \quad (2.107)$$

where

$$\begin{aligned} e^{\alpha\beta} &= (e_\phi^{\alpha\beta} \quad e_q^{\alpha\beta} \quad e_{b\alpha} \quad e_{b\beta})^t \\ f^{\alpha\beta} &= (f_\phi^{\alpha\beta} \quad f_q^{\alpha\beta} \quad f_{b\alpha} \quad f_{b\beta}) \end{aligned} \quad (2.108)$$

From (2.105) and (2.106), it gives:

$$\underbrace{\begin{pmatrix} 1 & 0 & 0 & 0 \\ 0 & 1 & -\gamma & \gamma-1 \\ 0 & 0 & -1 & 1 \\ 0 & 0 & .5g_{\alpha\beta} & .5g_{\alpha\beta} \end{pmatrix}}_{F^{\alpha\beta}} \begin{pmatrix} e_\phi^{\alpha\beta} \\ e_q^{\alpha\beta} \\ e_{b\alpha} \\ e_{b\beta} \end{pmatrix} + \underbrace{\begin{pmatrix} 0 & 0 & \gamma-1 & -\gamma \\ 0 & 0 & 0 & 0 \\ 1 & 0 & .5r_{\alpha\beta} & .5r_{\alpha\beta} \\ 0 & 1 & -1 & 1 \end{pmatrix}}_{E^{\alpha\beta}} \begin{pmatrix} f_\phi^{\alpha\beta} \\ f_q^{\alpha\beta} \\ f_{b\alpha} \\ f_{b\beta} \end{pmatrix} = 0 \quad (2.109)$$

with  $\gamma=1/2$  in the case of the approximations of Whitney for the 0-forms and the 1-forms. We denote the space of admissible efforts by  $e$ , and the domain of admissible flows by  $f$ , such that the following relation is satisfied by:

$$D = \{(f, e) \in \mathbb{R}^4 : E^{\alpha\beta} e^{\alpha\beta} + F^{\alpha\beta} f^{\alpha\beta} = 0\} \quad (2.110)$$

$D$  is a Dirac structure with respect to the bilinear form if and only if the following two conditions are satisfied:

$$\text{rank} \begin{bmatrix} E^{\alpha\beta} & F^{\alpha\beta} \end{bmatrix} = 4 \quad E^{\alpha\beta} (F^{\alpha\beta})^t + F^{\alpha\beta} (E^{\alpha\beta})^t = 0 \quad (2.111)$$

After computation we show that this is true and the two conditions are satisfied.

#### 2.4.4. Constitutive equations

To complete calculations, we will determine the expressions of the charge  $q_{\alpha\beta}(t)$  and the magnetic flux  $\phi_{\alpha\beta}(t)$  and their variations on the cell level.

$$\begin{aligned}\phi(t, x) &= \phi_{\alpha\beta}(t) {}^1w(x) \\ q(t, x) &= q_{\alpha\beta}(t) {}^1w(x)\end{aligned}\tag{2.112}$$

The total energy of the cell is given by

$$\begin{aligned}h_{\alpha\beta}(\phi_{\alpha\beta}, q_{\alpha\beta}) &= \int_{\Omega_c} \frac{1}{2c} q_{\alpha\beta} {}^1w \wedge q_{\alpha\beta} (*^1w) + \int_{\Omega_c} \frac{1}{2l} \phi_{\alpha\beta} {}^1w \wedge \phi_{\alpha\beta} (*^1w) \\ &= \left( \frac{\phi_{\alpha\beta}^2(t)}{2l} + \frac{q_{\alpha\beta}^2(t)}{2c} \right) \int_{\Omega_c} {}^1w \wedge (*^1w) \\ &= \frac{\phi_{\alpha\beta}^2(t)}{2l_{\alpha\beta}} + \frac{q_{\alpha\beta}^2(t)}{2c_{\alpha\beta}}\end{aligned}\tag{2.113}$$

with

$$l_{\alpha\beta} = \frac{l}{\int_{\Omega_c} {}^1w \wedge (*^1w)} = l(\beta - \alpha)\tag{2.114}$$

and

$$c_{\alpha\beta} = \frac{c}{\int_{\Omega_c} {}^1w \wedge (*^1w)} = c(\beta - \alpha)\tag{2.115}$$

In addition, we have the following bonds:

$$\frac{\partial q(t, x)}{\partial t} = \frac{dq_{\alpha\beta}}{dt} {}^1w(x) = f_q^{\alpha\beta}(t) {}^1w(x)\tag{2.116}$$

Then

$$\begin{aligned}\frac{dq_{\alpha\beta}}{dt} &= f_q^{\alpha\beta}(t) \\ \frac{d\phi_{\alpha\beta}}{dt} &= f_\phi^{\alpha\beta}(t)\end{aligned}\tag{2.117}$$

$$\begin{aligned}
 e_q^{\alpha\beta}(t) &= \frac{\partial h_{\alpha\beta}}{\partial q} = \frac{q_{\alpha\beta}}{c_{\alpha\beta}} \\
 e_\phi^{\alpha\beta}(t) &= \frac{\partial h_{\alpha\beta}}{\partial \phi} = \frac{\phi_{\alpha\beta}}{l_{\alpha\beta}}
 \end{aligned}
 \tag{2.118}$$

and from equation (2.106) we have :

$$\begin{aligned}
 e_q^{\alpha\beta} &= \frac{1}{2}(e_{b\alpha} + e_{b\beta}) \\
 e_\phi^{\alpha\beta} &= \frac{1}{2}(f_{b\alpha} + f_{b\beta})
 \end{aligned}
 \tag{2.119}$$

The dynamics of the cell are given then by:

$$\begin{aligned}
 \frac{d\phi_{\alpha\beta}}{dt} &= e_{b\alpha} - e_{b\beta} - r_{\alpha\beta} \frac{\phi_{\alpha\beta}}{l_{\alpha\beta}} \\
 \frac{dq_{\alpha\beta}}{dt} &= f_{b\alpha} - f_{b\beta} - g_{\alpha\beta} \frac{q_{\alpha\beta}}{c_{\alpha\beta}}
 \end{aligned}
 \tag{2.120}$$

The electrical representation of the transmission line at element level is presented in the next figure.

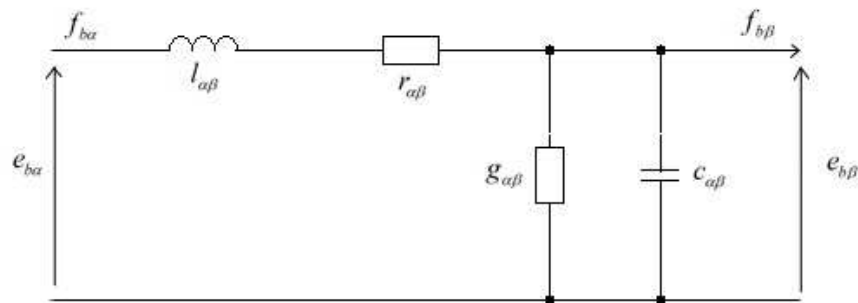


Fig.2.6. Elementary components representation of the transmission line

The corresponding bond graph representation [Nak 03] is the following :

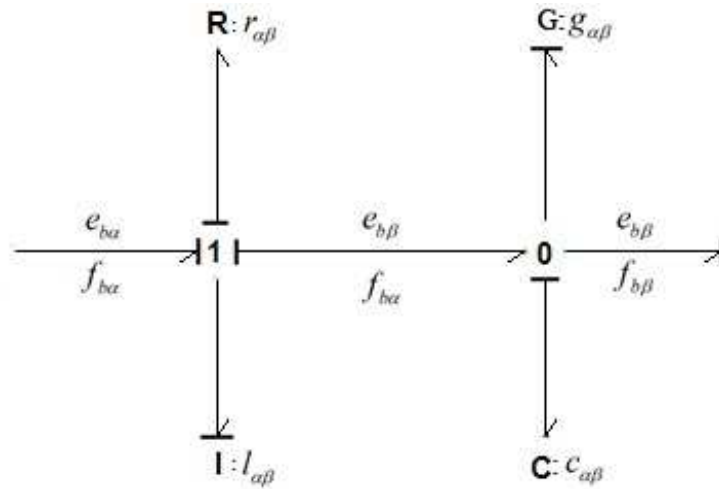


Fig.2.7. Bond Graph representation

It is known that the connection of two Dirac structures gives a Dirac structure. Thus the whole transmission line can be reconstructed by the connection of a fixed number of cells in advance.

## 2.5. Conclusion

The port Hamiltonian system has been used in the representation of the distributed parameter systems. Through the example of the telegrapher's equation, we have shown [Che 09] that using a special form of discretization for the space we made the calculation only on one element, considered as local and then concatenating the elements we can calculate the entire line of transmission.

The port Hamiltonian system is derived from the energy function (Hamiltonian), which is usually a good Lyapunov function, used in control.

## **Chapter 3.**

# **Traffic flow models**



## Contents

<b>Chapter 3. Traffic flow models</b> .....	91
3.1. Introduction .....	95
3.2. Model classification.....	97
3.3. Microscopic and mesoscopic models .....	98
3.3. Macroscopic models.....	99
3.4. Numerical methods.....	110
3.5. Implementation .....	114
3.5.1. Riemann problem in the LWR model.....	114
3.5.2. Influence of the choice of a numerical method on LWR model.....	115
3.5.3. Comparison of 1-equation model and 2-equation models	116
3.5.4. Comparison of LWR and Jiang models .....	118
3.6. Conclusions.....	120



## Chapter 3. Traffic flow models

### 3.1. Introduction

*“Because of congestion, there is a serious risk that Europe will lose economic competitiveness. The most recent study on the subject showed that the external costs of road traffic congestion alone amount to 0,5% of Community GDP. Traffic forecasts for the next 10 years show that if nothing is done, road congestion will increase significantly by 2010. The costs attributable to congestion will also increase by 142% to reach 80 billion a year, which is approximately 1% of Community GDP.” [Pap 03]*

In the context of economic globalization the need of circulation for goods and peoples has known a new growth. This growth in mobility is the principal cause for apparition of congestions.

The delays caused by congestions have an important impact over capacity of people life. The driver which is in a congestion has problems of stress, noise etc, driving to a growth of accident chance. This thing may be considered as an indirect cost (health problems). The congestions involve big losses of combustible. Hereby, in the world context, when the combustible price is higher and higher, this means a decrease of buying capacity. From ecological point of view, the congestions have a negative effect because they lead to a growth of

pollutions caused by the exhaust gases, which involves an exponential growth of economical and ecological costs.

The traffic congestion problems are socio-economical problems that need a solution which can be fast put into effect. The fastest and most easily is to build new infrastructures that are very expensive and reduce the available environmental space. Another solution for congestion decrease is to encourage the people to use public traffic infrastructure and to use train and ship for goods transport. But for doing this we need to ensure the way for train or ship. These imply also expensive costs.

Traffic flow theories try to describe in a mathematical way the flow theory for a better and a more easily way of understanding, using the interactions between the vehicles and their operators (mobile components and infrastructure). The infrastructure consists in all the highway system and its operational elements: signage, control devices, markings, etc.

All these theories lead to models and tools used in the design and operation of streets and highways. First study of traffic flow was made in the 1930's with the application of probability theory to the description of road traffic by Adams [Ada 36]. Also, Bruce D. Greenshields at the Yale Bureau of Highway Traffic studied the models relating volume and speed [Gre 35] and investigation of performance of traffic at intersections [Gre 47].

In the 50's theoretical developments based on a variety of approaches, such as car-following, traffic wave theory (hydrodynamic analogy) and queuing theory was developed. Between them we can include the works made by Wardrop [Wan 52], Pipes [Pip 53], Lighthill and Whitham [Lig 55], Richards [Ric 56], Chandler et al. [Cha 58].

In the 70's another approach had been introduced, considering the analogy with the fluid flow in fluid mechanics in Payne [Pay 71], Whitham [Whi 74].

In the last decades the domain knew a vast development, the authors trying to improve the existent models as Aw and Rascle [Aw 00], Zhang [Zha 02], Goatin [Goa 06], or to propose other models that are suitable for the new demands of the traffic as Zhang [Zha 98], Colombo [Col 02].

In this chapter we will present a classification of the models used in traffic flow representation followed by a short presentation of the principal schemes used in numerical simulation, and some results.

### ***3.2. Model classification***

The traffic models can be classified in function of some factors as: detail level, independent variables type, application scale, and processes representation [Hoo 01].

The detail level classification is a classification viewed from the level of the information about the vehicle where we are interested to arrive.

From a detail level point of view the models can be group as:

- *submicroscopic* models which describe the space-time behavior of each vehicle and their driver at the individual level and also the functioning of specific parts of the vehicle.

- *microscopic* models which describe also the space-time behavior of the vehicle and the drivers at the individual level.

- *mesoscopic* models which describe the behavior of individuals represented by groups of traffic entities, the activities and interactions of which are described at a low detail level. Some mesoscopic models are analog to the models used in gas-kinetic theory.

- *macroscopic* models are models where the traffic flow is seen as a flow without distinguishing its constituent parts. For the representation are used the flow-rate, density and velocity, and the

models can be classified according to the number of partial differential equations on the one hand and the order on the other hand.

When we want to simulate the traffic flow we must be aware that we have different conditions when we talk about a simulation of a highway or of an entire city. Thus, we must take in account the application scale which will be used: a lane, a highway, a city etc.

Usually, the traffic models describe dynamical systems. Thus, we can have: *continuous* models or *discrete* models in function of the moment when changes appear in the traffic system state.

In the suite we will make a short presentation of the microscopic and mesoscopic models then we will present the macroscopic models which are interesting for us.

### ***3.3. Microscopic and mesoscopic models***

The microscopic models are the models that arrive at a high level of detail for the vehicles, taking in account the vehicles as separable entities, their compartment in time and space and the interactions between them.

The first direction in research used the so-called follow the leader models. In this category we can include the safe-distance models developed by Pipes [Pip 53], Forbes [For 58], Pignataro [Pig 73], Leutzbach [Leu 88], Jespen [Jes 98], Dijkstra [Dij 98] and the stimulus-response car-following models developed by Chandler [Cha 58], Gazis [Gaz 61], Montroll [Mon 61], Payne [Pay 71].

Another directions used the cellular automata models developed by Nagel [Nag 1996], [Nag 98], Wu and Brilon [Wu 99], Esser [Ess 99] and the particle models developed by Eastwood [Eas 88], Van Aerde [Aer 94], Hoogendoorn and Bovy [Hoo 00].

The mesoscopic flow models describe the compartment of the vehicles in an aggregate-term using the probability distribution functions by example.

The most known models used to model the traffic flow at this level of detail are the headway distribution models developed by Buckley [Buc 68], Branston [Bra 76], Hoogendoorn and Bovy [Hoo 98], the cluster models developed by Prigogine [Pri 61], Prigogine and Herman [Pri 71], Botma [Bot 78] and the gas-kinetic continuum models developed by Prigogine and Herman [Pri 71], Paveri-Fontana [Pav 75], Nelson [Nel 95], Helbing [Hel 97], Klar and Wegener [Kla 98], Hoogendoorn and Bovy [Hoo 00].

### 3.3. Macroscopic models

The macroscopic traffic flow models are designed in a similar way to flow models of continuous media (fluid or gases) and use as macroscopic variables: density, velocity and vehicle flow.

The dynamics of the system are represented using partial differential equations (PDE). The independent variables of a continuous macroscopic flow model are location  $x$  and time instant  $t$ .

Consider a segment of highway  $[x, x + dx)$ . Density  $\rho = \rho(x, t)$  represents the expected number of vehicles on the roadway segment  $[x, x + dx)$  per unit length at instant  $t$ , the flow  $q = q(x, t)$  represents the expected number of vehicles flowing past  $x$  during  $[t, t + dt)$  per time unit and the velocity  $v = v(x, t)$  represents the expected velocity of the vehicles.

First model of traffic flow was proposed by Lighthill and Whitham [Lig 55] and Richards [Ric 56] (LWR).

Consider a section of highway between  $x_1$  and  $x_2$  ( $x_2 > x_1$ ). At time  $t$  the density on this section will be  $\rho(x, t)$ . The traffic flows that

enter into the section will be at a rate of  $q(x_1, t)$  and the flow that exits will be at a rate of  $q(x_2, t)$ .

If one supposes that it is a highway without entrances and exits, the number of vehicles must be conserved between  $x_1$  and  $x_2$  at any time  $t$ .

$$\frac{\partial}{\partial t} \int_{x_1}^{x_2} \rho(x, t) dx + q(x_2, t) - q(x_1, t) = 0 \quad (3.1)$$

LWR model also assumes for a homogenous highway:

$$q(x, t) = Q(\rho(x, t)) \quad (3.2)$$

where  $Q$  is a differentiable nonnegative function, that is zero if  $\rho = 0$  or  $\rho = \rho_{\max}$ . This is assumed to be true when flow and density vary with  $x$  and/or  $t$ .

Eq. (3.1) can be equivalently expressed as:

$$\frac{\partial \rho}{\partial t} + \frac{\partial q}{\partial x} = 0 \quad (3.3)$$

If  $\rho$  has a jump discontinuity at  $(x, t)$ , eq (3.3) is not more true, but the conservation principle still applies. At discontinuities a special kind of traffic waves appears and they are called shock waves (red light, accident). Because of them the solution of (3.3) has to be expanded to include the so-called weak solution. This is a function  $(\rho, q)(x, t)$  that is the solution of equation (3.3) everywhere except on a path  $x(t)$  where  $(\rho, q)(x, t)$  are discontinuous, but the integral form of the conservation law is respected.

The velocity of the jump,  $u$ , is:

$$u = [q] / [\rho] = [Q(\rho)] / [\rho] \quad (3.4)$$

where brackets denote the change in the enclosed variable across the discontinuity. Eq. (3.4) is also known as the Rankine-Hugoniot condition [LeV 92].

On substituting (3.2) into (3.3) we obtain a single quasilinear partial differential equation in  $\rho$ :

$$\frac{\partial \rho}{\partial t} + \frac{dQ(\rho)}{d\rho} \frac{\partial \rho}{\partial x} = 0 \quad (3.5)$$

which taken together with (3.4) defines the evolution of traffic flow over a specific road section, given a suitable set of initial/boundary conditions.

The LWR model assumes that the velocity depends only on the density:

$$v(\rho) = \left(1 - \frac{\rho}{\rho_{\max}}\right) V_{\max} \quad (3.6)$$

where  $V_{\max}$  is the maximal speed.

The corresponding fundamental diagram in the plane  $(\rho, \rho v)$  is in the figure 3.1. When there are not vehicles on the road the flow is equal to zero. It becomes to grow with density, but with a slower slope, until it arrives to the maximal flow. Starting from here the flow begins to decrease when the density grows. Continue until becomes zero at the maximal density, situation where the traffic is stopped because of congestion and the velocity is zero.

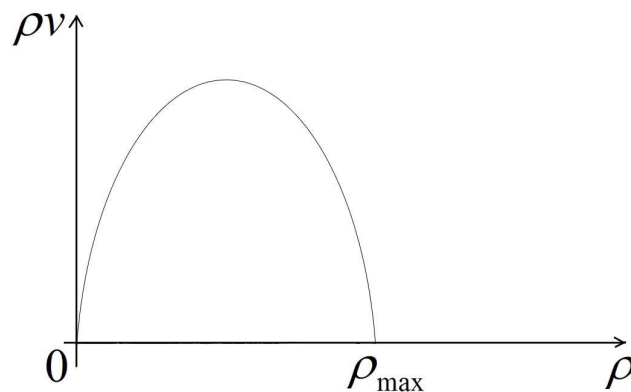


Fig.3.1. The fundamental diagram

Nevertheless, this diagram does not qualitatively match experimental data observed by Kerner [Ker 00], and presented below.

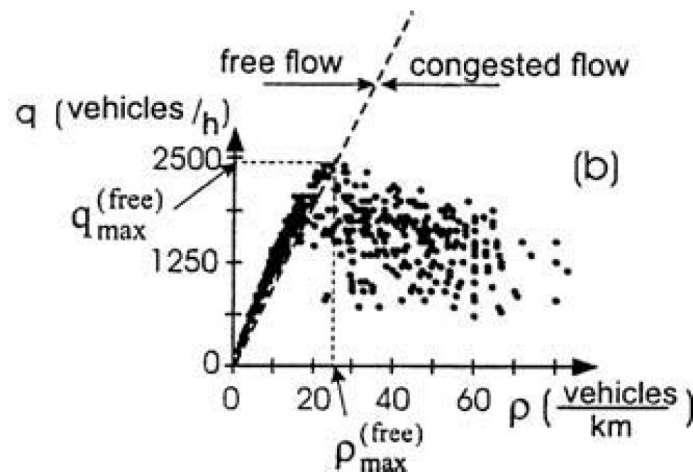


Fig.3.2. Experimental data [Ker 00]

When we have a light traffic and the passing is allowed, the queue of vehicle disperses from the front and back in a way that it is not predicted by the LWR theory. This comes from the fact that the LWR model does not take in consideration that there is a distribution of desired velocities across vehicles, in addition to a variation of the desired velocity for each vehicle.

When the passing is restricted, the LWR model has better results but also has some deficiencies related to the velocity of vehicle when passes through a shock, predicting an instantaneously speed change, and does not predict instabilities of the stop-and-go type.

To solve these problems, two directions have been followed. One in the kinetic theory with the capturing of dispersion effects by incorporating a velocity distribution and one that tried to describe what happening inside a shock using a high-order refinement of the LWR model.

Payne [Pay 71] and Whitham [Whi 74] used the second approach and considered the traffic flow as fluid flow in fluid mechanics.

Payne [Pay 71] proposed the continuum traffic flow model by a coupled system of two partial differential equations. He extended the LWR model by a partial differential equation describing the dynamics of the velocity  $v$ .

$$\frac{\partial v}{\partial t} + v \frac{\partial v}{\partial x} = (V_e(\rho) - v) / \tau - (c_0^2 / \rho) \frac{\partial \rho}{\partial x} \quad (3.7)$$

where  $c_0^2 = \zeta / \tau > 0$  is the anticipation constant, with  $\zeta = -dV_e/d\rho$ .

The second term of the left part, describing the changes due to inflowing and out flowing vehicles is the convection term. The first term of the right part describing the tendency of traffic flow to relax to an equilibrium velocity is the relaxation term and the second term of the right part, describing the drivers' anticipation on spatially changing traffic conditions downstream is the anticipation term.

But this approach is not realistic because there are essential differences between traffic and fluids. In the traffic flow a car is an anisotropic particle that responds to front stimuli, and in the fluid case a fluid particle responds to stimuli from the front and from behind. The traffic shock only encompasses a few vehicles, and in the traffic flow the vehicle, unlike molecules, have personalities that remain unchanged by motion.

Zhang [Zha 98] proposed another model starting from PW model, where only one term was different. The sound speed  $c_0$  in the PW model was replaced by  $c(\rho) = \rho V_e'(\rho)$ :

$$\frac{\partial v}{\partial t} + v \frac{\partial v}{\partial x} + \frac{c^2(\rho)}{\rho} \frac{\partial \rho}{\partial x} = \frac{V_e(\rho) - v}{\tau} \quad (3.8)$$

The model does not solve all the problems, but the effects if the gas-like behavior decays exponentially at a rate of  $\exp(-t/\tau)$ .

We write the equation in the vector form:

$$\frac{\partial U}{\partial t} + A(U) \frac{\partial U}{\partial x} = s(U) \quad (3.9)$$

where  $A$  is the Jacobian matrix and the eigenvalues of the  $A$  control the properties of the system.

We consider the PW-like model which has the same properties as Zhang model:

$$U = \begin{pmatrix} \rho \\ v \end{pmatrix} \quad A(U) = \begin{pmatrix} v & \rho \\ \frac{c^2(\rho)}{\rho} & v \end{pmatrix} \quad s(U) = (0, (V_e(\rho) - v)/\tau)^T \quad (3.10)$$

The eigenvalues are  $\lambda_1 = v + c(\rho)$  and  $\lambda_2 = v - c(\rho)$ . From  $\lambda_1 < \lambda_2$  results that the model is strictly hyperbolic which means that the information travel at finite speeds, and discontinuities or shocks in the state variable  $U$  arise in the solution under certain conditions.

As we can see the second eigenvalue  $\lambda_2$  is larger than  $v$  because  $c(\rho) < 0$ . This means that the waves associated with second characteristic reach vehicles from behind. This is not what one would expect to see in real traffic.

This is a gas-like traffic behavior; to solve the problem of the characteristic speed that exceeds vehicle speed, Zhang replaced  $c^2(\rho)/\rho$  by zero in the Jacobian matrix.

The new model proposed [Zha 02] is:

$$\frac{\partial v}{\partial t} + v \frac{\partial v}{\partial x} = -c(\rho) \frac{\partial v}{\partial x} \quad (3.11)$$

where  $c(\rho) = \rho V_e'(\rho)$  is the traffic sound at which the traffic disturbance are propagated relative to a moving traffic stream.

Now we can write the non-equilibrium traffic model in a vector form

$$\frac{\partial}{\partial t} \begin{pmatrix} \rho \\ v \end{pmatrix} + \begin{pmatrix} v & \rho \\ 0 & v + c(\rho) \end{pmatrix} \frac{\partial}{\partial x} \begin{pmatrix} \rho \\ v \end{pmatrix} = 0 \quad (3.12)$$

The eigenvalues of the flux Jacobian matrix are

$$\begin{aligned} \lambda_1 &= v + \rho V_e'(\rho) \\ \lambda_2 &= v \end{aligned} \quad (3.13)$$

We have  $\lambda_1 < \lambda_2$  and the eigenvectors

$$r_1 = \begin{pmatrix} 1 \\ V_e'(\rho) \end{pmatrix} \quad r_2 = \begin{pmatrix} 1 \\ 0 \end{pmatrix} \quad (3.14)$$

The model is strictly hyperbolic. The characteristics speed maximum is equal or smaller than traffic speed.

The first “second order” model proposed by Payne [Pay 71] and Whitham [Whi 74], was corrected by Aw and Rascle [Aw 00] replacing in the momentum equation, the space derivative of “pressure” by the convective derivative  $\frac{\partial}{\partial t} + v \frac{\partial}{\partial x}$ .

$$\begin{aligned} \frac{\partial \rho}{\partial t} + \frac{\partial(\rho v)}{\partial x} &= 0 \\ \frac{\partial}{\partial t}(v + p(\rho)) + v \frac{\partial}{\partial x}(v + p(\rho)) &= 0 \end{aligned} \quad (3.15)$$

where  $p$  is a smooth increasing function with the prototype:

$$p(\rho) = \rho^\gamma, \quad \gamma > 0 \quad (3.16)$$

If we set  $U := (\rho, v)$ , we can write the conservative form as:

$$\frac{\partial}{\partial t} U + A(U) \frac{\partial}{\partial x} U = 0 \quad (3.17)$$

where

$$A(U) = \begin{pmatrix} v & \rho \\ 0 & v - \rho p'(\rho) \end{pmatrix} \quad (3.18)$$

The eigenvalues are:

$$\lambda_1 = v - \rho p'(\rho) \leq \lambda_2 = v \quad (3.19)$$

The eigenvectors are:

$$r^1 = \begin{pmatrix} 1 \\ -p'(\rho) \end{pmatrix} \quad r^2 = \begin{pmatrix} 1 \\ 0 \end{pmatrix} \quad (3.20)$$

But this model has a problem near the vacuum; when the density is close to zero, the solution does not depend continuously on the initial data. Another problem arises when the road is empty. The maximal speed reached by vehicles depends on the initial data, which is wrong.

In [Col 02], there is proposed a traffic flow model described by:

$$\begin{cases} (\rho, q) \in \Lambda_{free} \\ \frac{\partial \rho}{\partial t} + \frac{\partial}{\partial x}(\rho \cdot v_f(\rho)) = 0 \\ v_f(\rho) = \left(1 - \frac{\rho}{\rho_{max}}\right) \cdot V \end{cases} \quad (3.21)$$

and

$$\begin{cases} (\rho, q) \in \Lambda_{cong} \\ \frac{\partial \rho}{\partial t} + \frac{\partial}{\partial x} (\rho \cdot v_c(\rho, q)) = 0 \\ \frac{\partial q}{\partial t} + \frac{\partial}{\partial x} [(q - Q) \cdot v_c(\rho, q)] = 0 \\ v_c(\rho, q) = \left(1 - \frac{\rho}{\rho_{max}}\right) \cdot \frac{q}{\rho} \end{cases} \quad (3.22)$$

where  $\rho$  is the vehicle density,  $v$  is the car speed,  $q$  is a weighted flow,  $\rho_{max}$  and  $V$  are respectively the maximal vehicle density and speed and  $Q$  is the weighted flow at the equilibrium value.

The set  $\Lambda_{cong}$  and  $\Lambda_{free}$  are defined by

$$\Lambda_{free} = \{(\rho, q) \in [0, \rho_{max}] \times [0, +\infty[ : v_f(\rho) \geq V_f, q = \rho \cdot V\} \quad (3.23)$$

$$\Lambda_{cong} = \left\{ (\rho, q) \in [0, \rho_{max}] \times [0, +\infty[ : v_c(\rho) \leq V_c, \frac{Q^- - Q}{\rho_{max}} \leq \frac{q - Q}{\rho} \leq \frac{Q^+ - Q}{\rho_{max}} \right\}$$

where  $V_f < V$  and  $V_c < V$  are threshold speed constants and the parameters  $Q^- \in ]0, Q[, Q^+ \in ]Q, +\infty[$  depend on environmental conditions.

If we assume that the following conditions are satisfied:

$$\begin{aligned} 0 < V_c < V_f < V \\ 0 < Q^- \leq Q \leq Q^+ \\ \frac{Q^+ - Q}{\rho_{max} V} < 1 \end{aligned} \quad (3.24)$$

$$V_f = \frac{V - Q^+ / \rho_{max}}{1 - (Q^+ - Q) / (\rho_{max} V)}$$

$$\left(1 - \frac{Q^+}{\rho_{max} V}\right) \cdot \left(\frac{Q^+}{Q} - 1\right) < 1$$

the model is a model where the vehicles may have only positive speed, the density at a red traffic light is the maximum possible and the vehicles stop only at maximum density.

When there is a light traffic the solution to the Riemann problem is quantitative different of the LWR model, in this case we have a phase-

transition wave followed by a rarefaction wave instead of only a single shock wave in the LWR case.

To solve the problems of the Aw and Rascle [Aw 00] model, Goatin [Goa 06] proposed to couple the AR model with the LWR equation, by introducing a transition dynamics from free to congested flow.

For the free flow:

$$\begin{aligned} (\rho, v) &\in \Lambda_f \\ \frac{\partial \rho}{\partial t} + \frac{\partial(\rho v)}{\partial x} &= 0 \\ v &= v_f(\rho) \end{aligned} \quad (3.25)$$

For the free phase there is only one independent variable, the density  $\rho$ . The velocity  $v_f$  is a function of  $\rho$  and is chosen to be a linear function:

$$v_f(\rho) = \left(1 - \frac{\rho}{\rho_{\max}}\right) V_{\max} \quad (3.26)$$

For the congested flow:

$$\begin{aligned} (\rho, v) &\in \Lambda_c \\ \begin{cases} \frac{\partial \rho}{\partial t} + \frac{\partial(\rho v)}{\partial x} = 0 \\ \frac{\partial(\rho(v + p(\rho)))}{\partial t} + \frac{\partial(\rho v(v + p(\rho)))}{\partial x} = 0 \end{cases} & \\ p(\rho) &= V_{ref} \ln(\rho / \rho_{\max}) \end{aligned} \quad (3.27)$$

For the congested phase we have two variables: density  $\rho$  and velocity  $v$ , or the conservative variables  $\rho$  and  $z = \rho v + \rho p(\rho)$ . Function  $p$  represents the driver reactions to the state of traffic in front of him.

Starting from the fact that it is impossible to have a queue form on a highway if you don't have cars, it is possible to assume that if the initial

data are in the free flow zone or in the congested zone, solution will remain there. Two domains result:

$$\begin{aligned}\Omega_{free} &= \{(\rho, v) \in [0, R_{free}] \times [V_{free}, V] : v = v_f(\rho)\}; \\ \Omega_{cong} &= \{(\rho, v) \in [0, R] \times [0, V_{cong}] : p(r) \leq v + p(\rho) \leq p(R)\}\end{aligned}\quad (3.28)$$

where  $V > V_{free} > V_{cong}$ . The parameter  $r \in ]0, R[$  represents the dimension of the congested region.  $R_{free}$  is the maximal density in the free-flow region must satisfy:

$$V_{free} + p(R_{free}) = p(R) \quad (3.29)$$

To have this condition, must be assumed that

$$V_{ref} < V \quad (3.30)$$

In this model the vehicles may have only positive speed, but the density at a red traffic light is not the maximum possible and the vehicle don't stop only at maximum density.

Jiang [Jia 02] proposed an anisotropic macroscopic continuum model which consists in two partial differential equations as follows:

$$\frac{\partial \rho}{\partial t} + \frac{\partial(\rho v)}{\partial x} = 0 \quad (3.31)$$

$$\frac{\partial v}{\partial t} + v \frac{\partial v}{\partial x} = \frac{V_e(\rho) - v}{\tau} + c_0 \frac{\partial v}{\partial x} \quad (3.32)$$

where  $v$  denotes the average vehicle velocity,  $\rho$  is the vehicle density. The right-hand side of the velocity eq. (3.32) contains a relaxation term reflecting the process when the driver adjusts the speed of vehicle to the equilibrium velocity  $V_e(\rho)$  in the relaxation time interval  $\tau$ , and an anticipation term representing the process when the driver reacts to the traffic ahead with the propagation speed of small disturbance  $c_0$ .

If we write the eq. (3.31) and (3.32) as

$$\frac{\partial U}{\partial t} + A \frac{\partial U}{\partial x} = E \quad (3.33)$$

with

$$U = \begin{pmatrix} \rho \\ v \end{pmatrix}, \quad A = \begin{pmatrix} v & \rho \\ 0 & v - c_0 \end{pmatrix}, \quad E = \begin{pmatrix} 0 \\ (V(\rho) - v) / \tau \end{pmatrix} \quad (3.34)$$

The eigenvalues of the matrix  $A$  are derived from:

$$\det|A - \lambda I| = 0 \quad (3.35)$$

where  $I$  is the identity matrix. We have  $\lambda_1 = v$ ,  $\lambda_2 = v - c_0$ . Since  $c_0 \geq 0$ , it follows that the characteristic speed  $dx/dt$  are always less than or equal to the macroscopic flow velocity  $v$ , which demonstrates the fundamental principle that vehicle flows are anisotropic and responded only to front stimuli.

In the process of modeling traffic flow, it is important to take in consideration also some important components of the road. We must study very carefully what happens at the intersection, looking from both possible situations: having a merge or a diverge. The problem of the merge has been studied by Daganzo [Dag 95], Holden and Risebro [Hol 95] and Lebacque [Leb 96]. In their model, Holden and Risebro have studied the traffic through a merge by an optimization problem. Daganzo and Lebacque based their models on locally supply and demand.

Starting from the LWR model, which analyzes the traffic evolution using the variables:  $\rho, v, q$ , and which in discrete representation used in numerical methods cut the road in equal segments named cells, Lebacque [Leb 96] and Daganzo [Dag 95] have developed a new method used to solve the problems which appear in this representation. In the LWR model, the number of the cars inside one cell is equal to the number of cars that enter minus the number of the cars that exit from this cell; in the Daganzo model the terms of sending flow and receiving flow are used. Lebacque [Leb 96] is the first who used the terms “supply” and “demand”. “The supply” is the flow rate when the traffic condition is overcritical and the flow capacity of the cell when is under-critical; “the

demand" is the flow capacity when the traffic condition is overcritical and its flow rate when is under critical.

To solve the boundary problem they used either the solution of the Riemann problem at the boundary or the demand-supply method where it calculates the supply and the demand for each cell, then chooses the minimum between them as boundary flow.

Daganzo added a condition to this method: because the outflow is smaller than or equal to the demand and the entrance flow is smaller or equal than supply, the total inflow is equal to the minimum between the sum of the outflows and the supply of the cell. So, what must be done is to assure a distribution of the flow for all the upstream cells. The attribution scheme of distribution functions is called the distribution scheme.

Lebacque proposed another modality. He considered that the supply of a downstream cell is distributed as virtual supply to the upstream cells. The outflows of these cells are equal to the minimum between the demand and the virtual supply, and the inflow in the downstream cell is equal with the outflows sum.

But to choose the appropriate distribution function, it must take into consideration some factors. Daganzo [Dag 95] and Lebacque [Leb 96] suggested considering: these to be proportional with the number of lane (Lebacque); to introduce priority and to consider that the upstream cells are priorities (Daganzo).

### ***3.4. Numerical methods***

In the belief that the behavior of freeway traffic at a given point in time-space is only affected by the state of the system in a neighborhood of that point, some researchers have examined the possibility of representing traffic phenomena by partial differential equations (PDEs).

One method to solve the LWR problem is to use the method of characteristics. The characteristics are curves in the plane space-time that start from one point where the initial conditions are known, with the property that the density along the curves does not change if  $\rho(x, t)$  is perturbed at any point not on the curves. The characteristic curves cannot intersect as result from definition. If they meet they must terminate at the meeting point, where a shock arises.

For the LWR model when the initial/boundary conditions are well-posed a family of characteristic curves exists and every point not on a shock is reached from exactly one characteristic that extends backward in time to some initial boundary point. The characteristic curves, define the path of disturbance, because any modification that appear at any point it must propagate only on characteristic that passes through that point.

The solution can be obtain for a special kind of problem called Riemann problem which implies two constant density separated by a jump [LeV 92].

$$\rho(x, t = 0) = \begin{cases} \rho_l & x < 0 \\ \rho_r & x > 0 \end{cases} \quad (3.36)$$

The solution of the Riemann problem can be either a shock, when it is a density growing (fig. 3.3):

$$\rho(x, t) = \begin{cases} \rho_l & x < st \\ \rho_r & x > st \end{cases} \quad (3.37)$$

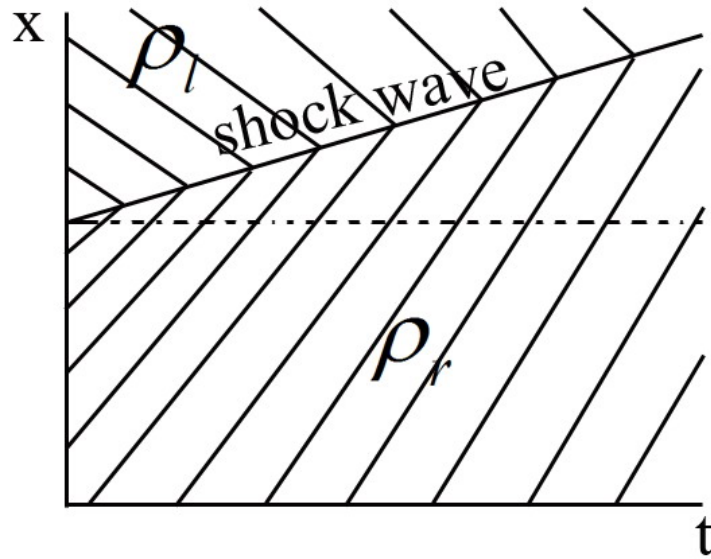


Fig.3.3. Shock wave

or a rarefaction wave, when the density profile decreases. The characteristics of the initial state are divergent, so we have a number of solutions, and the physical one is chosen using the entropy criterion, which in the traffic flow corresponds to a range of characteristics (fig. 3.4).

$$\rho(x,t) = \begin{cases} \rho_l & x < c_l t \\ (q')^{-1}\left(\frac{x}{t}\right) & c_l t \leq x \leq c_r t \\ \rho_r & x > c_r t \end{cases} \quad (3.38)$$

where  $c_{r,l} = q(\rho_{r,l})$ .

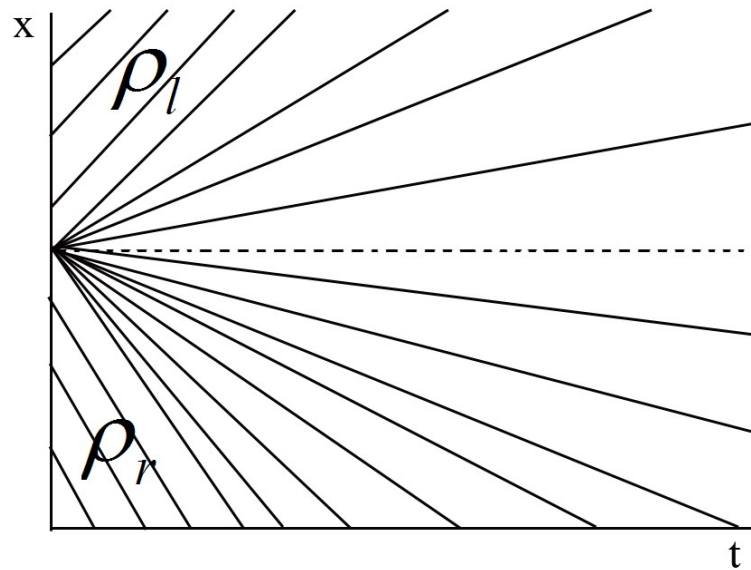


Fig.3.4. Rarefaction waves

Another method used is the approximation of the conservation laws using numerical methods. These are in general methods that consist in a time-dimension discretization.

Consider the case of simple linear equation:

$$\frac{\partial u}{\partial t} + a \frac{\partial u}{\partial x} = 0, \quad x \in \mathbb{R}, t > 0 \quad (3.39)$$

$$u(x, 0) = u_0(x), \quad x \in \mathbb{R} \quad (3.40)$$

where  $a > 0$ .

We discretize the  $(x, t)$  -plane by the mesh  $(x_i, t_n)$  with

$$x_i = ih \ (i \in \mathbb{Z}), \quad t_n = nk \ (n \in \mathbb{N}_0) \quad (3.41)$$

and  $h, k > 0$ .

For simplicity we take  $h=k$ .

There are some schemes that can be used in simulation for find the solution of equation (3.39). About some of them we have discussed in Chapter 1. Here we give some examples of the methods that are usually used in solving the macroscopic traffic flow models.

Godunov's first order upwind scheme:

$$\frac{\partial u}{\partial t} = \frac{u_i^{n+1} - u_i^n}{\Delta t} \quad (3.42)$$

$$\frac{\partial u}{\partial x} = \frac{u_i^n - u_{i-1}^n}{\Delta x}$$

and the scheme become

$$u_i^{n+1} = u_i^n - c(u_i^n - u_{i-1}^n) \quad (3.43)$$

Lax-Friedrichs scheme:

$$u_i^{n+1} = \frac{1}{2}(1+c)u_{i-1}^n + \frac{1}{2}(1-c)u_{i+1}^n \quad (3.44)$$

Lax-Wendroff Scheme:

$$u_i^{n+1} = \frac{1}{2}c(1+c)u_{i-1}^n + (1-c^2)u_i^n - \frac{1}{2}c(1-c)u_{i+1}^n \quad (3.45)$$

FTCS Scheme:

$$u_i^{n+1} = u_i^n + \frac{1}{2}c(u_{i+1}^n - u_{i-1}^n) \quad (3.46)$$

### 3.5. Implementation

For simulation we have considered three models: LWR model, AR model and Zhang model, and we made simulation applying different numerical methods, all based on finite differences. The road length (100 km) has been split into 1000 sections.

#### 3.5.1. Riemann problem in the LWR model

At  $t = 0$ , the density is a square signal with maximum value at 350 veh/km, as shown figure 3.5. At  $t = 0^+$ , the front begins to move to the right (switching to green of a traffic light). On figure 3.5. is shown the shape of the car front after 10 sec.

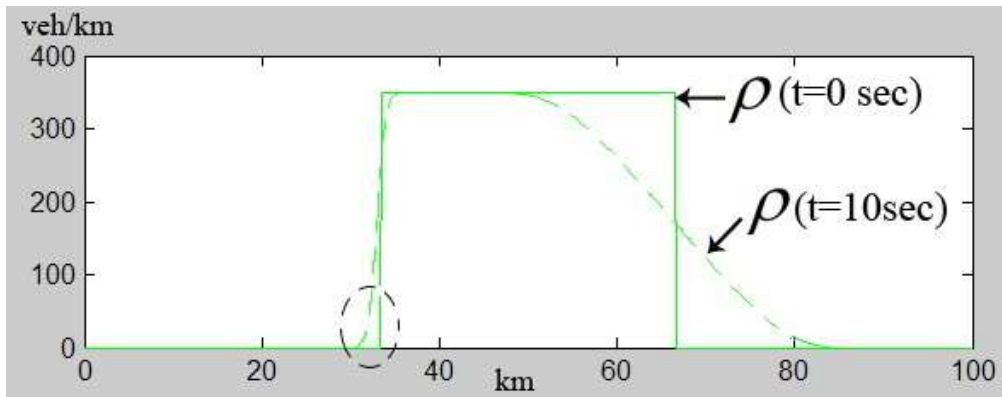
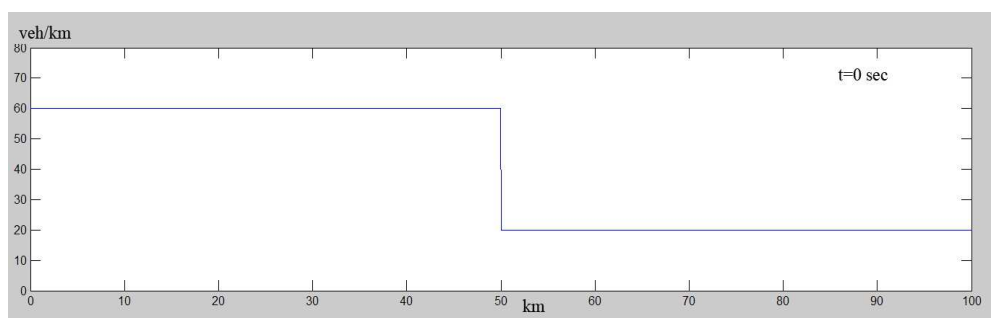


Fig.3.5. LWR solution using the Lax-Friedrichs method

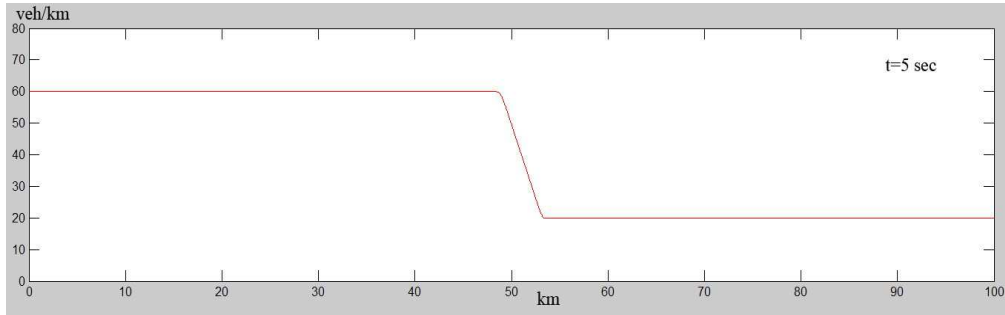
In the back of the car front we have a displacement of vehicles which is not true in reality (no back motion), this problem being one of the drawbacks of the LWR method. It is due to the fact that  $\rho = \rho_{\max}$  ( $t = 10s$ ). As soon as  $\rho(x, t)$  will be less than  $\rho_{\max}$ , this problem will disappear.

### 3.5.2. Influence of the choice of a numerical method on LWR model

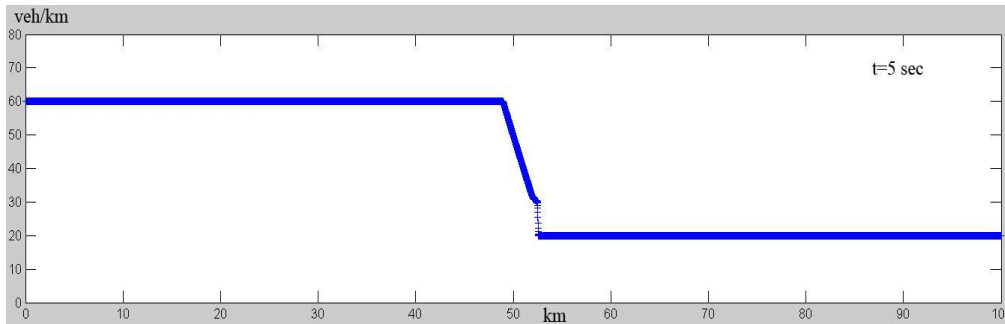
We make a comparison between the Lax-Friedrichs and FTCS method. Figure 3.6. (a) shows the initial conditions of  $\rho(x, t = 0)$ . At  $t = 0^+$ , the car front begins to move to the right. Figure 3.6. (b) and (c) show the shape of the front car at  $t = 5$  sec using the two different numerical methods.



a)



b)



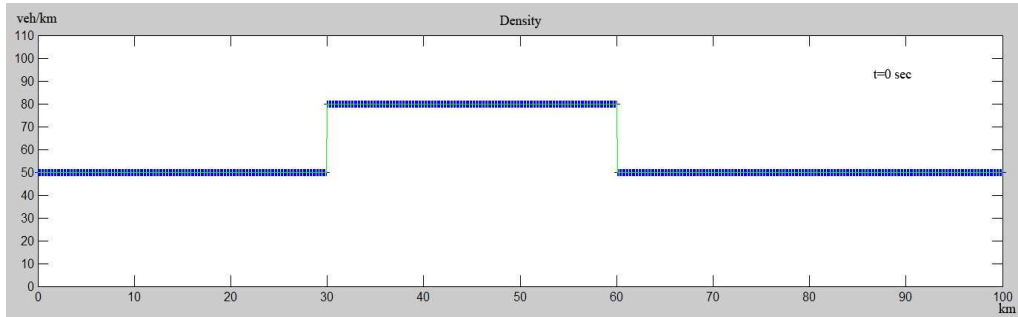
c)

**Fig.3.6. Comparisons of density with Lax-Friedrichs and FTCS for LWR (a-initial conditions, b-Lax-Friedrichs, c- FTCS)**

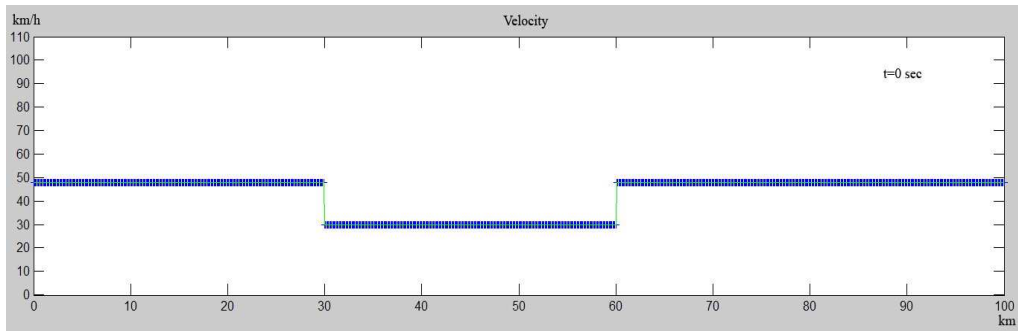
It appears that the Lax-Friedrichs method gives better results (no discontinuity).

### **3.5.3. Comparison of 1-equation model and 2-equation models**

We consider three models: 1-equation model LWR and 2-equation models AR and Zhang. At  $t=0$ , we have the initial conditions as shown figure 3.7 for density (a) and velocity (b).



a)

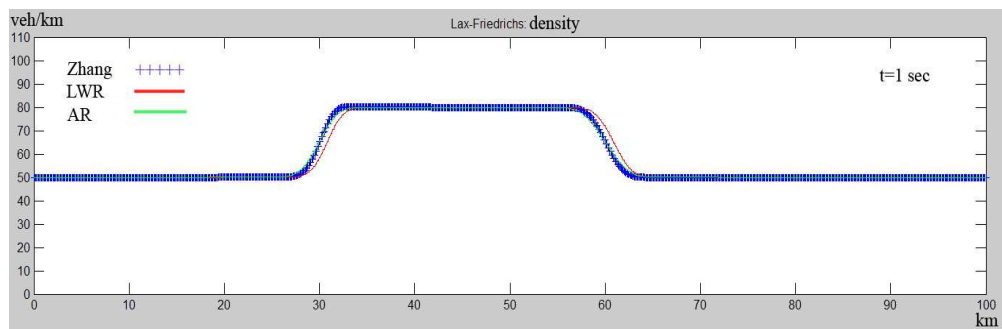


b)

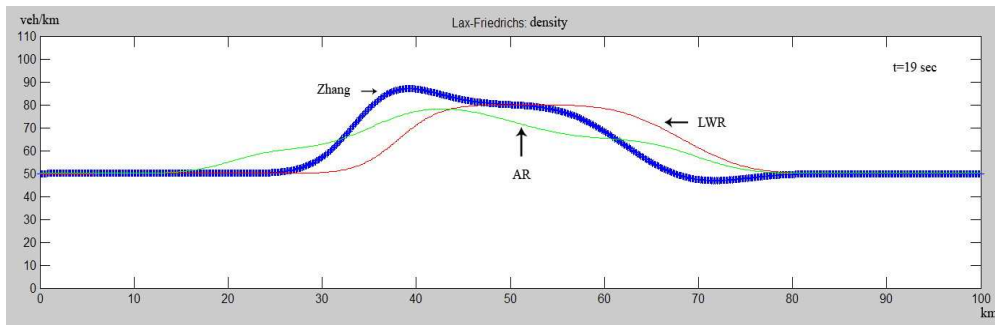
Fig. 3.7. Initial conditions (a- density, b- velocity)

Applying the Lax-Friedrichs numerical method, we obtain the results presented in the following figures:

Figure 3.8. a) t=1 sec. We have the same drawbacks (motion at the back of the front).



a)



b)

Fig. 3.8. Simulation density results

Figure 3.8. b)  $t=19$  sec. Globally the results are better obtained for the LWR model. The AR model presents an important displacement of the back car front. The Zhang model presents a displacement of the back front and also an accumulation of vehicle in the back of the queue.

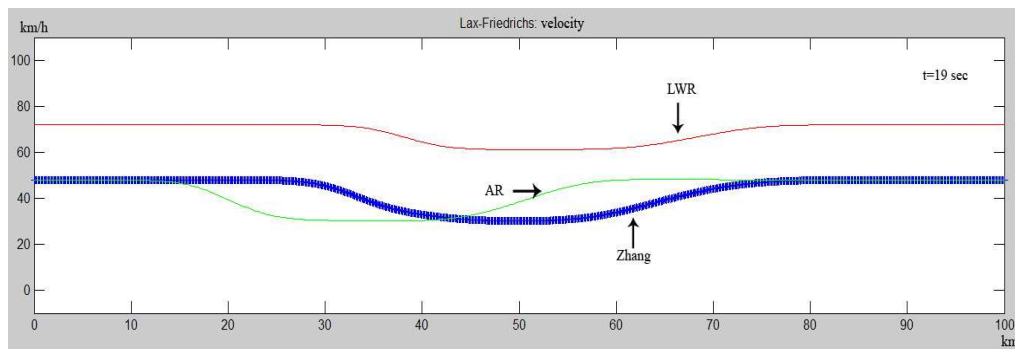


Fig. 3.9. Simulation velocity results

For the velocity, it appears from figure 3.9 that it is algebraically related to density in the LWR model, and that it behaves independently in the other two.

### 3.5.4. Comparison of LWR and Jiang models

Consider the LWR model discretized using the Lax-Friedrichs scheme and the model proposed by Jiang [Jia 02]. This model will be used in chapter 4 as starting mathematical model for CFD

representation. This model was discretized in using [Jia 02] the following scheme:

$$\rho_i^{n+1} = \rho_i^n + \frac{\Delta t}{\Delta x} \rho_i^n (v_i^n - v_{i+1}^n) + \frac{\Delta t}{\Delta x} v_i^n (\rho_{i-1}^n - \rho_i^n) \quad (3.47)$$

for the density, and for velocity:

-if the traffic is heavy ( $v_i^n < c_0$ )

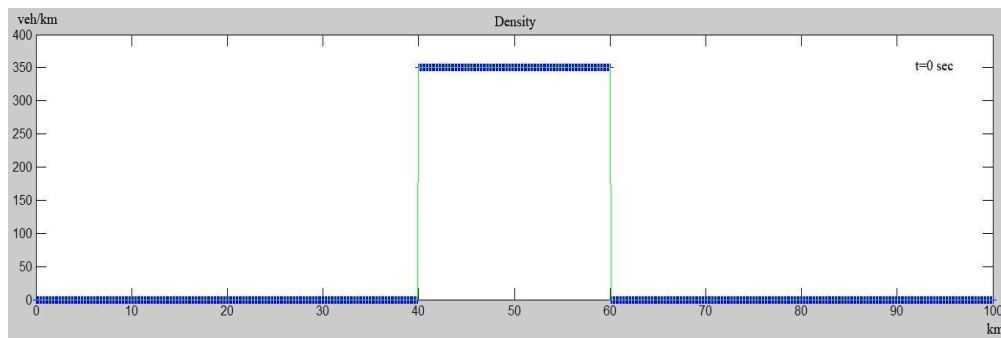
$$v_i^{n+1} = v_i^n + \frac{\Delta t}{\Delta x} (c_0 - v_i^n)(v_{i+1}^n - v_i^n) - \frac{\Delta t}{T} (v_i^n - v_{eq}) \quad (3.48)$$

-if the traffic is light ( $v_i^n \geq c_0$ )

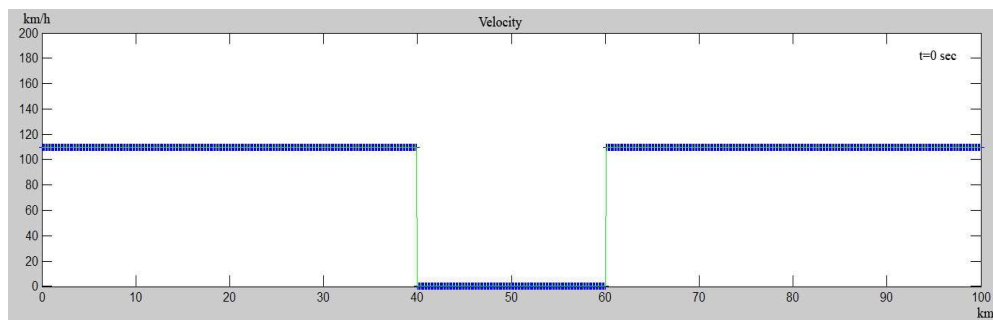
$$v_i^{n+1} = v_i^n + \frac{\Delta t}{\Delta x} (c_0 - v_i^n)(v_i^n - v_{i-1}^n) - \frac{\Delta t}{T} (v_i^n - v_{eq}) \quad (3.49)$$

where  $c_0$  is the propagation speed of the disturbance,  $T$  is the relaxation time,  $i$  represents the road section and  $j$  represents time.

At  $t=0$ , the initial conditions are presented in figure 3.9. At time  $t = 0^+$ , the car front begins to move to the right.



a)



b)

Fig.3.9. Initial conditions (a-density, b-velocity)

Figure 3.10 and figure 3.11., show the shape of the density and velocity of the car front after 9 sec.

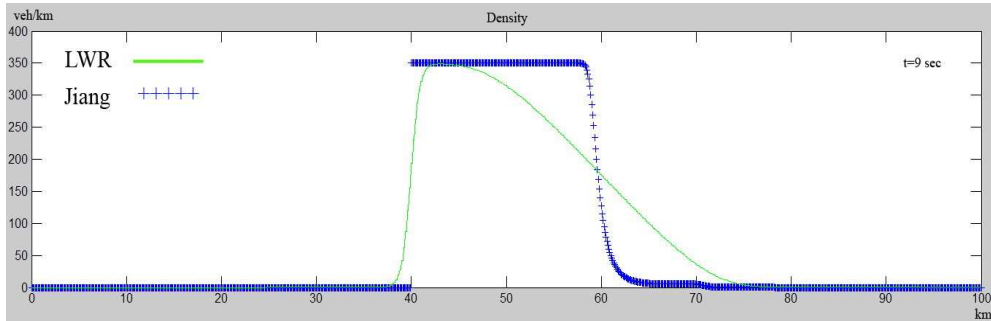


Fig.3.10. Comparison between Jiang and LWR model (density)

It appears that the Jiang model gives better result in the back of the front. In the front of the queue, the behavior of the two models is different. It would be interesting to have experimental data to be able to conclude which model is physically more consistent.

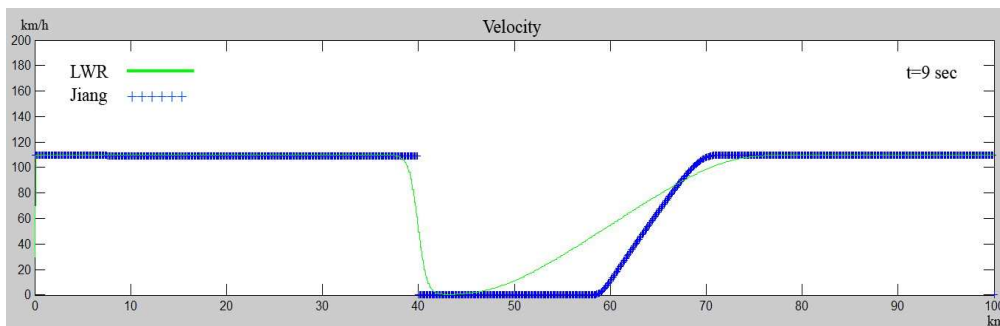


Fig. 3.11. Comparison between Jiang and LWR models (velocity)

At the velocity level there is an algebraically relation with the density in the LWR model. In the Jiang model the velocity behaves independently.

### 3.6. Conclusions

In this chapter we have presented a few models used in macroscopic traffic flow representation, starting with the well known

LWR model and arriving to new models developed by Zhang or Aw and Rascole. The LWR model is a model which has been used for a long period of time in simulation and it was considered as the best model for the representation of the traffic flow. But in the latest years some researchers showed that this model has some drawbacks. Thus, new models have been developed trying to eliminate the inadvertences with the real life situation.

Through simulation of the models found in the literature we have seen the advantages and drawbacks of each of them. In the meantime, we have tried to see which numerical method (based on finite difference) is more appropriate to be used in discretization of the models.

In the next chapter, we will show how the Jiang's model [Jia 02] can be represented using CFD technique.



## **Chapter 4.**

# **Transport equations modeled by CFD**



## Contents

Chapter 4. Transport equations modeled by CFD .....	123
4.1. Introduction .....	127
4.1.1. Two-equation traffic models .....	128
4.2. Power balance per unit volume.....	128
4.2.1. Kinetic energy.....	128
4.2.2. Balance equations .....	129
4.3. Discretization.....	130
4.3.1. Description of the flow fields.....	130
4.3.2. Integrated variables .....	131
4.4. System integration.....	132
4.4.1. Kinetic energy.....	132
4.4.2. System $IC$ -field.....	134
4.4.3 Resistance field .....	135
4.5. State equations.....	136
4.5.1. Mass port.....	136
4.5.2. Velocity port.....	138
4.6. Coupling matrices .....	139
4.6.1. Coupling between the velocity and mass ports.....	139
4.7. System Bond Graph.....	140
4.8. Initial and boundary conditions .....	141
4.8.1. Initial conditions.....	141
4.8.2. Boundary conditions.....	142
4.9. Integrated variables .....	142

4.9.1. Shape and weight functions .....	143
4.9.2. Diagonal volume matrix .....	147
4.9.3. Nodal vector of mass.....	147
4.9.4. Inertia matrix.....	148
4.9.5. Nodal vectors of potentials.....	149
4.9.6. State equations, mass port.....	149
4.9.7. State equations, velocity port.....	155
4.10. Implementation.....	159
4.11. Conclusions.....	165

## Chapter 4. Transport equations modeled by CFD

### 4.1. Introduction

As seen in the previous chapter, starting with the models of Lighthill and Whitham [Lig 55], Richards [Ric 56], continuing with Payne [Pay 71] and more recently Zhang [Zha 02], the study of traffic flow had known an important development. The proposed models and the modality of approach vary from one author to another.

The models where the dynamic part is consider only for the vehicle density have a few drawbacks like: the velocity is determined by a equilibrium speed density, no fluctuation of speed around the equilibrium is allowed, thus the model is not suitable for the description of non-equilibrium situations like stop-and-go, etc. To overcome these drawbacks a new type of models were proposed, considering two dynamical equations, one for vehicle density and one for vehicle velocity.

One way for modeling these systems is by using the classical approximation methods like Lax-Friedrichs, FTCS, Godunov etc [Str 04], [Ago 85].

In moving fluids, the transport of mass, momentum and energy are represented using the differential equations. In the early 1960s was

developed the Computational Fluid Dynamics (CFD) [And 95], [Dat 05], [Hir 07], [Jiy 08] with the objective to find the numerical solution for these equations. Today, CFD is extensively used in basic applied research, in design of engineering equipment, and in calculation of environmental and geophysical phenomena.

In the recent years, there was a development of CFD using the bond graph approach [Bal 06]. Starting from this approach in this chapter we will present a new way of modeling the traffic flow, using computational fluid dynamics. Some simulations will be done to validate the model.

#### 4.1.1. Two-equation traffic models

Two-equation traffic models consider one-dimensional flow with one continuity equation for vehicle density  $\rho(x, t)$ :

$$\frac{\partial \rho}{\partial t} + \frac{\partial}{\partial x}(\rho v) = 0 \quad (4.1)$$

and one transport equation for vehicle velocity  $v(x, t)$ . For the velocity equation, different models appearing in the literature can be written as:

$$\frac{\partial v}{\partial t} + v \frac{\partial v}{\partial x} = \frac{v_e}{\tau} + G - \frac{v}{\tau} \quad (4.2)$$

where  $\tau$  is the reactive time,  $v_e(\rho)$  is the equilibrium velocity distribution and  $G$  is a source term.

### 4.2. Power balance per unit volume

#### 4.2.1. Kinetic energy

In the two-equation model, total energy corresponds to kinetic energy. The kinetic energy density  $T_v$  is:

$$T_v = \frac{1}{2} \rho v^2 \quad (4.3)$$

The following potentials (kinetic energy per unit vehicle and vehicle momentum density) are defined as:

$$\kappa = \frac{\partial T_v}{\partial \rho} = \frac{1}{2} v^2 \quad (4.4)$$

$$q_v = \frac{\partial T_v}{\partial v} = \rho v \quad (4.5)$$

These potentials satisfy Maxwell's relations:

$$\frac{\partial \kappa}{\partial v} = \frac{\partial q_v}{\partial \rho} = v \quad (4.6)$$

The time derivative of the kinetic energy density can be written as:

$$\frac{\partial T_v}{\partial t} = \kappa \frac{\partial \rho}{\partial t} + q_v \frac{\partial v}{\partial t} \quad (4.7)$$

#### 4.2.2. Balance equations

The balance equations are power density equations corresponding to each one of the terms that contributes to the time derivative of the total energy density.

Multiplying Eq. (4.1) by  $\kappa$ , the density balance equation results:

$$\kappa \frac{\partial \rho}{\partial t} = -\kappa \frac{\partial}{\partial x} (\rho v) = -\frac{\partial}{\partial x} (\kappa \rho v) + \rho v \frac{\partial \kappa}{\partial x} \quad (4.8)$$

Multiplying Eq. (4.2) by  $q_v$ , the velocity balance equation results:

$$q_v \frac{\partial v}{\partial t} = \rho v \left( \frac{v_e}{\tau} + G \right) - \rho \frac{v^2}{\tau} - \rho v^2 \frac{\partial v}{\partial x} \quad (4.9)$$

Since

$$\frac{\partial \kappa}{\partial x} = v \frac{\partial v}{\partial x} \quad (4.10)$$

it can be seen that the last term in Eq. (4.8) and (4.9) is a coupling term.

### 4.3. Discretization

#### 4.3.1. Description of the flow fields

In order to formulate the model at the discrete level, it is necessary to specify the description of the fields corresponding to the independent variables in the domain  $\Omega$ , as shown in Fig. 4.1. As it is done in the Finite Element Method [Whi 99], this description is made in terms of a finite set of nodal values and interpolation functions:



Fig. 4.1. Domain  $\Omega$  with boundaries

$$\rho(x, t) = \sum_{k=1}^{n_\rho} \rho_k(t) \phi_{\rho k}(x) = \underline{\rho}^T \cdot \underline{\phi}_\rho \quad (4.11)$$

$$v(x, t) = \sum_{m=1}^{n_v} v_m(t) \phi_{vm}(x) = \underline{v}^T \cdot \underline{\phi}_v \quad (4.12)$$

where  $\underline{\rho}$  and  $\underline{v}$  are time-dependent nodal vectors and  $\underline{\phi}_\rho$  and  $\underline{\phi}_v$  are nodal vectors of interpolation or shape functions, with the properties:

$$\sum_{k=1}^{n_\rho} \phi_{\rho k}(x) = 1 \quad \forall x \in \Omega \quad (4.13)$$

$$\sum_{m=1}^{n_v} \phi_{vm}(x) = 1 \quad \forall x \in \Omega \quad (4.14)$$

For simplicity in the treatment of the boundary conditions, it is also required for the interpolation function to be equal to unity at the reference node, and to be equal to zero at the rest of the nodes, this is:

$$\phi_{\rho k}(x_n) = \delta_{kn} \text{ for a density node located at position } x_n \quad (4.15)$$

$$\phi_{vm}(x_n) = \delta_{mn} \text{ for a velocity node located at position } x_n \quad (4.16)$$

In Eq. (4.15),  $\delta_{kn}$  is the Kronecker's delta ( $\delta_{kn} = 1$  if  $k = n$ ,  $\delta_{kn} = 0$  otherwise).

The representation of the flow fields in terms of nodal values and interpolation functions allows to define the corresponding values at any position, so it is possible to calculate univocally all the integrals corresponding to the state equations; this is not evident for other methodologies like Finite Differences or Finite Volumes, where only nodal values are defined and additional considerations must be made in order to integrate the differential equations. Besides, the chosen representation can make use of the considerable amount of computational tools already available for the popular Finite Element Method.

### 4.3.2. Integrated variables

A nodal vector of mass is defined, related to the nodal vector of density as:

$$\underline{m} = \underline{\underline{\Omega}}_{\rho} \cdot \underline{\rho} \quad (4.17)$$

where the diagonal volume matrix  $\underline{\underline{\Omega}}_{\rho}$  associated to the density is defined as:

$$\left( \underline{\underline{\Omega}}_{\rho} \right)_{kn} = \Omega_{\rho k} \delta_{kn} \quad (4.18)$$

where:

$$\Omega_{\rho k} = \int_{\Omega} \phi_{\rho k} dx \quad (4.19)$$

The system mass  $m$  is related to the corresponding nodal vector as follows:

$$m = \int_{\Omega} \rho dx = \sum_{k=1}^{n_{\rho}} m_k \quad (4.20)$$

#### 4.4. System integration

##### 4.4.1. Kinetic energy

The system kinetic energy  $T$  is defined as:

$$T = \int_{\Omega} T_v dx \quad (4.21)$$

From Eq. (4.12) and (4.21), it can be easily shown that the system kinetic energy can be expressed as the following bilinear form:

$$T = \frac{1}{2} \underline{v}^T \cdot \underline{\underline{M}} \cdot \underline{v} \quad (4.22)$$

where  $\underline{\underline{M}}$  is the system inertia matrix (size  $n_v$ , symmetric and regular):

$$(M)_{mn} = \int_{\Omega} \rho \phi_{vm} \phi_{vn} dx \quad (4.23)$$

The following potentials are defined:

$$\underline{K}(\underline{v}) = \frac{\partial T}{\partial \underline{m}} = \underline{\underline{\Omega}}_{\rho}^{-1} \cdot \left( \int_{\Omega} \kappa \phi_{\rho} dx \right) \quad (4.24)$$

$$\underline{q}(\underline{m}, \underline{v}) = \frac{\partial T}{\partial \underline{v}} = \int_{\Omega} q_v \phi_v dx = \underline{\underline{M}} \cdot \underline{v} \quad (4.25)$$

where  $\underline{K}$  and  $\underline{q}$  are correspondingly nodal vectors of kinetic energy per unit vehicle and vehicle momentum.

As in the continuum formulation, it can be shown that the Maxwell relations also holds for the nodal vectors of potentials:

$$\frac{\partial \underline{K}}{\partial \underline{v}} = \left( \frac{\partial \underline{q}}{\partial \underline{m}} \right)^T = \underline{\underline{\Omega}}_{\rho}^{-1} \cdot \left( \int_{\Omega} v \underline{\phi}_{\rho} \underline{\phi}_{v} dx \right) \quad (4.26)$$

It is important to notice that Eq. (4.25) defines, in the bond graph terminology, a modulated multibond transformer relating the nodal vectors of velocity and vehicle momentum, as shown in Fig. 4.2. According to the power conservation across the transformer, the generalized effort  $\underline{F}$  is given by:

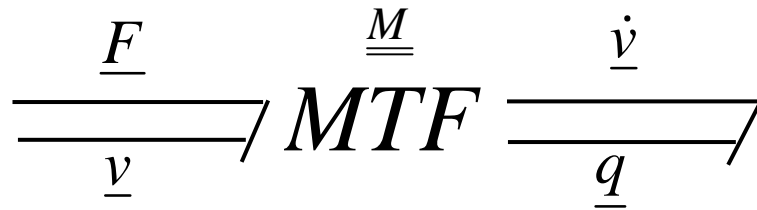


Fig. 4.2. Modulated transformer relating nodal vectors of velocity and vehicle momentum.

$$\underline{F} = \underline{\underline{M}} \cdot \dot{\underline{v}} \quad (4.27)$$

According to Eq. (4.25), the nodal vector of vehicle momentum can be regarded as a system integral of the local values weighted by the velocity interpolation function. It can be easily shown that the system vehicle momentum  $Q$  can be obtained as:

$$Q = \int_{\Omega} q_v dx = \sum_{m=1}^{n_v} q_m \quad (4.28)$$

According to Eq. (4.24), the nodal vector  $\underline{K}$  can be regarded as a system domain average of the corresponding local values, weighted by the interpolation functions. Therefore, it is important to realize that the values of the nodal vectors may be different from the corresponding values calculated with the local variables at the nodal positions.

The time derivative of the system kinetic energy can be written as:

$$\dot{T} = \underline{K}^T \cdot \dot{\underline{m}} + \underline{q}^T \cdot \dot{\underline{v}} \quad (4.29)$$

It can also be shown that the volume integrals of the right side term of Eq. (4.7) can be calculated as:

$$\int_{\Omega} \kappa \frac{\partial \rho}{\partial t} dx = \underline{K}^T \cdot \dot{\underline{m}} \quad (4.30)$$

$$\int_{\Omega} q_v \frac{\partial v}{\partial t} dx = \underline{q}^T \cdot \dot{\underline{v}} \quad (4.31)$$

#### 4.4.2. System $IC$ -field

Equation (4.21), constitutive relations (4.24) and (4.25) and Maxwell relation (4.26) define a multibond  $IC$  -field associated to the system kinetic energy, as shown in Fig. 4.3. The generalized effort variables are  $\underline{K}$  and  $\dot{\underline{v}}$ , while the generalized flow variables are correspondingly  $\dot{\underline{m}}$  and  $\underline{q}$ .

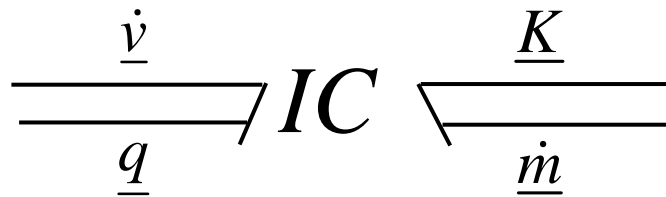


Fig. 4.3. System  $IC$  -field representing kinetic energy storage.

In Fig. 4.3, the generalized effort and flow of the multibonds connected to the capacitive and inertial ports are nodal vectors whose elements are scalar variables; these types of multibonds are equivalent to  $n$  single bonds, as shown in Fig. 4.4.

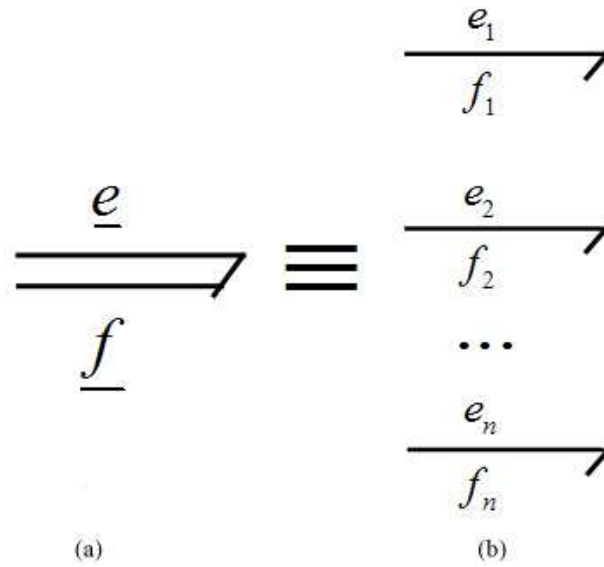


Fig. 4.4. Multibond with nodal vector of scalar variables (a), equivalent to  $n$  single bonds (b).

#### 4.4.3 Resistance field

The  $l$ -element of the resistance force is:

$$F_{Rl} = \int_{\Omega} \rho \frac{v}{\tau} \phi_{vl} dx \quad (4.32)$$

The discretization for the velocity field is:

$$v(x, t) = \sum_{m=1}^{n_v} v_m(t) \phi_{vm}(x) \quad (4.33)$$

Substituting, we have:

$$F_{Rl} = \sum_{m=1}^{n_v} v_m \left( \int_{\Omega} \frac{\rho}{\tau} \phi_{vl} \phi_{vm} dx \right) = \sum_{m=1}^{n_v} F_{Rlm} v_m \quad (4.34)$$

where:

$$F_{Rlm} = \int_{\Omega} \frac{\rho}{\tau} \phi_{vl} \phi_{vm} dx \quad (4.35)$$

This represents a  $R$ -field with resistance causality (efforts are a function of flows), as shown in Figure 5. In this case, the coefficients  $F_{Rlm}$

of the linear relation (4.34) are modulated by the density. The matrix relation for the field is:

$$\underline{F}_R = \underline{F}_R \cdot \underline{v} \quad (4.36)$$

where the elements of the square matrix  $\underline{F}_R$  are defined by (4.35).

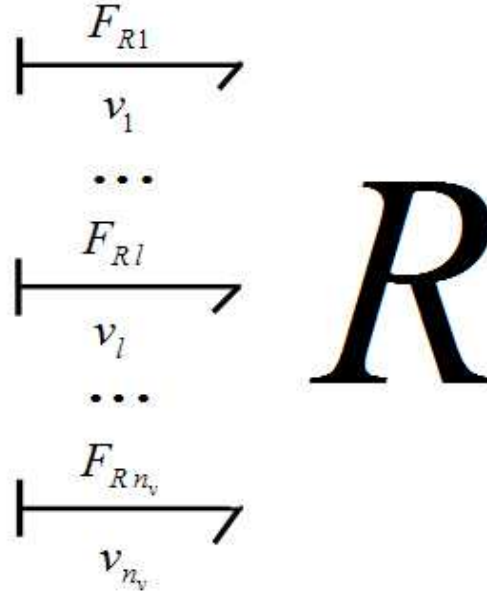


Fig.4.5. Resistance field

## 4.5. State equations

### 4.5.1. Mass port

Nodal density weight functions  $w_{\rho k}(x, t)$  are introduced, with the following properties:

$$\sum_{k=1}^{n_\rho} w_{\rho k}(x, t) = 1 \quad \forall x \in \Omega, \forall t \quad (4.37)$$

$$w_{\rho k}(x_n, t) = \delta_{kn} \text{ for a density node located at position } x_n \quad (4.38)$$

The nodal density weight functions are introduced to satisfy the power interchanged by the system through the boundary conditions, as well as to share the importance of different power terms among

neighboring nodes. These functions can be used to introduce schemes in the numerical solution.

As it is done in the Petrov-Galerkin method [Cuv 86], each term of the mass balance equation (4.8) is multiplied by the test function  $w_{\rho k}$ ; then, the resulting terms are integrated over the domain  $\Omega$  and Green's theorem is applied whenever necessary, obtaining:

$$\underline{K} \cdot \underline{\dot{m}} = \underline{W}_B^{(\Gamma)} + \underline{W}_B + \underline{W}_K \quad (4.39)$$

where the different nodal vectors of power are:

$$\underline{W}_B^{(\Gamma)} = - \left[ \left( \underline{w}_\rho \kappa \rho v \right)_L - \left( \underline{w}_\rho \kappa \rho v \right)_0 \right] \quad (4.40)$$

$$\underline{W}_B = \int_{\Omega} \frac{\partial w_\rho}{\partial x} \kappa \rho v dx \quad (4.41)$$

$$\underline{W}_K = \int_{\Omega} \underline{w}_\rho \rho v^2 \frac{\partial v}{\partial x} dx \quad (4.42)$$

Alternatively, it can be written:

$$\underline{\dot{m}} = \underline{\dot{m}}_B^{(\Gamma)} + \underline{\dot{m}}_B + \underline{\dot{m}}_K \quad (4.43)$$

where the different nodal vectors of mass rates are:

$$\underline{\dot{m}}_B^{(\Gamma)} = \underline{K}^{-1} \cdot \underline{W}_B^{(\Gamma)} \quad (4.44)$$

$$\underline{\dot{m}}_B = \underline{K}^{-1} \cdot \underline{W}_B \quad (4.45)$$

$$\underline{\dot{m}}_K = \underline{K}^{-1} \cdot \underline{W}_K \quad (4.46)$$

The square matrix  $\underline{K}$  (size  $n_\rho$ ) is defined as:

$$(K)_{kj} = \frac{1}{\Omega_{\rho j}} \int_{\Omega} \kappa w_{\rho k} \phi_{\rho j} dx \quad (4.47)$$

The nodal vector  $\underline{K}$  is related to the corresponding matrix as:

$$K_j = \sum_{k=1}^{n_\rho} (K)_{kj} \quad (4.48)$$

Taking into account Eq. (4.48) it can be verified that the product  $\underline{K}^T \cdot \underline{\dot{m}}_x$ , where  $\underline{\dot{m}}_x$  is any nodal vector of mass rate, recovers the corresponding power term integrated in the system. So, the product  $\underline{K}^T \cdot \underline{\dot{m}}_B^{(\Gamma)}$  recovers the power due to the flux of free kinetic energy through the system boundary, while  $\underline{K}^T \cdot \underline{\dot{m}}_B$  is a power term that vanishes, because of Eq.(4.37). Notice that  $\underline{\dot{m}}_B^{(\Gamma)}$  may be nonzero only for the nodes located at the system boundary. Making the product of  $\underline{K}$  times Eq.(4.43), it can be easily shown that the integral density balance equation is satisfied, this is:

$$\int_{\Omega} \kappa \frac{\partial \rho}{\partial t} dx = -(\kappa \rho v)_L + (\kappa \rho v)_0 + \int_{\Omega} \rho v^2 \frac{\partial v}{\partial x} dx + \int_{\Omega} \kappa \rho v dx \quad (4.49)$$

### 4.5.2. Velocity port

As it is done in the Galerkin method [Cuv 86], the momentum conservation equation is multiplied by the test function  $\phi_{vm}$  and integrated over the domain  $\Omega$ , obtaining:

$$\underline{\underline{M}} \cdot \dot{\underline{v}} = \underline{F}_E + \underline{F}_G - \underline{F}_R - \underline{F}_K \quad (4.50)$$

where:

$$\underline{F}_E = \int_{\Omega} \rho \left( \frac{v_e}{\tau} \right) \phi_v dx \quad (4.51)$$

$$\underline{F}_G = \int_{\Omega} \rho G \phi_v dx \quad (4.52)$$

$$\underline{F}_R = \int_{\Omega} \rho \frac{v}{\tau} \phi_v dx \quad (4.53)$$

$$\underline{F}_K = \int_{\Omega} \rho v \frac{\partial v}{\partial x} \phi_v dx \quad (4.54)$$

Alternatively, it can be written:

$$\dot{\underline{v}} = \underline{\underline{M}}^{-1} \cdot (\underline{F}_E + \underline{F}_G - \underline{F}_R - \underline{F}_K) \quad (4.55)$$

Adding the nodal components of Eq. (4.50) it can be easily shown that the integral velocity equation is satisfied, this is:

$$\int_{\Omega} \rho \frac{\partial v}{\partial t} dx = \int_{\Omega} \rho \left( \frac{v_e - v}{\tau} + G - v \frac{\partial v}{\partial x} \right) dx \quad (4.56)$$

Since the interpolation function were chosen as test functions, the product  $\underline{F}_x^T \cdot \underline{v}$ , where  $\underline{F}_x$  is any nodal vector of force, recovers the corresponding power term integrated in the system. Making the product of Eq. (4.50) times  $\underline{v}$ , it can be easily shown that the integral velocity balance equation is satisfied, this is:

$$\int_{\Omega} q_v \frac{\partial v}{\partial t} dx = \int_{\Omega} \rho v \left( \frac{v_e - v}{\tau} + G - v \frac{\partial v}{\partial x} \right) dx \quad (4.57)$$

## 4.6. Coupling matrices

Once defined the generalized effort and flow variables, it is necessary to represent the power coupling, appearing in the balance equations, to a discretized level. This representation is performed through a coupling matrix, which relates generalized nodal variables whose product gives rise to power terms appearing in a pair of multiports. Since the nodal vectors may have different size, the coupling matrix is rectangular, thus setting a restriction in the allowable causalities.

### 4.6.1. Coupling between the velocity and mass ports

From Eq. (4.46) and (4.54):

$$\underline{\dot{m}}_K = \left( \underline{K}^{-1} \cdot \underline{M}_K \right) \cdot \underline{v} \quad (4.58)$$

$$\underline{F}_K = \left( \underline{K}^{-1} \cdot \underline{M}_K \right)^T \cdot \underline{K} \quad (4.59)$$

where  $\underline{M}_K$  is a rectangular matrix ( $n_\rho$  rows and  $n_v$  columns) defined as:

$$(M_K)_{km} = \int_{\Omega} w_{\rho k} \phi_{vm} \rho v \frac{\partial v}{\partial x} dx \quad (4.60)$$

Eq. (4.58) and (4.59) define a multibond transformer modulated by the state variables, as shown in Fig. 4.6.

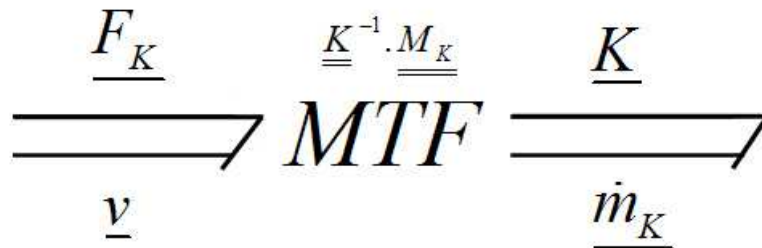


Fig. 4.6. Modulated transformer coupling the velocity and mass ports.

#### 4.7. System Bond Graph

The system Bond Graph is shown in Fig. 4.7. Kinetic energy storing is represented by a  $IC$  - field.

At the 0-junction with common  $\underline{K}$  all the nodal mass rates are added; in this way, the flow balance represents the mass conservation equations for the nodal mass values. At the 1-junction with common  $\underline{v}$  all the nodal forces are added; in this way, the effort balance represents the momentum conservation equations for the nodal velocity values.

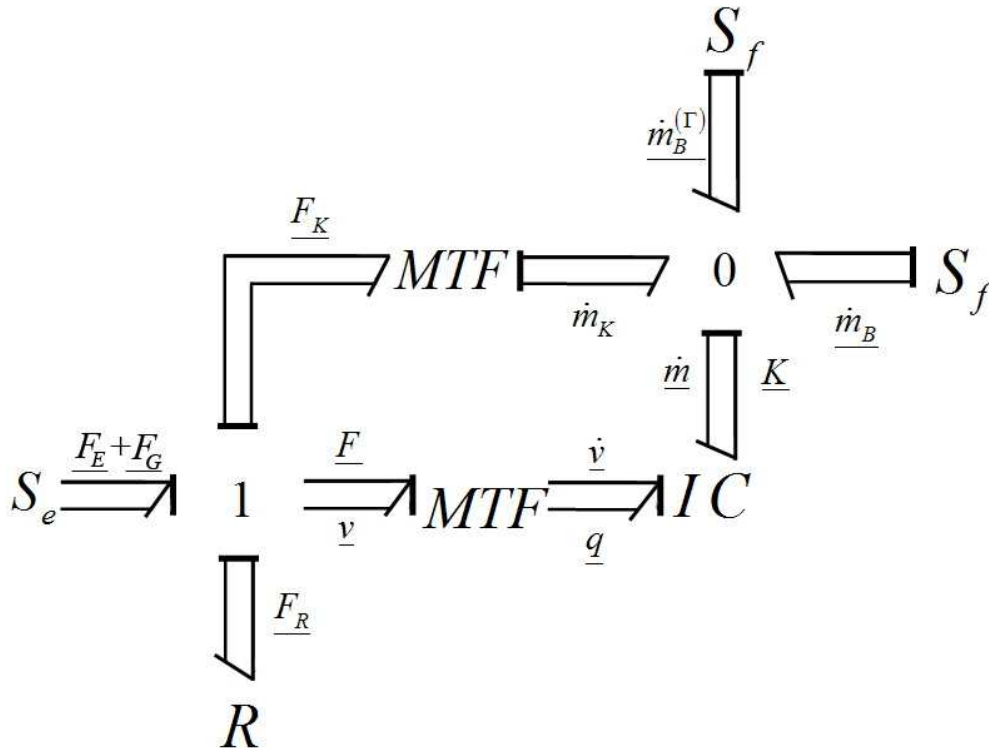


Fig. 4.7. Bond graph for the two-equation traffic flow model.

## 4.8. Initial and boundary conditions

### 4.8.1. Initial conditions

In order to solve the state equations, it is needed to set initial and boundary conditions. The nodal initial values may be readily specified as:

$$\underline{m}(t=0) = \underline{m}_0 \quad (4.61)$$

$$\underline{v}(t=0) = \underline{v}_0 \quad (4.62)$$

Alternatively, if spatial functions  $\rho_0(x)$  and  $v_0(x)$  are specified for the initial time for density and velocity, the nodal values must be determined in order to conserve the system mass and momentum. In this case, it can be easily shown that:

$$m_{0k} = \int_{\Omega} \rho_0(x) \phi_{\rho k} dx \quad (4.63)$$

$$v_{0m} = \frac{\int_{\Omega} \rho_0(x) v_0(x) \phi_{v m} dx}{\int_{\Omega} \rho_0(x) \phi_{v m} dx} \quad (4.64)$$

#### 4.8.2. Boundary conditions

The boundary conditions establish relationships among the variables corresponding to the nodes located at the system boundary and can be regarded (in the bond graph methodology) as the input variables. It is necessary, for the model being mathematically well defined, that the boundary conditions allow determining the causality for all the bonds in the resulting bond graph. The boundary conditions are introduced through the bonds corresponding to the superficial source terms  $\dot{m}_B^{(\Gamma)}$ .

It is worth noting that, since the interpolation functions are zero at the boundary for inner nodes, causality is assigned by definition at these bonds. Thus, zero-flow sources are connected to an inner  $\dot{m}_{Bk}^{(\Gamma)}$ , and these bonds could be removed from the graph.

Since the two-equation model is second order, it is possible to establish boundary conditions in both  $x = 0$  and  $x = L$ , being possible the treatment of problems in which boundary conditions are established at both ends (stop-and-go problems).

#### 4.9. Integrated variables

We set linear shape functions for density and velocity, as well as linear weight functions for density. For simplicity, we consider  $n_p = n_v = n$  and regular grid of spacing  $h$  for an inner node ( $1 < l < n$ ), and  $\frac{h}{2}$  for the first and last nodes.

### 4.9.1. Shape and weight functions

#### 4.9.1.1. Inner node

For an inner node, we consider the following shape and weight functions (see Figure 4.8):

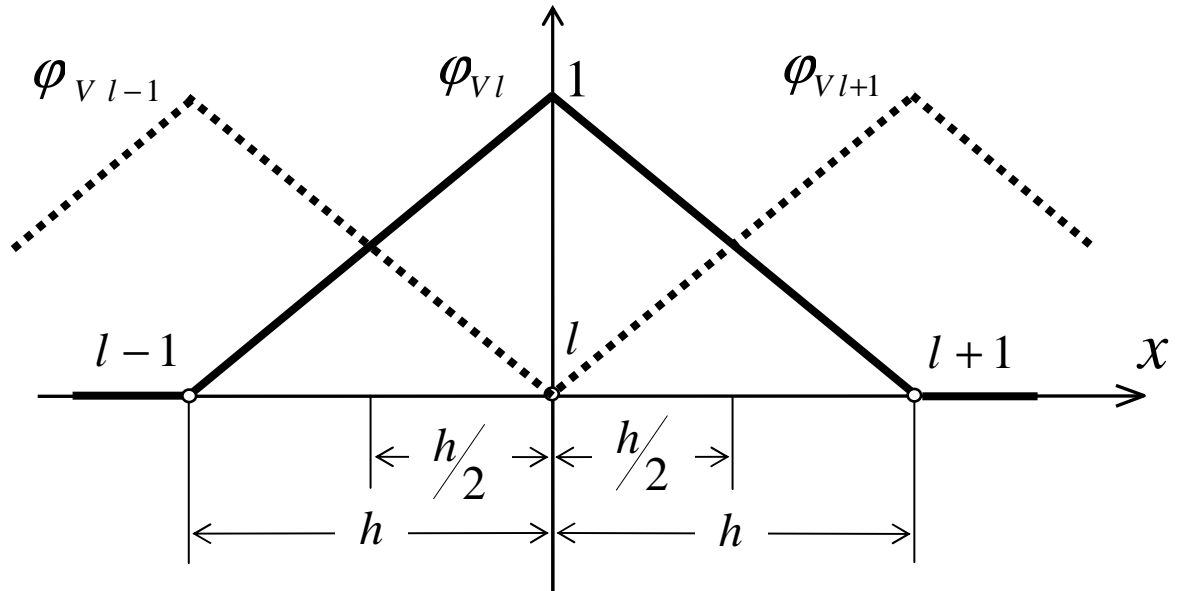


Fig.4. 8. Shape and weight functions for an inner node (shape function is shown in continuous line).

$$\phi_{pl} = \phi_{vl} = w_{pl} = \begin{cases} 0 & x \leq -h \\ 1 + \frac{x}{h} & -h < x < 0 \\ 1 & x = 0 \\ 1 - \frac{x}{h} & 0 < x < h \\ 0 & x \geq h \end{cases} \quad (4.65)$$

$$\frac{\partial \phi_{\rho l}}{\partial x} = \frac{\partial \phi_{v l}}{\partial x} = \frac{\partial w_{\rho l}}{\partial x} = \begin{cases} 0 & x \leq -h \\ \frac{1}{h} & -h < x < 0 \\ -\frac{1}{h} & 0 < x < h \\ 0 & x \geq h \end{cases} \quad (4.66)$$

As:

$$\rho = \sum_{l=1}^n \rho_l \phi_{\rho l} \quad (4.67)$$

$$v = \sum_{l=1}^n v_l \phi_{v l} \quad (4.68)$$

it is obtained, for  $-h \leq x \leq h$  :

$$\rho = \begin{cases} -\rho_{l-1} \frac{x}{h} + \rho_l \left(1 + \frac{x}{h}\right) & -h < x < 0 \\ \rho_l \left(1 - \frac{x}{h}\right) + \rho_{l+1} \frac{x}{h} & 0 < x < h \end{cases} \quad (4.69)$$

$$v = \begin{cases} -v_{l-1} \frac{x}{h} + v_l \left(1 + \frac{x}{h}\right) & -h < x < 0 \\ v_l \left(1 - \frac{x}{h}\right) + v_{l+1} \frac{x}{h} & 0 < x < h \end{cases} \quad (4.70)$$

As:

$$\frac{\partial \rho}{\partial x} = \sum_{l=1}^n \rho_l \frac{\partial \phi_{\rho l}}{\partial x} \quad (4.71)$$

$$\frac{\partial v}{\partial x} = \sum_{l=1}^n v_l \frac{\partial \phi_{v l}}{\partial x} \quad (4.72)$$

it is obtained, for  $-h \leq x \leq h$  :

$$\frac{\partial \rho}{\partial x} = \begin{cases} \frac{\rho_l - \rho_{l-1}}{h} & -h < x < 0 \\ \frac{\rho_{l+1} - \rho_l}{h} & 0 < x < h \end{cases} \quad (4.73)$$

$$\frac{\partial v}{\partial x} = \begin{cases} \frac{v_l - v_{l-1}}{h} & -h < x < 0 \\ \frac{v_{l+1} - v_l}{h} & 0 < x < h \end{cases} \quad (4.74)$$

#### 4.9.1.2. First node

For the first node (see Figure 4.9) it results:

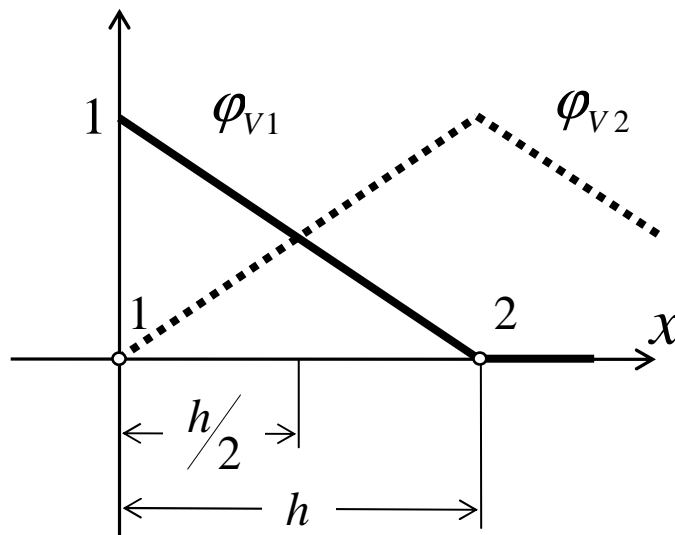


Fig. 4.9. Shape and weight functions for the first node (shape function is shown in continuous line)

$$\phi_{\rho 1} = \phi_{v 1} = w_{\rho 1} = \begin{cases} 1 - \frac{x}{h} & 0 \leq x < h \\ 0 & x \geq h \end{cases} \quad (4.75)$$

$$\frac{\partial \phi_{\rho 1}}{\partial x} = \frac{\partial \phi_{v 1}}{\partial x} = \frac{\partial w_{\rho 1}}{\partial x} = \begin{cases} -\frac{1}{h} & 0 < x < h \\ 0 & x \geq h \end{cases} \quad (4.76)$$

$$\rho = \rho_1 \left(1 - \frac{x}{h}\right) + \rho_2 \frac{x}{h} \quad 0 < x < h \quad (4.77)$$

$$v = v_1 \left(1 - \frac{x}{h}\right) + v_2 \frac{x}{h} \quad 0 < x < h \quad (4.78)$$

$$\frac{\partial \rho}{\partial x} = \frac{\rho_2 - \rho_1}{h} \quad 0 < x < h \quad (4.79)$$

$$\frac{\partial v}{\partial x} = \frac{v_2 - v_1}{h} \quad 0 < x < h \quad (4.80)$$

#### 4.9.1.3. Last node

For the last node (see Figure 4.10) it results:

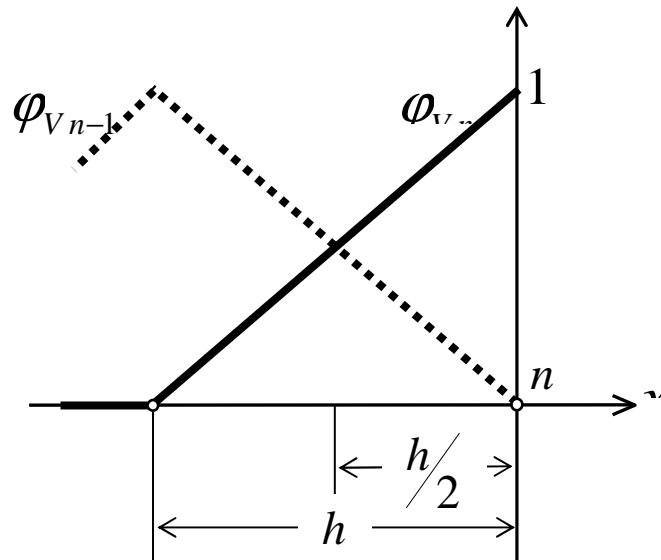


Fig. 4.10. Shape and weight functions for the last node (shape function is shown in continuous line).

$$\phi_{\rho n} = \phi_{v n} = w_{\rho n} = \begin{cases} 0 & x \leq -h \\ 1 + \frac{x}{h} & -h < x < 0 \end{cases} \quad (4.81)$$

$$\frac{\partial \phi_{\rho_n}}{\partial x} = \frac{\partial \phi_{v_n}}{\partial x} = \frac{\partial w_{\rho_n}}{\partial x} = \begin{cases} 0 & x \leq -h \\ \frac{1}{h} & -h < x < 0 \end{cases} \quad (4.82)$$

$$\rho = -\rho_{n-1} \frac{x}{h} + \rho_n \left(1 + \frac{x}{h}\right) \quad -h < x < 0 \quad (4.83)$$

$$v = -v_{n-1} \frac{x}{h} + v_n \left(1 + \frac{x}{h}\right) \quad -h < x < 0 \quad (4.84)$$

$$\frac{\partial \rho}{\partial x} = \frac{\rho_n - \rho_{n-1}}{h} \quad -h < x < 0 \quad (4.85)$$

$$\frac{\partial v}{\partial x} = \frac{v_n - v_{n-1}}{h} \quad -h < x < 0 \quad (4.86)$$

#### 4.9.2. Diagonal volume matrix

$$\Omega_{\rho_l} = h \quad (1 < l < n) \quad (4.87)$$

$$\Omega_{\rho_1} = \Omega_{\rho_n} = \frac{1}{2}h \quad (4.88)$$

#### 4.9.3. Nodal vector of mass

$$m_l = h \rho_l \quad (1 < l < n) \quad (4.89)$$

$$m_1 = \frac{1}{2}h \rho_1 \quad (4.90)$$

$$m_n = \frac{1}{2}h \rho_n \quad (4.91)$$

#### 4.9.4. Inertia matrix

For the inner node, we have:

$$M_{l-1,l} = \int_{-h}^h \rho \phi_{v_{l-1}} \phi_{v_l} dx = \frac{h}{12} (\rho_{l-1} + \rho_l) \quad (4.92)$$

$$M_{l,l} = \int_{-h}^h \rho \phi_{v_l}^2 dx = \frac{h}{12} (\rho_{l-1} + 6\rho_l + \rho_{l+1}) \quad (4.93)$$

$$M_{l+1,l} = \int_{-h}^h \rho \phi_{v_l} \phi_{v_{l+1}} dx = \frac{h}{12} (\rho_l + \rho_{l+1}) \quad (4.94)$$

For the first and last nodes, we have:

$$M_{1,1} = \int_0^h \rho \phi_{v_1}^2 dx = \frac{h}{12} (3\rho_1 + \rho_2) \quad (4.95)$$

$$M_{2,1} = \int_0^h \rho \phi_{v_1} \phi_{v_2} dx = \frac{h}{12} (\rho_1 + \rho_2) \quad (4.96)$$

$$M_{n-1,n} = \int_{-h}^h \rho \phi_{v_{n-1}} \phi_{v_n} dx = \frac{h}{12} (\rho_{n-1} + \rho_n) \quad (4.97)$$

$$M_{n,n} = \int_{-h}^0 \rho \phi_{v_n}^2 dx = \frac{h}{12} (\rho_{n-1} + 3\rho_n) \quad (4.98)$$

The nodal vector of vehicle momentum results, for an inner node:

$$q_l = M_{l-1,l} v_{l-1} + M_{l,l} v_l + M_{l+1,l} v_{l+1} \quad (4.99)$$

For the first and last nodes, we have:

$$q_1 = M_{1,1} v_1 + M_{1,2} v_2 \quad (4.100)$$

$$q_n = M_{n-1,n} v_{n-1} + M_{n,n} v_n \quad (4.101)$$

### 4.9.5. Nodal vectors of potentials

The nodal vector of kinetic energy per unit vehicle results, for an inner node:

$$\begin{aligned}
 K_l &= \frac{1}{h} \int_{-h}^h \frac{1}{2} v^2 \phi_{\rho l} dx = \\
 &= \frac{1}{h} \int_{-h}^0 \frac{1}{2} \left[ -v_{l-1} \frac{x}{h} + v_l \left( 1 + \frac{x}{h} \right) \right]^2 \left( 1 + \frac{x}{h} \right) dx \\
 &\quad + \frac{1}{h} \int_0^h \frac{1}{2} \left[ v_l \left( 1 - \frac{x}{h} \right) + v_{l+1} \frac{x}{h} \right]^2 \left( 1 - \frac{x}{h} \right) dx
 \end{aligned} \tag{4.102}$$

$$K_l = \frac{1}{24} (v_{l-1}^2 + 2v_{l-1}v_l + 6v_l^2 + 2v_lv_{l+1} + v_{l+1}^2) \tag{4.103}$$

For the first and the last nodes, we have:

$$K_1 = \frac{2}{h} \int_0^h \frac{1}{2} v^2 \phi_{\rho 1} dx = \frac{1}{12} (3v_1^2 + 2v_1v_2 + v_2^2) \tag{4.104}$$

$$K_n = \frac{2}{h} \int_{-h}^0 \frac{1}{2} v^2 \phi_{\rho n} dx = \frac{1}{12} (v_{n-1}^2 + 2v_{n-1}v_n + 3v_n^2) \tag{4.105}$$

### 4.9.6. State equations, mass port

#### 4.9.6.1. Matrix $\underline{\underline{K}}$

For an inner node ( $1 < l < n$ ):

$$(K)_{l-1,l} = \frac{1}{\Omega_{\rho l}} \int_{\Omega} \kappa w_{\rho l-1} \phi_{\rho l} dx = \frac{1}{h} \int_{-h}^0 \frac{1}{2} v^2 w_{\rho l-1} \phi_{\rho l} dx \tag{4.106}$$

As  $w_{\rho l-1} = 1 - w_{\rho l}$  for  $(-h \leq x \leq 0)$ , it results:

$$\begin{aligned}
(K)_{l-1,l} &= \frac{1}{h} \int_{-h}^0 \frac{1}{2} v^2 (1 - w_{\rho l}) \phi_{\rho l} dx = \\
&= \frac{1}{h} \int_{-h}^0 \frac{1}{2} \left[ -v_{l-1} \frac{x}{h} + v_l \left( 1 + \frac{x}{h} \right) \right]^2 \left( -\frac{x}{h} \right) \left( 1 + \frac{x}{h} \right) dx
\end{aligned} \tag{4.107}$$

$$(K)_{l-1,l} = \frac{1}{120} (3v_{l-1}^2 + 4v_{l-1}v_l + 3v_l^2) \tag{4.108}$$

$$\begin{aligned}
(K)_{l,l} &= \frac{1}{\Omega_{\rho l}} \int_{\Omega} \kappa w_{\rho l} \phi_{\rho l} dx = \frac{1}{h} \int_{-h}^h \frac{1}{2} v^2 w_{\rho l} \phi_{\rho l} dx = \\
&= \frac{1}{h} \int_{-h}^0 \frac{1}{2} \left[ -v_{l-1} \frac{x}{h} + v_l \left( 1 + \frac{x}{h} \right) \right]^2 \left( 1 + \frac{x}{h} \right)^2 dx + \\
&+ \frac{1}{h} \int_0^h \frac{1}{2} \left[ v_l \left( 1 - \frac{x}{h} \right) + v_{l+1} \frac{x}{h} \right]^2 \left( 1 - \frac{x}{h} \right)^2 dx
\end{aligned} \tag{4.109}$$

$$(K)_{l,l} = \frac{1}{60} (v_{l-1}^2 + 3v_{l-1}v_l + 12v_l^2 + 3v_l v_{l+1} + v_{l+1}^2) \tag{4.110}$$

$$(K)_{l+1,l} = \frac{1}{\Omega_{\rho l}} \int_{\Omega} \kappa w_{\rho l+1} \phi_{\rho l} dx = \frac{1}{h} \int_0^h \frac{1}{2} v^2 w_{\rho l+1} \phi_{\rho l} dx \tag{4.111}$$

As  $w_{\rho l+1} = 1 - w_{\rho l}$  for  $(0 \leq x \leq h)$ , it results:

$$\begin{aligned}
(K)_{l+1,l} &= \frac{1}{h} \int_0^h \frac{1}{2} v^2 (1 - w_{\rho l}) \phi_{\rho l} dx \\
&= \frac{1}{h} \int_0^h \frac{1}{2} \left[ v_l \left( 1 - \frac{x}{h} \right) + v_{l+1} \frac{x}{h} \right]^2 \frac{x}{h} \left( 1 - \frac{x}{h} \right) dx
\end{aligned} \tag{4.112}$$

$$(K)_{l+1,l} = \frac{1}{120} (3v_l^2 + 4v_l v_{l+1} + 3v_{l+1}^2) \tag{4.113}$$

It is verified:

$$(K)_{l-1,l} + (K)_{l,l} + (K)_{l+1,l} = K_l \tag{4.114}$$

For the first node:

$$\begin{aligned}
(K)_{1,1} &= \frac{1}{\Omega_{\rho_1}} \int_{\Omega} \kappa w_{\rho_1} \phi_{\rho_1} dx = \frac{2}{h} \int_0^h \frac{1}{2} v^2 w_{\rho_1} \phi_{\rho_1} dx \\
&= \frac{2}{h} \int_0^h \frac{1}{2} \left[ v_1 \left( 1 - \frac{x}{h} \right) + v_2 \frac{x}{h} \right]^2 \left( 1 - \frac{x}{h} \right)^2 dx
\end{aligned} \tag{4.115}$$

$$(K)_{1,1} = \frac{1}{30} (6v_1^2 + 3v_1v_2 + v_2^2) \tag{4.116}$$

$$\begin{aligned}
(K)_{2,1} &= \frac{1}{\Omega_{\rho_1}} \int_{\Omega} \kappa w_{\rho_2} \phi_{\rho_1} dx = \frac{2}{h} \int_0^h \frac{1}{2} v^2 w_{\rho_2} \phi_{\rho_1} dx \\
&= \frac{2}{h} \int_0^h \frac{1}{2} v^2 (1 - w_{\rho_1}) \phi_{\rho_1} dx = \frac{2}{h} \int_0^h \frac{1}{2} \left[ v_1 \left( 1 - \frac{x}{h} + v_2 \frac{x}{h} \right) \right]^2 \frac{x}{h} \left( 1 - \frac{x}{h} \right) dx
\end{aligned} \tag{4.117}$$

$$(K)_{2,1} = \frac{1}{60} (3v_1^2 + 4v_1v_2 + 3v_2^2) \tag{4.118}$$

It is verified:

$$(K)_{1,1} + (K)_{2,1} = K_1 \tag{4.119}$$

For the last node:

$$\begin{aligned}
(K)_{n,n} &= \frac{1}{\Omega_{\rho_n}} \int_{\Omega} \kappa w_{\rho_n} \phi_{\rho_n} dx = \frac{2}{h} \int_{-h}^0 \frac{1}{2} v^2 w_{\rho_n} \phi_{\rho_n} dx \\
&= \frac{2}{h} \int_{-h}^0 \frac{1}{2} \left[ -v_{n-1} \frac{x}{h} + v_n \left( 1 + \frac{x}{h} \right) \right]^2 \left( 1 + \frac{x}{h} \right)^2 dx
\end{aligned} \tag{4.120}$$

$$(K)_{n,n} = \frac{1}{30} (v_{n-1}^2 + 3v_{n-1}v_n + 6v_n^2) \tag{4.121}$$

$$\begin{aligned}
(K)_{n-1,n} &= \frac{1}{\Omega_{\rho_n}} \int_{\Omega} \kappa w_{\rho_{n-1}} \phi_{\rho_n} dx = \frac{2}{h} \int_{-h}^0 \frac{1}{2} v^2 w_{\rho_{n-1}} \phi_{\rho_n} dx \\
&= \frac{2}{h} \int_{-h}^0 \frac{1}{2} v^2 (1 - w_{\rho_n}) \phi_{\rho_n} dx
\end{aligned} \tag{4.122}$$

$$= \frac{2}{h} \int_{-h}^0 \frac{1}{2} \left[ -v_{n-1} \frac{x}{h} + v_n \left( 1 + \frac{x}{h} \right) \right]^2 \left( -\frac{x}{h} \right) \left( 1 + \frac{x}{h} \right) dx$$

$$(K)_{n-1,n} = \frac{1}{60} (3v_{n-1}^2 + 4v_{n-1}v_n + 3v_n^2) \tag{4.123}$$

It is verified:

$$(K)_{n-1,n} + (K)_{n,n} = K_n \quad (4.124)$$

#### 4.9.6.2. Nodal vector $\underline{W}_B^{(\Gamma)}$

For an inner node ( $1 < l < n$ ):

$$W_{Bl}^{(\Gamma)} = 0 \quad (4.125)$$

For the first and last nodes:

$$W_{B1}^{(\Gamma)} = \kappa_1 \rho_1 v_1 = \frac{1}{2} \rho_1 v_1^3 \quad (4.126)$$

$$W_{Bn}^{(\Gamma)} = -\kappa_n \rho_n v_n = -\frac{1}{2} \rho_n v_n^3 \quad (4.127)$$

#### 4.9.6.3. Nodal vector $\underline{W}_B$

For an inner node ( $1 < l < n$ ):

$$\begin{aligned} W_{Bl} &= \int_{-h}^h \frac{\partial w_{\rho l}}{\partial x} \kappa \rho v dx = \int_{-h}^h \frac{\partial w_{\rho l}}{\partial x} \frac{1}{2} \rho v^3 dx \\ &= \frac{1}{h} \int_{-h}^0 \frac{1}{2} \left[ -\rho_{l-1} \frac{x}{h} + \rho_l \left( 1 + \frac{x}{h} \right) \right] \left[ -v_{l-1} \frac{x}{h} + v_l \left( 1 + \frac{x}{h} \right) \right]^3 dx \\ &\quad - \frac{1}{h} \int_0^h \frac{1}{2} \left[ \rho_l \left( 1 - \frac{x}{h} \right) + \rho_{l+1} \frac{x}{h} \right] \left[ v_l \left( 1 - \frac{x}{h} \right) + v_{l+1} \frac{x}{h} \right]^3 dx \end{aligned} \quad (4.128)$$

$$\begin{aligned} W_{Bl} &= \frac{1}{40} (4v_{l-1}^3 + 3v_{l-1}^2 v_l + 2v_{l-1} v_l^2 + v_l^3) \rho_{l-1} \\ &\quad + \frac{1}{40} (4v_{l-1}^3 + 2v_{l-1}^2 v_l + 3v_{l-1} v_l^2 - 3v_l^2 v_{l+1} - 2v_l v_{l+1}^2 - v_{l+1}^3) \rho_l \\ &\quad + \frac{1}{40} (-v_l^3 - 2v_l^2 v_{l+1} - 3v_l v_{l+1}^2 - 4v_{l+1}^3) \rho_{l+1} \end{aligned} \quad (4.129)$$

For the first and last nodes:

$$\begin{aligned} W_{B1} &= \int_0^h \frac{\partial w_{\rho_1}}{\partial x} \kappa \rho v dx = \int_0^h \frac{\partial w_{\rho_1}}{\partial x} \frac{1}{2} \rho v^3 dx \\ &= -\frac{1}{2} \int_0^h \frac{1}{2} \left[ \rho_1 \left( 1 - \frac{x}{h} \right) + \rho_2 \frac{x}{h} \right] \left[ v_1 \left( 1 - \frac{x}{h} \right) + v_2 \frac{x}{h} \right]^3 dx \end{aligned} \quad (4.130)$$

$$\begin{aligned} W_{B1} &= \frac{1}{40} \left( -4v_1^3 - 3v_1^2 v_2 - 2v_1 v_2^2 - v_2^3 \right) \rho_1 \\ &+ \frac{1}{40} \left( -v_1^3 - 2v_1^2 v_2 - 3v_1 v_2^2 - 4v_2^3 \right) \rho_2 \end{aligned} \quad (4.131)$$

$$\begin{aligned} W_{Bn} &= \int_{-h}^0 \frac{\partial w_{\rho_n}}{\partial x} \kappa \rho v dx = \int_{-h}^0 \frac{\partial w_{\rho_n}}{\partial x} \frac{1}{2} \rho v^3 dx \\ &= \frac{1}{h} \int_{-h}^0 \frac{1}{2} \left[ -\rho_{n-1} \frac{x}{h} + \rho_n \left( 1 + \frac{x}{h} \right) \right] \left[ -v_{n-1} \frac{x}{h} + v_n \left( 1 + \frac{x}{h} \right) \right]^3 dx \end{aligned} \quad (4.132)$$

$$\begin{aligned} W_{Bn} &= \frac{1}{40} \left( 4v_{n-1}^3 + 3v_{n-1}^2 v_n + 2v_{n-1} v_n^2 + v_n^3 \right) \rho_{n-1} \\ &+ \frac{1}{40} \left( v_{n-1}^3 + 2v_{n-1}^2 v_n + 3v_{n-1} v_n^2 + 4v_n^3 \right) \rho_n \end{aligned} \quad (4.133)$$

#### 4.9.6.4. Nodal vector $\underline{W}_K$

For an inner node ( $1 < l < n$ ):

$$\begin{aligned} W_{Kl} &= \int_{-h}^h w_{\rho_l} \rho v^2 \frac{\partial v}{\partial x} dx \\ &= \frac{(v_l - v_{l-1})}{h} \int_{-h}^0 \left( 1 + \frac{x}{h} \right) \left[ -\rho_{l-1} \frac{x}{h} + \rho_l \left( 1 + \frac{x}{h} \right) \right] \left[ -v_{l-1} \frac{x}{h} + v_l \left( 1 + \frac{x}{h} \right) \right]^2 dx \\ &+ \frac{(v_{l+1} - v_l)}{h} \int_0^h \left( 1 - \frac{x}{h} \right) \left[ \rho_l \left( 1 - \frac{x}{h} \right) + \rho_{l+1} \frac{x}{h} \right] \left[ v_l \left( 1 - \frac{x}{h} \right) + v_{l+1} \frac{x}{h} \right]^2 dx \end{aligned} \quad (4.134)$$

$$\begin{aligned}
W_{Kl} &= \frac{1}{60}(v_l - v_{l-1})(3v_{l-1}^2 + 4v_{l-1}v_l + 3v_l^2)\rho_{l-1} \\
&+ \frac{1}{60}\left[(v_l - v_{l-1})(2v_{l-1}^2 + 6v_{l-1}v_l + 12v_l^2) \right. \\
&+ (v_{l+1} - v_l)(12v_l^2 + 6v_lv_{l+1} + 2v_{l+1}^2)\left. \right]\rho_l \\
&+ \frac{1}{60}(v_{l+1} - v_l)(3v_l^2 + 4v_lv_{l+1} + 3v_{l+1}^2)\rho_{l+1}
\end{aligned} \tag{4.135}$$

For the first and last nodes:

$$\begin{aligned}
W_{K1} &= \int_0^h w_{\rho_1} \rho v^2 \frac{\partial v}{\partial x} dx \\
&= \frac{(v_2 - v_1)}{h} \int_0^h \left(1 - \frac{x}{h}\right) \left[ \rho_1 \left(1 - \frac{x}{h}\right) + \rho_2 \frac{x}{h} \right] \left[ v_1 \left(1 - \frac{x}{h}\right) + v_2 \frac{x}{h} \right]^2 dx \tag{4.136}
\end{aligned}$$

$$\begin{aligned}
W_{K1} &= \frac{1}{60}(v_2 - v_1)(12v_1^2 + 6v_1v_2 + 2v_2^2)\rho_1 \\
&+ \frac{1}{60}(v_2 - v_1)(3v_1^2 + 4v_1v_2 + 3v_2^2)\rho_2
\end{aligned} \tag{4.137}$$

$$\begin{aligned}
W_{Kn} &= \int_{-h}^0 w_{\rho_n} \rho v^2 \frac{\partial v}{\partial x} dx \\
&= \frac{(v_n - v_{n-1})}{h} \int_{-h}^0 \left(1 + \frac{x}{h}\right) \left[ -\rho_{n-1} \frac{x}{h} + \rho_n \left(1 + \frac{x}{h}\right) \right] \left[ -v_{n-1} \frac{x}{h} + v_n \left(1 + \frac{x}{h}\right) \right]^2 dx \tag{4.138}
\end{aligned}$$

$$\begin{aligned}
W_{Kn} &= \frac{1}{60}(v_n - v_{n-1})(3v_{n-1}^2 + 4v_{n-1}v_n + 3v_n^2)\rho_{n-1} \\
&+ \frac{1}{60}(v_n - v_{n-1})(2v_{n-1}^2 + 6v_{n-1}v_n + 12v_n^2)\rho_n
\end{aligned} \tag{4.139}$$

### 4.9.7. State equations, velocity port

#### 4.9.7.1. Nodal vector $\underline{F}_R$

We consider as a constat. For an inner node ( $1 < l < n$ ):

$$\begin{aligned}
 F_{Rl} &= \int_{-h}^h \rho \frac{v}{\tau} \phi_{vl} dx \\
 &= \frac{1}{\tau} \int_{-h}^0 \left[ -\rho_{l-1} \frac{x}{h} + \rho_l \left( 1 + \frac{x}{h} \right) \right] \left[ -v_{l-1} \frac{x}{h} + v_l \left( 1 + \frac{x}{h} \right) \right] \left( 1 + \frac{x}{h} \right) dx \\
 &\quad + \frac{1}{\tau} \int_0^h \left[ \rho_l \left( 1 - \frac{x}{h} \right) + \rho_{l+1} \frac{x}{h} \right] \left[ v_l \left( 1 - \frac{x}{h} \right) + v_{l+1} \frac{x}{h} \right] \left( 1 - \frac{x}{h} \right) dx
 \end{aligned} \quad (4.140)$$

$$F_{Rl} = \frac{h}{12\tau} (\rho_{l-1} + \rho_l) v_{l-1} + \frac{h}{12\tau} (\rho_{l-1} + 6\rho_l + \rho_{l+1}) v_l + \frac{h}{12\tau} (\rho_l + \rho_{l+1}) v_{l+1} \quad (4.141)$$

For the first and last nodes:

$$\begin{aligned}
 F_{R1} &= \int_0^h \rho \frac{v}{\tau} \phi_{v1} dx \\
 &= \frac{1}{\tau} \int_0^h \left[ \rho_1 \left( 1 - \frac{x}{h} \right) + \rho_2 \frac{x}{h} \right] \left[ v_1 \left( 1 - \frac{x}{h} \right) + v_2 \frac{x}{h} \right] \left( 1 - \frac{x}{h} \right) dx
 \end{aligned} \quad (4.142)$$

$$F_{R1} = \frac{h}{12\tau} (3\rho_1 + \rho_2) v_1 + \frac{h}{12\tau} (\rho_1 + \rho_2) v_2 \quad (4.143)$$

$$\begin{aligned}
 F_{Rn} &= \int_{-h}^0 \rho \frac{v}{\tau} \phi_{vn} dx \\
 &= \frac{1}{\tau} \int_{-h}^0 \left[ -\rho_{n-1} \frac{x}{h} + \rho_n \left( 1 + \frac{x}{h} \right) \right] \left[ -v_{n-1} \frac{x}{h} + v_n \left( 1 + \frac{x}{h} \right) \right] \left( 1 + \frac{x}{h} \right) dx
 \end{aligned} \quad (4.144)$$

$$F_{Rn} = \frac{h}{12\tau} (\rho_{n-1} + \rho_n) v_{n-1} + \frac{h}{12\tau} (\rho_{n-1} + 3\rho_n) v_n \quad (4.145)$$

#### 4.9.7.2. Nodal vector $\underline{F}_E$

We assume as the equilibrium relation:

$$v_e(\rho) = v_{\max} \left( 1 - \frac{\rho}{\rho_{\max}} \right) \quad (4.146)$$

where  $v_{\max}$  and  $\rho_{\max}$  are positive constants.

For an inner node ( $1 < l < n$ ):

$$\begin{aligned} F_{El} &= \int_{-h}^h \rho \frac{v_e}{\tau} \phi_{vl} dx \\ &= \frac{v_{\max}}{\tau} \int_{-h}^0 \left[ -\rho_{l-1} \frac{x}{h} + \rho_l \left( 1 + \frac{x}{h} \right) \right] \left\{ 1 - \frac{1}{\rho_{\max}} \left[ -\rho_{l-1} \frac{x}{h} + \rho_l \left( 1 + \frac{x}{h} \right) \right] \right\} \left( 1 + \frac{x}{h} \right) dx \\ &\quad + \frac{v_{\max}}{\tau} \int_0^h \left[ \rho_l \left( 1 - \frac{x}{h} \right) + \rho_{l+1} \frac{x}{h} \right] \left\{ 1 - \frac{1}{\rho_{\max}} \left[ \rho_l \left( 1 - \frac{x}{h} \right) + \rho_{l+1} \frac{x}{h} \right] \right\} \left( 1 - \frac{x}{h} \right) dx \end{aligned} \quad (4.147)$$

$$\begin{aligned} F_{El} &= \frac{hv_{\max}}{12\tau\rho_{\max}} \left[ \rho_{\max} (2\rho_{l-1} + 8\rho_l + 2\rho_{l+1}) - \rho_{l-1}^2 - 2\rho_{l-1}\rho_l \right. \\ &\quad \left. - 6\rho_l^2 - 2\rho_l\rho_{l+1} - \rho_{l+1}^2 \right] \end{aligned} \quad (4.148)$$

For the first and last nodes:

$$\begin{aligned} F_{E1} &= \int_0^h \rho \frac{v_e}{\tau} \phi_{v1} dx \\ &= \frac{v_{\max}}{\tau} \int_0^h \left[ \rho_1 \left( 1 - \frac{x}{h} \right) + \rho_2 \frac{x}{h} \right] \left\{ 1 - \frac{1}{\rho_{\max}} \left[ \rho_1 \left( 1 - \frac{x}{h} \right) + \rho_2 \frac{x}{h} \right] \right\} \left( 1 - \frac{x}{h} \right) dx \end{aligned} \quad (4.149)$$

$$F_{E1} = \frac{hv_{\max}}{12\tau\rho_{\max}} \left[ \rho_{\max} (4\rho_1 + 2\rho_2) - 3\rho_1^2 - 2\rho_1\rho_2 + \rho_2^2 \right] \quad (4.150)$$

$$\begin{aligned} F_{En} &= \int_{-h}^0 \rho \frac{v_e}{\tau} \phi_{vn} dx \\ &= \frac{v_{\max}}{\tau} \int_{-h}^0 \left[ -\rho_{n-1} \frac{x}{h} + \rho_n \left( 1 + \frac{x}{h} \right) \right] \left\{ 1 - \frac{1}{\rho_{\max}} \left[ -\rho_{n-1} \frac{x}{h} + \rho_n \left( 1 + \frac{x}{h} \right) \right] \right\} \left( 1 + \frac{x}{h} \right) dx \end{aligned} \quad (4.151)$$

$$F_{En} = \frac{h\nu_{\max}}{12\tau\rho_{\max}} \left[ \rho_{\max} (2\rho_{n-1} + 4\rho_n) - \rho_{n-1}^2 - 2\rho_{n-1}\rho_n - 3\rho_n^2 \right] \quad (4.152)$$

#### 4.9.7.3. Nodal vector $\underline{F}_G$ for the SG model

In the speed gradient (SG) model [Jia 02]:

$$G = c \frac{\partial v}{\partial x} \quad (4.153)$$

where  $c$  (assumed constant) is the propagation speed of small perturbations.

For an inner node ( $1 < l < n$ ):

$$\begin{aligned} F_{Gl} &= \int_{-h}^h \rho c \frac{\partial v}{\partial x} \phi_{vl} dx \\ &= c \frac{v_l - v_{l-1}}{h} \int_{-h}^0 \left[ -\rho_{l-1} \frac{x}{h} + \rho_l \left( 1 + \frac{x}{h} \right) \right] \left( 1 + \frac{x}{h} \right) dx \\ &\quad + c \frac{v_{l+1} - v_l}{h} \int_0^h \left[ \rho_l \left( 1 - \frac{x}{h} \right) + \rho_{l+1} \frac{x}{h} \right] \left( 1 - \frac{x}{h} \right) dx \end{aligned} \quad (4.154)$$

$$F_{Gl} = -\frac{1}{6}c(\rho_{l-1} + 2\rho_l)v_{l-1} - \frac{1}{6}c(\rho_{l+1} - \rho_{l-1})v_l + \frac{1}{6}c(2\rho_l + \rho_{l+1})v_{l+1} \quad (4.155)$$

For the first and last nodes:

$$\begin{aligned} F_{G1} &= \int_0^h \rho c \frac{\partial v}{\partial x} \phi_{v1} dx \\ &= c \frac{v_2 - v_1}{h} \int_0^h \left[ \rho_1 \left( 1 - \frac{x}{h} \right) + \rho_2 \frac{x}{h} \right] \left( 1 - \frac{x}{h} \right) dx \end{aligned} \quad (4.156)$$

$$F_{G1} = -\frac{1}{6}c(2\rho_1 + \rho_2)v_1 + \frac{1}{6}c(2\rho_1 + \rho_2)v_2 \quad (4.157)$$

$$F_{Gn} = \int_{-h}^0 \rho c \frac{\partial v}{\partial x} \phi_{vn} dx$$

$$= c \frac{v_n - v_{n-1}}{h} \int_{-h}^0 \left[ -\rho_{n-1} \frac{x}{h} + \rho_n \left( 1 + \frac{x}{h} \right) \right] \left( 1 + \frac{x}{h} \right) dx \quad (4.158)$$

$$F_{Gn} = -\frac{1}{6} c (\rho_{n-1} + 2\rho_n) v_{n-1} + \frac{1}{6} c (\rho_{n-1} + 2\rho_n) v_n \quad (4.159)$$

#### 4.9.7.4. Nodal vector $\underline{F_K}$

For an inner node ( $1 < l < n$ ):

$$\begin{aligned} F_{Kl} &= \int_{-h}^h \rho v \frac{\partial v}{\partial x} \phi_{v_l} dx \\ &= \frac{v_l - v_{l-1}}{h} \int_{-h}^0 \left[ -\rho_{l-1} \frac{x}{h} + \rho_l \left( 1 + \frac{x}{h} \right) \right] \left[ -v_{l-1} \frac{x}{h} + v_l \left( 1 + \frac{x}{h} \right) \right] \left( 1 + \frac{x}{h} \right) dx \\ &\quad + \frac{v_{l+1} - v_l}{h} \int_0^h \left[ \rho_l \left( 1 - \frac{x}{h} \right) + \rho_{l+1} \frac{x}{h} \right] \left[ v_l \left( 1 - \frac{x}{h} \right) + v_{l+1} \frac{x}{h} \right] \left( 1 - \frac{x}{h} \right) dx \quad (4.160) \\ F_{Kl} &= -\frac{1}{12} [v_{l-1} (\rho_{l-1} + \rho_l) + v_l (\rho_{l-1} + 3\rho_l)] v_{l-1} \\ &\quad + \frac{1}{12} [v_{l-1} (\rho_{l-1} + \rho_l) - v_l (\rho_{l+1} - \rho_{l-1}) - v_{l+1} (\rho_l + \rho_{l+1})] v_l \quad (4.161) \\ &\quad + \frac{1}{12} [v_l (3\rho_l + \rho_{l+1}) + v_{l+1} (\rho_l + \rho_{l+1})] v_{l+1} \end{aligned}$$

For the first and last nodes:

$$\begin{aligned} F_{K1} &= \int_0^h \rho v \frac{\partial v}{\partial x} \phi_{v_1} dx \\ &= \frac{v_2 - v_1}{h} \int_0^h \left[ \rho_1 \left( 1 - \frac{x}{h} \right) + \rho_2 \frac{x}{h} \right] \left[ v_1 \left( 1 - \frac{x}{h} \right) + v_2 \frac{x}{h} \right] \left( 1 - \frac{x}{h} \right) dx \quad (4.162) \end{aligned}$$

$$\begin{aligned} F_{K1} &= -\frac{1}{12} [v_1 (3\rho_1 + \rho_2) + v_2 (\rho_1 + \rho_2)] v_1 \\ &\quad + \frac{1}{12} [v_1 (3\rho_1 + \rho_2) + v_2 (\rho_1 + \rho_2)] v_2 \quad (4.163) \end{aligned}$$

$$F_{K_n} = \int_{-h}^0 \rho v \frac{\partial v}{\partial x} \phi_{v_n} dx$$

$$= \frac{v_n - v_{n-1}}{h} \int_{-h}^0 \left[ -\rho_{n-1} \frac{x}{h} + \rho_n \left( 1 + \frac{x}{h} \right) \right] \left[ -v_{n-1} \frac{x}{h} + v_n \left( 1 + \frac{x}{h} \right) \right] \left( 1 + \frac{x}{h} \right) dx \quad (4.164)$$

$$F_{K_n} = -\frac{1}{12} [v_{n-1} (\rho_{n-1} + \rho_n) + v_n (\rho_{n-1} + 3\rho_n)] v_{n-1}$$

$$+ \frac{1}{12} [v_{n-1} (\rho_{n-1} + \rho_n) + v_n (\rho_{n-1} + 3\rho_n)] v_n \quad (4.165)$$

#### 4.10. Implementation

Considers the following parameters:

$$h = 100 \text{ m}; \rho_{\max} = 0.25 \text{ veh/m}; v_{\max} = 33 \text{ m/s}; \tau = 10 \text{ s}; c = 11 \text{ m/s} \quad (4.166)$$

where  $h$  – the length of the section;

$c$  – the propagation speed of small perturbations;

$\tau$  – the reactive time;

$\rho_{\max}, v_{\max}$  – the maximal values for density and velocity.

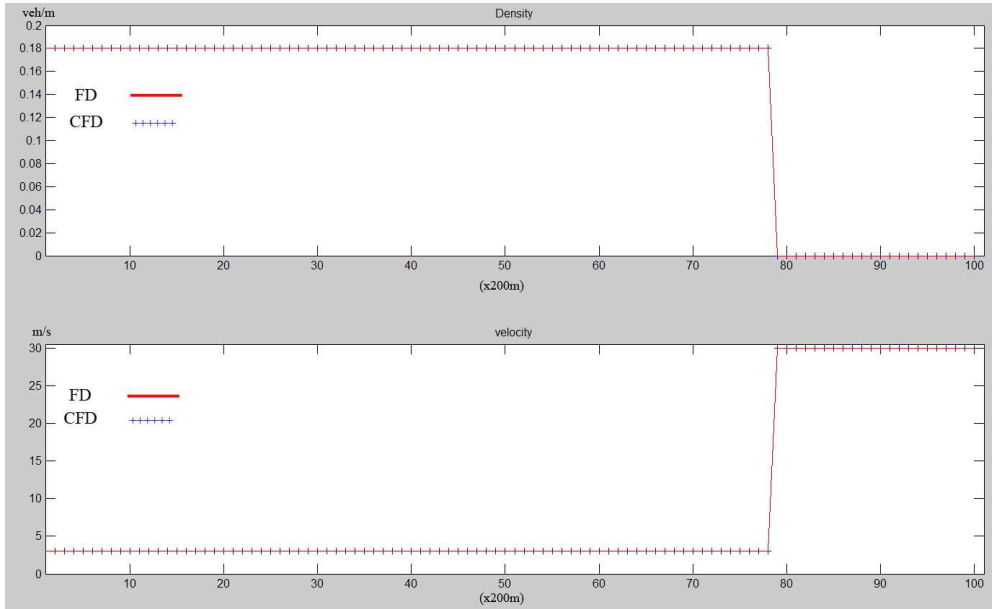
##### a) Comparison CFD and finite difference approach

In order to compare the time evolution of density and velocity obtained from the 2-equation method using CFD approach and finite difference numerical method, we have chosen Matlab as simulation medium.

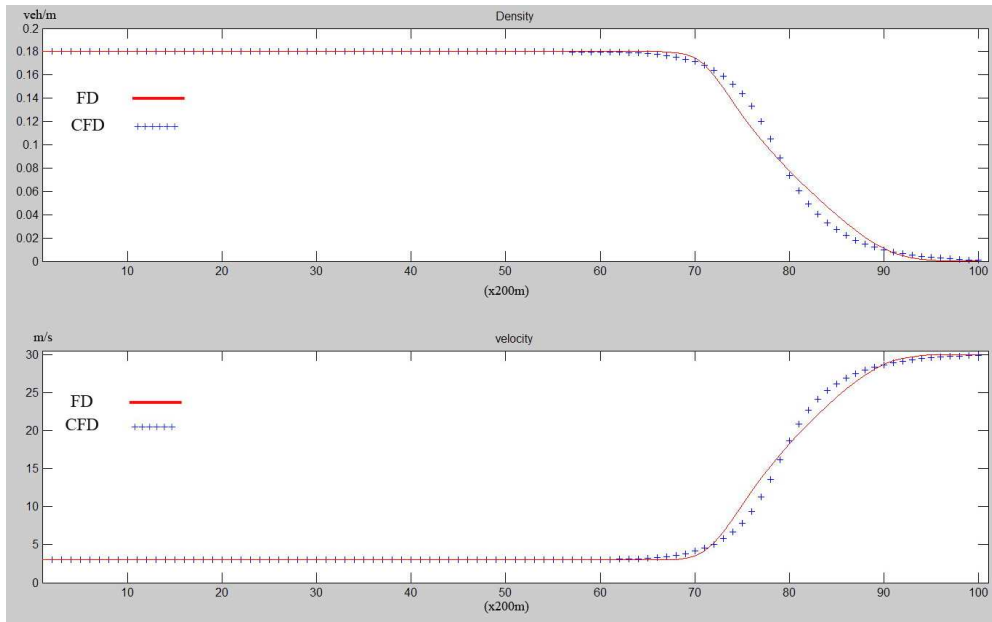
## Scenario 1: rarefaction wave

### Data:

$$\begin{aligned} \rho_{left} &= 0.18 \text{ veh/m}; \rho_{right} = 0.0 \text{ veh/m}; \\ v_{left} &= 3 \text{ m/s}; v_{right} = 30 \text{ m/s}; \end{aligned} \quad (4.167)$$



a)



b)

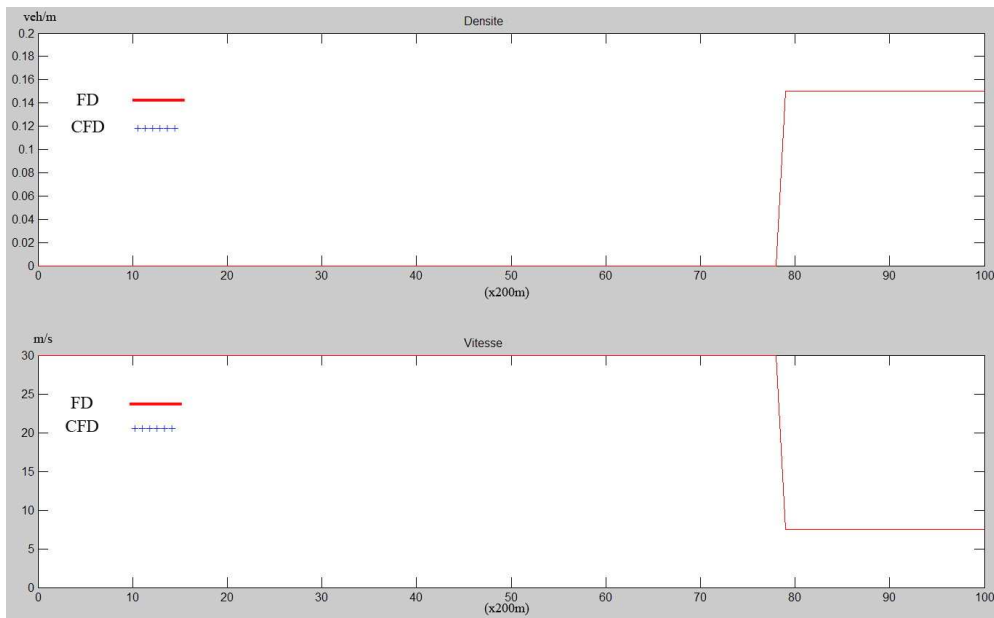
Fig. 4.11. Comparison CFD- FD: rarefaction wave.  
a) initial conditions  
b) values at t=60s

We consider the rarefaction wave, which appears in the case of a stop and go situation (red color) with the initial conditions presented in figure 4.11. a). The color change into green and the vehicles start to move to the right. We observe that after 60 seconds the shapes of the density and velocity are the same in finite differences (FD) as also in Computational Fluid Dynamic (CFD) approach (fig. 4.11. b)).

### Scenario 2: shock wave

#### Data:

$$\begin{aligned} \rho_{left} &= 0.0 \text{ veh}/m; \rho_{right} = 0.15 \text{ veh}/m; \\ v_{left} &= 30 \text{ m}/s; v_{right} = 7.5 \text{ m}/s; \end{aligned} \quad (4.168)$$



a)

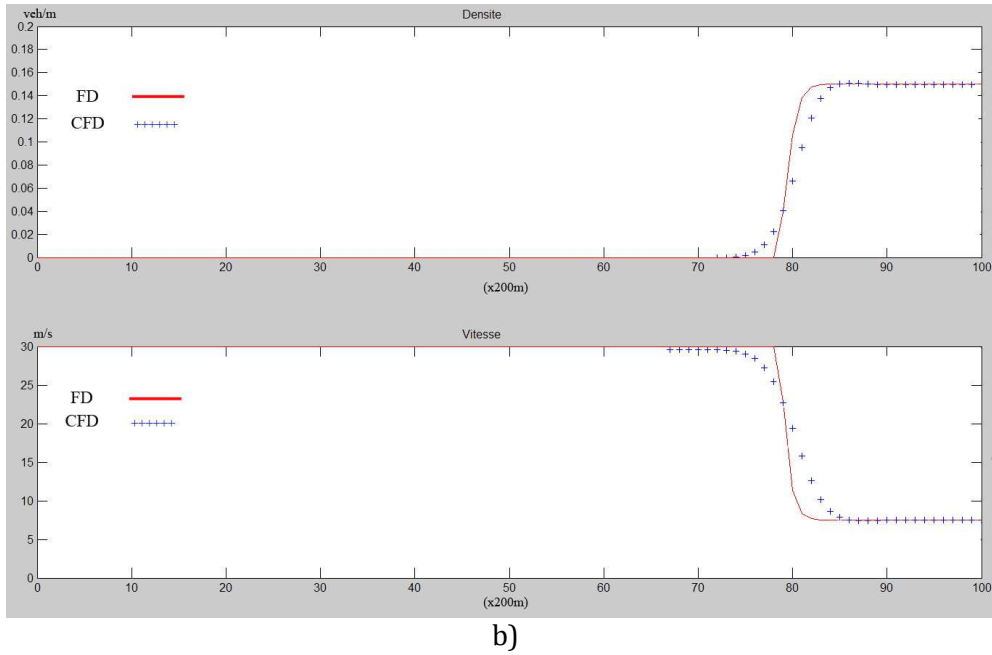


Fig.4.12. Comparison CFD- FD: shock wave.  
 c) initial conditions  
 d) values at t=40s

When we have a queue of vehicles that produce in the back a shock wave, with initial conditions presented in figure 4.12.a), after 40 second we obtain the graphic from figure 4.12.b). We have almost the same shape for the density and velocity in both cases with a little bump in the back of the front in the CFD approach. The bump appears due to the linear approximations used that have a  $C_0$  continuity near the discontinuity. To overcome this problem artificial diffusivity is used [Bes 85].

$$\mu = \frac{1}{1 + e^{-\gamma}} \quad (4.169)$$

$$\gamma = \frac{(\rho_{i+1} - \rho_{i-1})}{\rho_{\max}} \quad i = 2, \dots, n_p - 1$$

where  $n_p$  represent the number of elements.

We adjust the value of  $\Delta t$  in order to get the right velocity of propagation of shock wave [Jia 02].

$$U = \frac{q(\rho_2) - q(\rho_1)}{\rho_2 - \rho_1} \quad (4.170)$$

A smaller  $\Delta t$  will determine a smaller bump with diffusion in the back front and a velocity smaller than the propagation velocity of shock wave. A higher  $\Delta t$  will determine a higher bump, without diffusion in the back front and a higher velocity.

We can say that the model obtained by CFD approach satisfies the main characteristics that a traffic flow model must fulfill.

### b) Problems in the development of simulation

In simulation we met some problems concerning the apparition of singular matrices. In fluid dynamics, the field where the CFD approach is used, the density is considered to be different from zero on every segment so the matrices are matrices that have the entire diagonal element different from zero. In our application we met situation where we do not have vehicles on some sections thus the corresponding elements in the matrices are equal to zero conducting to singular matrices.

$$\begin{bmatrix} k_{11} & k_{12} & 0 & \dots & \dots & \dots & 0 \\ 0 & 0 & 0 & 0 & \dots & \dots & 0 \\ \dots & \dots & \dots & \dots & \dots & \dots & \dots \\ 0 & \dots & \dots & k_{n-1n-2} & k_{n-1n-1} & k_{n-1n} & \dots \\ 0 & \dots & \dots & \dots & k_{nn-1} & k_{nn} & \dots \end{bmatrix} \begin{bmatrix} \dot{m}_1 \\ \dot{m}_2 \\ \dots \\ \dots \\ \dot{m}_n \end{bmatrix} = \begin{bmatrix} w_{b1}^i \\ w_{b2}^i \\ \dots \\ \dots \\ w_{bn}^i \end{bmatrix} \quad (4.171)$$

To overcome this problem we apply the following steps:

- 1) we find the lines with all elements equal to zero and put one on the diagonal;
- 2) we put the value from the previous step in the right vector of the system.

$$\begin{bmatrix} k_{11} & k_{12} & 0 & \dots & 0 \\ 0 & \mathbf{1} & 0 & 0 & \dots & 0 \\ \dots & \dots & \dots & \dots & \dots & \dots \\ 0 & \dots & \dots & k_{n-1n-2} & k_{n-1n-1} & k_{n-1n} \\ 0 & \dots & \dots & k_{nn-1} & k_{nn} & \dots \end{bmatrix} \begin{bmatrix} \dot{m}_1 \\ \dot{m}_2 \\ \vdots \\ \dot{m}_n \end{bmatrix} = \begin{bmatrix} w_{b1}^i \\ w_{b2}^{i-1} \\ \vdots \\ w_{bn}^i \end{bmatrix} \tag{4.172}$$

**c) Further development**

As a further development we propose a structure composed by a number of elements that are concatenated to obtain the structure of the entire road.

The decomposed structure of the entire road in bond graph representation is illustrated in fig. 4.13, where we chose only three cells. In theory, the number of cells should be infinite to have a perfect representation of the distributed phenomena. Each section has the same structure which can be called “generic”.

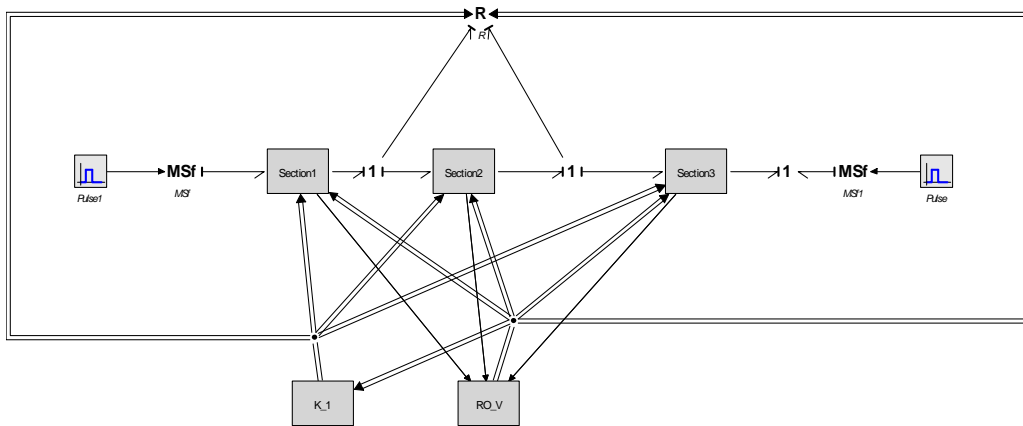


Fig.4.13. Three sections model

At the section level the structure is represented in fig. 4.14, where can be found the different bond graph elements presented before.



Some limitations in the simulation have been pointed out. They are due to the fact that some singularities appear in the matrices to be inverted, due to null values of density or velocity which may occur during the simulation. Specific algorithms have to be developed to solve this problem and allow simulations in all cases.

**Conclusions**

**Future developments**



## Conclusions - Future developments

Modeling and simulation of distributed parameter systems are heavy tasks. Approximations have to be performed either on the PDE model itself or on its solution for simulation purpose.

The objectives of the thesis were to combine PDE models and bond graph approach, with application to traffic flow.

In chapter 1, some classical methods used for approximation of partial differential equations are recalled and the corresponding bond graph model is designed. For each of them advantages and drawbacks are presented.

In the second chapter, the port-Hamiltonian approach for distributed parameter system is presented.

The port Hamiltonian system has been used in the representation of the distributed parameter systems. Through the example of the telegrapher's equation, we have shown [Che 09] that using a special form of discretization for space we made the calculation only on one element, considered as local and then concatenating the elements we can calculate the entire line of transmission.

The port Hamiltonian system is derived from the energy function (Hamiltonian), which is usually a good Lyapunov function, used in control.

In the third chapter, the main models used for traffic flow representation are presented and some of them are implemented in simulation. A comparison is done on one hand on different numerical

methods applied on the first class of models (1-equation model) and on the other hand between 1-equation and 2- equation models.

In chapter 4, we have proposed an original approach extending Computational Fluid Dynamics bond graph representation to traffic flow, using Jiang's model [Jia 02].

A theoretical development of a bond graph approach for representing the two-equation traffic model was developed. The state equations were obtained in terms of the state variables, which resulted from nodal values of mass and velocity.

The set of generalized effort and flow variables was derived based on energy considerations, while the state equations are obtained as a Petrov-Galerkin formulation for the mass port and a Galerkin formulation for the velocity port; as a consequence, the computational tools developed for the Finite Element Method, as well for other numerical methods, can be used to solve the resulting state equations.

Regarding the CFD approach, some work are still to be done:

- development of a solver algorithm dealing with singularities in matrices;
- determination of the right number of sections to use to have a stabilized solution;
- more precise study on velocity and comparison with LWR model in different scenarios.

Further developments in the area of traffic flow study are wide and promising:

- the proposed CFD bond graph model concerns a road, it has now to be extended to crossing sections;
- the road is supposed to be single line. It could be extended to two line road as highway;
- we supposed that we have the same type of vehicles. It could be extended considering different types of vehicles, with different velocities;

- the road is supposed to be without ramp. We can study the case where we have a entry/exit ramp;
- the model is an open loop model, with no perturbations. A control strategy [Nak 05a], [Nak 05b], [Nak 07], linked to traffic flow objectives, has to be studied. The state space model derived from bond graph can be used.



## References



## References

- [Ada 36] W. F. Adams (1936). "*Road Traffic Considered as a Random Series*", J. Inst. Civil Engineers, 4, pp. 121-130, U.K
- [Aer 94] M. van Aerde (1994). "*INTEGRATION: A model for simulating integrated traffic networks*", Transportation System Research Group
- [Ago 85] V. Agochkov, "*Introduction aux méthodes des éléments finis*", Mir, 1985
- [And 95] J.D. Anderson (1995). "*Computational Fluid Dynamics: the basic with application*", McGraw-Hill
- [Arn 89] V. I. Arnold, A. Weinstein, and K. Vogtmann. (1989) "*Mathematical Methods of Classical Mechanics*", Springer-Verlag
- [Aw 00] A. Aw, M. Rascle (2000). "Resurrection of "second order" models of traffic flow", SIAM J. Appl. Math. 60, pp.916-938
- [Baa 08] A.Baaiu, F. Couenne, Y. Le Gorrec, L. Lefevre, M. Tayakout (2008). "*Port based modelling of a multiscale adsorption column*", Mathematical and Computer Modelling of Dynamical Systems, Volume 14, Issue 3 , pp. 195 – 211

- [Bal 06] J.L. Balino, A.E. Larreteguy, E.F. Gandolfo Raso (2006). "*A general bond graph approach for computational fluid dynamics*", Simulation Modelling Practice and theory 14, pp.884-908
- [Bes 85] D.E. Beskos, P.G. Michalopoulos, J.K. Lin (1985). "*Analysis of traffic flow by the finite element method*", Appl. Mathematics Modelling, vol. 9, pp.358-364
- [Bey 78] Beylich (1978). "*Elements of a kinetic theory of traffic flow*", Proceeding of the Eleventh International Symposium on Rarefied Gas-Dynamics, Vol.1, Cannes, France, pp.129-138
- [Bos 91] A.Bossavit, C. Emson and I. Mayergoyz, (1991). "*Méthodes numériques en électromagnétisme*", Eyrolles (Paris).
- [Bot 78] H. Botma (1978). "*State-of-the-art report "Traffic flow models"*", Research Report R-78-40, SWOV
- [Bra 76] D.Branston (1976). "*Models of single lane time headway distributions*", Transportation Science 10, pp.125-148
- [Buc 68] D.J. Buckley (1968). "*A semi-poisson model of traffic flow*", Transportation Science 2(2), pp.107-132
- [Cha 58] R. E. Chandler, R. Herman and E. W. Montroll (1958). "*Traffic Dynamics: Studies in Car Following*", Opns. Res. 6, pp. 165-183
- [Cha 58] R.E. Chandler, R. Herman, E.W. Montroll (1958). "*Traffic dynamics: studies in car following*", Operation Research 6, pp.165-184

- [Che 07] C. Chera, A. Nakrachi, Dauphin Tanguy.(2007) "*Approximation of the telegrapher's equations with dissipation*", IFAC MCPL 2007, Sibiu, Romania
- [Che 09] C. Chera, A. Nakrachi, G. Dauphin-Tanguy, D.Popescu (2009). "*Approximation of a dissipative system with Dirac structure conservation: Case study*", Mathmod'09, Wien
- [Che 09] C. Chera, A. Nakrachi, G. Dauphin-Tanguy, D.Popescu (2009). "*Whitney Forms for an Infinite Dimensional port-Hamiltonian System Approximation*", CSCS-17, Bucarest, Roumanie
- [Col 02] R.M. Colombo (2002) "*On a 2x2 hyperbolic traffic flow model*", Math. Comput. Modelling, 35, pp. 683-688
- [Cou 90] T.J. Courant (1990). "*Dirac manifolds*", Trans. American Math. Soc., 319, pp.631-661
- [Cuv 86] C. Cuvelier, A. Segal, A. van Steenhoven (1986). "*Finite Element methods and Navier-Stokes Equations*", D.Reidel Publishing Company, Holland
- [Dag 95] C.F. Daganzo (1995). "*The cell transmission model part II: Network traffic*", Transportation Research Part B 29 (2), pp.79-93
- [Dal 99] M. Dalsmo & A.J. van der Schaft (1999). "*On representations and integrability of mathematical structures in energy-conserving physical systems*", SIAM J. Control and Optimization, 37, pp.54-91
- [Dat 05] A.W.Date (2005). "*Introduction to Computational Fluid Dynamics*", Cambridge University Press
- [Dau 00] G. Dauphin-Tanguy & all, "*Les bond graph*", Hermes, 2000

- [Der 05] A. Derkaoui, E. Bideaux, S. Scavarda, "*Finite Element local structure assembly and shape functions influence on bond graph modelling*", International Conference on Bond Graph Modeling and Simulation (ICBGM'05), New Orleans, SUA, 2005
- [Der 05] A. Derkaoui (2005). "*Dimensionnement sous des critères dynamiques et énergétiques de systèmes mécatroniques comportant des sous-systèmes à paramètres répartis- Approche par méthode inverse*", Doctorat soutenu le 18 novembre 2005 à l'INSA de Lyon
- [Des 06] Desbrun M., Kanso E., Tong Y. (2006). "*Discret Differential Forms for Computational Modeling*", SIGGRAPH
- [Dij 98] T. Dijkstra, P.H. Bovy, R. Vermijs (1998). "*Car-following under congested conditions: empirical findings*", Transport Research Record 1644, pp.20-28
- [Dor 93] I. Dorfman (1993). "*Dirac Structures and Integrability of Nonlinear Evolution Equations*", John Wiley
- [Ess 99] J.L. Esser, L. Neubert, J. Wahle, M. Schreckenberg (1999). "*Microscopic online simulations of urban traffic*", Proceedings of the 14<sup>th</sup> International Symposium of Transportation and Traffic Theory, Jerusalem, pp.517-534.
- [For 58] T.W. Forbes, H.J. Zagorski, E.L. Holshouser and W.A. Deterline (1958). "*Measurement of driver reactions to tunnel conditions*", Highway Research Board, Proceedings 37, pp. 345-357
- [Gaz 61] D.C. Gazis, R. Herman, R.W. Rothery (1961). "*Nonlinear follow the leader models of traffic flow*", Operation Research 9, pp.545-567

- [Ger 87] P. Germain-Lacour, "*Mathématique et CAO. Volume 3*", Hermes, 1987
- [Goa 06] P. Goatin (2006). "*The Aw-Rascle vehicular traffic flow model with phase transitions*", *Mathematical and Computer Modelling* 44, p287-303
- [Gol 02] G. Golo, V. Talasila, A.J. van der Schaft, (2002). "*Approximation of the telegrapher's equations*", *41<sup>st</sup> IEEE conf. on decision and control*, Las Vegas
- [Gol 04] G. Golo, V. Talasila, A.J. van der Schaft, B.M. Maschke, (2004). "*Hamiltonian discretization of boundary control systems*", *Automatica*, vol. 40/5, pp. 757--711.
- [Gre 35] B. D. Greenshields (1935). "*A Study in Highway Capacity*" Highway Research Board, Proceedings, Vol. 14, p. 458.
- [Gre 47] B. D. Greenshields, D. Schapiro and E. L. Erickson (1947). "*Traffic Performance at Urban Intersections*", Bureau of Highway Traffic, Technical Report No. 1. Yale University Press, New Haven, CT.
- [Gue 63] A.O. Guelfond, "*Calcul des différences finies*", Dunod, 1963
- [Hel 97] D. Helbing (1997). "*Modeling multi-lane traffic flow with queuing effects*" *Physica A* 242, pp.175-194
- [Her 92] R. Herman (1992). "*Technology, Human Interaction, and Complexity: Reflections on Vehicular Traffic Science*", *Operations Research*, 40(2), pp. 199-212.

- [Hir 07] C.Hirsch (2007). "*Numerical computation of internal & external flows. Vol.1. Fundamentals of Computational Fluid Dynamics*", John Wiley & Sons
- [Hol 95] H. Holden, N.H. Risebro (1995). "*A mathematical model of traffic flow on a network of unidirectional roads*", SIAM Journal on Mathematical Analysis 26 (4), pp.999–1017
- [Hoo 98] S.P.Hoogendoorn, P.H.L. Bovy (1998). "*A new estimation technique for vehicle-type specific headway distributions*", Transportation Research Record 1646, pp.18-28
- [Hoo 00] S.P.Hoogendoorn, P.H.L. Bovy (2000). "*Modelling multiple user-class traffic flow*", Transportation Research B (34)2, pp.123-146
- [Hoo 01] S.P. Hoogendoorn, P.H.L. Bovy (2001). "*State-of-the-art of vehicular traffic flow modelling*", *Proceedings of the Institution of Mechanical Engineers*, **215** (1): 283–303.
- [Jes 98] M. Jespen (1998). "*On the speed-flow relationships in road traffic: a model of driver behaviour*", Proceedings for the Third International Symposium on Highway capacity, 279-313, Copenhagen, Danemark
- [Jia 02] R. Jiang et al (2002). "*A new continuum model for traffic flow and numerical tests*", Transportation Research Part B 36, pp. 405-419
- [Jiy 08] T. Jiyuan, Guan Heng, Chaoqun Liu (2008). "*Computational Fluid Dynamics: a practical approach*", Elsevier
- [Kan 06] K. Kang, Chris Weinberger, Wei Cai (2006). "*A Short Essay on Variational Calculus*", Department of Mechanical Engineering, Stanford University

- [Kar 90] D.C. Karnopp, D.L. Margolis, R.C. Rosenberg, "*System dynamics: a unified approach*", John-Wiley & Sons, 1990
- [Ker 00] B.S. Kerner (2000). "*Phase transitions in traffic flow*", Traffic and Granular Flow '99, pp.253-283, Springer Verlag
- [Kla 98] A. Klar, Wegener (1998). "*A hierarchy of models for multilane vehicular traffic I & II: modelling*", SIAM Journal of Applied Mathematics
- [Leb 96] J.P. Lebacque (1996). "*The Godunov scheme and what it means for first order traffic flow models*", The International Symposium on Transportation and Traffic Theory, Lyon, France
- [Leu 88] W. Leutzbach (1988). "*An introduction to the theory of traffic flow*", Springer-Verlag, Berlin
- [LeV 92] R. LeVeque (1992). "*Numerical methods for conservation laws*", Birkhäuser Verlag
- [Lew 91] P.E.Lewis, "*The finite element method- Principles and applications*", Addison-Wesley, 1991
- [Lig 55] M.H. Lighthill, G.B. Whitham (1955) "*On kinematic waves II: a theory of traffic flow on long, crowded roads*", Proceeding of the Royal Society of London series A, 229, pp.317-345
- [Loh 01] R.Lohner (2001). "*Applied CFD Techniques: An Introduction Based on Finite element Method*", John Wiley & Sons
- [Mas 05] B.M. Maschke, A.J. van der Schaft, (2005). "*Compositional Modelling of Distributed-Parameter Systems*", pp. 115--154 in /Advanced Topics in Control Systems Theory,/ Lecture Notes

from FAP 2004, Springer Lect. Notes in Control and Information Sciences 311, Springer, London

[Mon 61] E.W. Montroll (1961). "*Acceleration noise and clustering tendency of vehicular traffic*", Hermand, Theory of traffic flow, pp.147-157

[Nag 96] K. Nagel (1996). "*Particle hopping models and traffic flow theory*", Physical Review E 53, pp.4655-4672

[Nag 98] K.Nagel (1998). "*From particle hopping models to traffic flow theory*", Transportation Research Record 1644, pp. 1-9

[Nak 03] A. Nakrachi, G. Dauphin-Tanguy (2003). "*Bond Graph for distributed parameter systems : The telegrapher equation case*", IMACS-IEEE "CESA'03" Lille

[Nak 05a] A. Nakrachi, C. Chera, C. Lupu et I. Matei (2005). "*Flexible modelling in adaptive control applications*", IMACS 2005, Paris, France

[Nak 05b] A. Nakrachi, C. Chera (2005). "*Air-stream and temperature plant remote control*", IMAACA 2005, Marseilles, France

[Nak 07] A. Nakrachi, C. Chera, N.Christov et C. Petrescu (2007). "*Remote control for multivariable systems*", CSCS-16, Bucarest, Roumanie

[Nel 95] P. Nelson (1995). "*A kinetic theory of vehicular traffic and its associated bimodal equilibrium solutions*", Transport Theory and Statistical Physics 24(1-3), pp.383-409

- [Nel 97] P. Nelson, D.D.Bui, A. Sopasakis (1997). "A novel traffic stream model deriving from a bimodal kinetic equilibrium", Proceeding of the IFAC conference, pp.799-804
- [New 55] G.F. Newell (1955). "Mathematical Models for Freely Flowing Highway Traffic", Operations Research 3, pp. 176-186.
- [Ort 01] R. Ortega, A.J. van der Schaft, I. Mareels, & B.M. Maschke (2001). "Putting energy back in control", *Control Systems Magazine*, 21, pp. 18-33
- [Pap 03] M. Papageorgiou et all. (2003). "Review of road traffic control strategies", Proceedings of the IEEE, vol. 91, Nr.12
- [Pav 75] S.L. Paveri-Fontana (1975). "On Boltzmann-like treatments for traffic flow: a critical review of the basic model and an alternative proposal for dilute traffic analysis", Transportation Research B 9, pp.225-235
- [Pay 71] H.J. Payne (1971). "Models of freeway traffic and control", Math. Models Publ. Sys, 28, pp.51-61
- [Pig 73] L.J. Pignataro (1973). "Traffic engineering- theory and practice", Prentice-Hall, Englewood Cliffs
- [Pip 53] L.A. Pipes (1953). "An Operational Analysis of Traffic Dynamics", J. Appl. Phys., 24(3), pp. 274-281.
- [Pri 61] I. Prigogine (1961). "A Boltzmann-like approach to the statistical theory of traffic flow", Theory of traffic flow
- [Pri 71] I. Prigogine, R.Herman (1971). "Kinetic theory of vehicular traffic", American Elsevier New-York

- [Ram 06] P. Ramkrishna, (2006). "*On Analysis and Control of Interconnected Finite and Infinite-dimensional Physical Systems*", Phd Thesis, University of Twente, Nederland.
- [Red 93] J.N.Reddy, "*An introduction to the finite element method*", McGraw-Hill, 1993
- [Ric 56] P.I.Richards (1956). "*Shockwaves on the highway*", Opns. Research, 4, pp.42-51
- [Sab 86] J.C. Sabonnadiere, J.L.Coulomb, "*Eléments finis et CAO*", Hermes, 1986
- [Sch 02] A.J. van der Schaft, (2002). "*Port-Hamiltonian systems: network modeling and control of nonlinear physical systems*", pp. 127--168 in *Advanced Dynamics and Control of Structures and Machines*, CISM Courses and lectures No. 444, CISM International Centre for Mechanical Sciences, Udine, Italy, April 15--19, 2002 (Eds. H. Irshik, K. Schlacher), Springer, Wien, New York, 2004.
- [Sch 05] A.J. van der Schaft, (2005). "*Theory of port-Hamiltonian systems. Chapter 3: Compositional modelling of distributed-parameter systems*"
- [Sch 95] A.J. van der Schaft & B.M. Maschke (1995) "*The Hamiltonian formulation of energy conserving physical systems with external ports*", Archiv für Elektronik und Übertragungstechnik, 49, pp. 362-371
- [Str 04] J.C. Strikwerda, "*Finite Difference Schemes and Partial Differential Equations*", SIAM, 2004

- [Wan 07] X.P. Wang, "*Partial differential equations and applications*", Société mathématique de France, 2007
- [War 52] J.G. Wardrop (1952). "*Some Theoretical Aspects of Road Traffic Research*", Proceedings of the Institution of Civil Engineers, Part II, 1(2), pp. 325-362, U.K.
- [Whi 56] G.B. Whitham (1974). "*Linear and nonlinear waves*", New York: Wiley
- [Whi 99] G.B. Whitham (1999). "*Linear and Nonlinear Waves*", John Wiley & Sons
- [Wu 99] N. Wu, W. Brilon (1999). "*Cellular automata for highway traffic flow simulation*", Proceeding 14<sup>th</sup> International Symposium on transport and traffic theory, pp.1-18
- [Zha 02] H.M. Zhang (2002). "*A non-equilibrium traffic model devoid of gas-like behavior*", Transportation Research Part B 36, pp.275-290
- [Zha 98] H.M. Zhang (1998). "*A theory of non-equilibrium traffic flow*", Transportation Research B 32 (7), pp.485-498



# **Appendices**



## Appendices 1

### 1.1. The weak formulation [Red 93]

The development of weighted-integral statement of a differential equation is made to have  $N$  linearly independent algebraic relations among the coefficient  $b_i$  of the approximation:

$$u \approx U_N = \sum_{i=1}^N b_i \phi_i(x) + \phi_0(x) \quad (\text{A.1.1})$$

This is accomplished by choosing  $N$  linearly independent weight functions in the integral statement.

To develop the weak form there are three steps that must be followed:

1) To express the original equation in the weighted-integral or weighted-residual statement.

We make this by moving all expressions to one side, multiplying the entire equation by a function  $w$ , called the weight function and integrating over the domain  $\Omega = (0, L)$ .

If we consider the equation (A.1.2):

$$-\frac{d}{dx} \left( EA(x) \frac{du}{dx} \right) = q(x) \quad \forall x \in \Omega \quad (\text{A.1.2})$$

$$u(0) = u_0, \quad EA \frac{du}{dx} \Big|_{x=L} = Q_0 \quad (\text{A.1.3})$$

we have:

$$0 = \int_0^L w \left[ -\frac{d}{dx} \left( EA(x) \frac{du}{dx} \right) - q \right] dx \quad (\text{A.1.4})$$

The integral statement allows us to choose  $N$  linearly independent functions for  $w$  and obtain  $N$  equations for  $b_1, b_2, \dots, b_N$ . The weight function can be any nonzero integral function.

2) The approximation functions  $\phi_i$  must be of the form that make  $U_N$  differentiable as many times as called for in the original differential equation and satisfies the specified boundary conditions.

If the differentiation is distributed between the approximate solution  $U_N$  and the weight function  $w$ , the resulting integral form will require weakened continuity conditions on  $\phi_j$ , and hence the weighted-integral statement is called the weak form. The weak formulation has two characteristics: it requires weaker continuity of the dependent variable and the natural boundary conditions of the problem are included in the weak form, and therefore the approximate solution  $U_N$  is required to satisfy only the essential boundary conditions of the problem.

Integrating first term by parts we obtain:

$$\begin{aligned} 0 &= \int_0^L \left\{ w \left[ -\frac{d}{dx} \left( EA(x) \frac{du}{dx} \right) \right] - wq \right\} dx \\ &= \int_0^L \left( \frac{dw}{dx} EA(x) \frac{du}{dx} - wq \right) dx - \left[ wEA(x) \frac{du}{dx} \right]_0^L \end{aligned} \tag{A.1.5}$$

To identify the natural and essential boundary conditions we must do the following:

After completing step 2, we must examine all boundary terms of the integral statement, which will involve both the dependent variable and the weight function.

Coefficient of the weight function and its derivative on the boundary expression constitutes the natural boundary conditions NBC. In our case  $\left( EA(x) \frac{du}{dx} \right)$ .

The dependent variable of the problem, expressed in the same form as the weight function appearing in the boundary term, constitutes the essential boundary conditions (EBC).

The weak form is:

$$\begin{aligned}
 0 &= \int_0^L \left( EA(x) \frac{dw}{dx} \frac{dv}{dx} - wq \right) dx - \left[ wEA(x) \frac{du}{dx} \right]_0^L \\
 &= \int_0^L \left( EA(x) \frac{dw}{dx} \frac{du}{dx} - wq \right) dx - \left( wEA(x) \frac{du}{dx} n_x \right) \Big|_{x=0} \\
 &\quad - \left( wEA(x) \frac{du}{dx} n_x \right) \Big|_{x=L} \\
 &= \int_0^L \left( EA(x) \frac{dw}{dx} \frac{du}{dx} - wq \right) dx - (wQ)_0 - (wQ)_L
 \end{aligned} \tag{A.1.6}$$

where  $n_x$  -cosine of the angle between the  $x$  axis and the normal to the boundary.

3) To impose in the weak formulation the boundary conditions of the problem under consideration.

$$w(0) = 0 \text{ because } u(0) = u_0$$

$$\text{Since } w(0) = 0 \text{ and } Q(L) = \left( EA(x) \frac{du}{dx} \right) \Big|_{x=L} = Q_0, \text{ (A.1.6) reduces to}$$

the expression:

$$0 = \int_0^L \left( EA(x) \frac{dw}{dx} \frac{du}{dx} - wq \right) dx - w(L)Q_0 \tag{A.1.7}$$

With the weak formulation we pass from a punctual formulation, where  $u$  is an application defined on the space of continuum derivable functions, named classical formulation, to a formulation where we rewrite the relations between functions through integrals.

The weak formulation uses an approximation of the unknown variable using a base of functions, named base functions or form functions in finite element approximation or projection function in the case of spectral methods. It simplifies the problem giving equivalent to initial problem new equations.

When we have a problem with multiple dimensions, to reduce the derivation order of one unity, we apply the Green formula, which is the generalization for multiple dimensions of the integration by parts formula:

$$\int_{\Omega} u \frac{\partial w}{\partial x_i} d\Omega = - \int_{\Omega} \frac{\partial u}{\partial x_i} w d\Omega + \int_{\partial\Omega} uw \cdot n_{x_i} d(\partial\Omega) \quad (\text{A.1.8})$$

where  $n_{x_i}$  is the normal to  $\partial\Omega$  in the  $x_i$  direction.

The integration by parts form is:

$$\int_a^b u \frac{\partial u}{\partial x} dx = - \int_a^b \frac{\partial u}{\partial x} w dx + [uw]_a^b \quad (\text{A.1.9})$$

Starting from the weak formulation, the approximation methods like finite elements and spectral methods give a general approximation of the variable  $u$  using the two relations and put the approximation

under the form  $u_N(x,t) = \sum_{i=0}^N b_i(t)\phi_i(x)$ , where  $\phi_i$  are used as basis

functions.

The new unknowns are now the  $b_i$  which are found solving the new system:

$$Kb_i = F_i \quad (\text{A.1.10})$$

where  $K$  and  $F$  depend by  $\phi_i$  and  $w$ .

## 1.2. The Bond Graph [Kar 90]

A bond graph is composed of bonds (half arrows and elements). The bonds carry 2 variables, effort variable  $e$  and flow variable  $f$  whose product  $P=ef$  is the instantaneous power carried by the bond.

### Passive elements

They can be elements which dissipate energy as heat or store energy.

The 1-port **resistor** is represented by **R**:

$$\begin{array}{c} e \\ \hline f \end{array} \rightarrow R$$

There is a static relation between effort and flow variables. It is a energy dissipative element.

The constitutive relation between  $e$  and  $f$  is:

$$\begin{aligned} \Phi_R(e,f) &= 0 \quad \text{or} \quad e - R \cdot f = 0 \quad \text{in the linear case} \\ \text{Power} &= e \cdot f \end{aligned} \quad (\text{A.1.11})$$

An electrical resistor, a mechanical damper or dashpot, porous plug in fluid lines, and other analogous passive elements can be represented using this element.

The 1-port **capacitor** is represented by **C**:

$$\begin{array}{c} e \\ \hline f = dq/dt \end{array} \rightarrow C$$

There is a static constitutive relation between an effort ( $e$ ) and a displacement ( $q$ ). It is an element which stores and gives up energy without loss.

$$q = \int_{-\infty}^t f dt \quad (\text{A.1.12})$$

$$\Phi_C(e, \int f dt) = 0 \quad (\text{A.1.13})$$

In physical terms, the analogy is a spring, a torsion bar, an electrical capacitor, a gravity tank or an accumulator.

The 1-port **inertial** is represented by **I**:

$$\begin{array}{c} e = dp/dt \\ \hline f \end{array} \rightarrow I$$

It is a storage energy element, characterized by a static constitutive law between the flow ( $f$ ) and the momentum ( $p$ ).

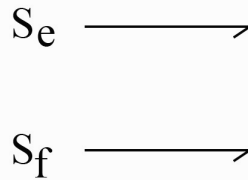
$$p = \int_{-\infty}^t e dt \quad (\text{A.1.14})$$

$$\Phi_t \left( \int e dt, f \right) = 0 \quad (\text{A.1.15})$$

It is used to model inductance in electrical systems and mass or inertia effects in mechanical or fluid systems.

### Active elements

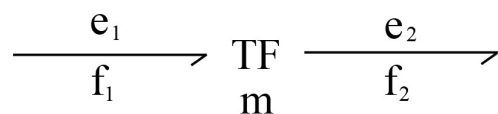
The source is used to supply power to the model and impresses either an effort or a flow. We have **effort source** ( $S_e$ ) and **flow source** ( $S_f$ ):



### Junction elements

They are used to connect passive and active elements. They are power conservative.

The 2-port **transformer** element is represented by **TF**:

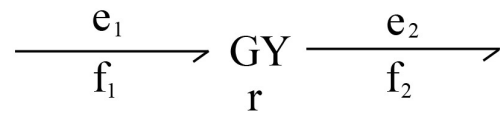


The constitutive laws to dimension the modulus  $m$  are:

$$\begin{aligned} e_1 &= m e_2 \\ f_2 &= m f_1 \end{aligned} \quad (\text{A.1.16})$$

It can represent an electrical transformer, a rigid lever or a hydraulic ram.

In the same class of elements we find the 2-port **gyrator** represented by **GY**:



The constitutive laws to dimension  $r$  are:

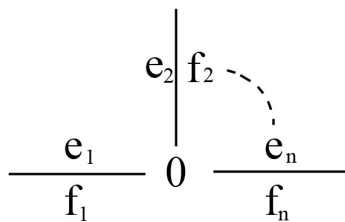
$$\begin{aligned} e_1 &= rf_2 \\ e_2 &= rf_1 \end{aligned} \quad (\text{A.1.17})$$

It is used in motor models or for physical domain change without power loss.

The **0-junction** or common effort junction it is characterized by the properties:

- the efforts on all bonds are identical;
- the algebraic sum of all flows always vanishes.

$$\begin{aligned} e_1 &= e_2 = \dots = e_n \\ \sum_{i=1}^n f_i &= 0 \end{aligned} \quad (\text{A.1.18})$$



The **1-junction** of common flow junction has the properties:

- all the bond has the same flow;
- the algebraic sum of all efforts always vanishes.

$$\begin{aligned} f_1 &= f_2 = \dots = f_n \\ \sum_{i=1}^n e_i &= 0 \end{aligned} \quad (\text{A.1.19})$$

$$\frac{e_1}{f_1} \quad 1 \quad \frac{e_n}{f_n}$$

The diagram shows a central node labeled '1'. To the left of node '1', there is a horizontal line with 'e<sub>1</sub>' above it and 'f<sub>1</sub>' below it. To the right of node '1', there is a horizontal line with 'e<sub>n</sub>' above it and 'f<sub>n</sub>' below it. Above node '1', there is a vertical line with 'e<sub>2</sub>' to its left and 'f<sub>2</sub>' to its right. A dashed arc connects 'e<sub>2</sub>' and 'f<sub>2</sub>'.

## Appendices 2

### 2.1. The Dirac structure [Sch 05]

In the port-Hamiltonian system formalism, the physical system can be expressed in terms of energy exchange, as a network, with the elements interconnected and these connections are non-dissipative, with the power balance through connection equal to zero. This is represented by a Dirac structure.

If we consider two dual linear spaces:  $F$  a  $\ell$ -dimensional one, and  $F^*$  its dual, the product space  $F \times F^*$  is considered to be the space of power variables.

The power is defined by

$$P = \langle f^* | f \rangle, \quad (f, f^*) \in F \times F^* \quad (\text{A.1.20})$$

where  $\langle f^* | f \rangle$  is the dual product.

$F$  is called the space of *flows*  $f$ , and  $F^*$  the space of *efforts*  $e$ . The power of an element  $(f, e) \in F \times F^*$  is denoted as  $\langle e | f \rangle$ .

If  $F$  is endowed with an *inner product* structure  $\langle, \rangle$ , then  $F^*$  can be naturally identified with  $F$  in such a way that  $\langle e | f \rangle = \langle e, f \rangle$ ,  $f \in F, e \in F^* \simeq F$ .

On  $F \times F^*$  can be seen that there exist a canonically defined symmetric bilinear form

$$\langle (f_1, e_1), (f_2, e_2) \rangle_{F \times F^*} := \langle e_1 | f_2 \rangle + \langle e_2 | f_1 \rangle \quad (\text{A.1.21})$$

for  $f_i \in F, e_i \in F^*, i = 1, 2$ .

If consider a linear subspace, with dimension  $p$ :

$$S \subset F \times F^* \quad (\text{A.1.22})$$

its orthogonal complement with respect to the bilinear form  $\langle, \rangle_{F \times F^*}$  on  $F \times F^*$ , is denoted as

$$S^\perp \subset F \times F^* \quad (\text{A.1.23})$$

and has dimension  $2\ell - p$ . ( $\dim(F \times F^*) = 2\ell$ , and  $\langle, \rangle_{F \times F^*}$  is a non-degenerate form.)

**Definition.** A constant Dirac structure on  $F$  is a linear subspace  $D \subset F \times F^*$  such that  $D = D^\perp$ .

Result that the dimension of  $D$  on a  $\ell$ -dimensional linear space is equal to  $\ell$ .

Let  $(f, e) \in D = D^\perp$ . Then

$$0 = \langle (f, e), (f, e) \rangle_{F \times F^*} = 2 \langle e | f \rangle \quad (\text{A.1.24})$$

Thus for all  $(f, e) \in D$  we obtain

$$\langle e | f \rangle = 0 \quad (\text{A.1.25})$$

Hence a Dirac structure  $D$  on  $F$  defines a power-conserving relation between the power variables  $(f, e) \in F \times F^*$ .

**Different matrix representations of a Dirac structure.**

Let  $F$  be a  $\ell$ -dimensional space. We define a constant Dirac structure  $D \subset F \times F^*$ . Then  $D$  can be represented as

1. (Kernel and Image representation)

$$D = \{(f, e) \in F \times F^* \mid Ff + Ee = 0\} \quad (\text{A.1.26})$$

for  $\ell \times \ell$  matrices  $F$  and  $E$  satisfying

$$\begin{aligned} EF^T + FE^T &= 0 \\ \text{rank}[F \mid E] &= \ell \end{aligned} \quad (\text{A.1.27})$$

Equivalently,

$$D = \{(f, e) \in F \times F^* \mid f = E^T \lambda, e = F^T \lambda, \lambda \in \mathbb{R}^\ell\} \quad (\text{A.1.28})$$

2. (Constrained input-output representation)

$$D = \{(f, e) \in F \times F^* \mid f = Je + G\lambda, G^T e = 0\} \quad (\text{A.1.29})$$

for an  $\ell \times \ell$  skew-symmetric matrix  $J$ , and a matrix  $G$  such that  $\text{Im } G = \{f \mid (f, 0) \in D\}$ . Furthermore,  $\text{Ker } J = \{e \mid (0, e) \in D\}$ .

### 3. (Hybrid input-output representation)

Let  $D$  be given as in 1. Suppose  $\text{rank } F = \ell^1 (\leq \ell)$ . Select  $\ell^1$  independent columns of  $F$ , and group them into a matrix  $F^1$ . Write (possibly after permutation)  $F = [F^1 \mid E^2]$ ,  $f = \begin{bmatrix} f^1 \\ f^2 \end{bmatrix}$ ,  $e = \begin{bmatrix} e^1 \\ e^2 \end{bmatrix}$ . Then the matrix  $[F^1 \mid E^2]$  can be shown to be invertible, and

$$D = \left\{ \left( \begin{array}{c} f^1 \\ f^2 \end{array} \right), \left( \begin{array}{c} e^1 \\ e^2 \end{array} \right) \middle| \left( \begin{array}{c} f^1 \\ e^2 \end{array} \right) = J \left( \begin{array}{c} e^1 \\ f^2 \end{array} \right) \right\} \quad (\text{A.1.30})$$

with  $J := -[F^1 \mid E^2]^{-1} [F^2 \mid E^1]$  skew-symmetric.

## 2.2. Stokes-Dirac structures [Sch 05]

Let  $Z$  be an  $n$ -dimensional smooth manifold with smooth  $(n-1)$ -dimensional boundary  $\partial Z$ , representing the space of spatial variables.

Denote by  $\Omega^k(Z)$ ,  $k = 0, 1, \dots, n$ , the space of exterior  $k$ -forms on  $Z$ , and by  $\Omega^k(\partial Z)$ ,  $k = 0, 1, \dots, n-1$ , the space of  $k$ -forms on  $\partial Z$ . (Note that  $\Omega^0(Z)$ , respectively  $\Omega^0(\partial Z)$ , is the space of smooth functions on  $Z$ , respectively  $\partial Z$ .) Clearly,  $\Omega^k(Z)$  and  $\Omega^k(\partial Z)$  are (infinite-dimensional) linear spaces (over  $\mathbb{R}$ ). Furthermore, there is a natural pairing between  $\Omega^k(Z)$  and  $\Omega^{n-k}(Z)$  given by

$$\langle \beta \mid \alpha \rangle := \int_Z \beta \wedge \alpha \quad (\in \mathbb{R}) \quad (\text{A.1.31})$$

with  $\alpha \in \Omega^k(Z)$ ,  $\beta \in \Omega^{n-k}(Z)$ , where  $\wedge$  is the usual wedge product of differential forms yielding the  $n$ -form  $\beta \wedge \alpha$ . In fact, the pairing (A.1.31)

is non-degenerate in the sense that if  $\langle \beta | \alpha \rangle = 0$  for all  $\alpha$ , respectively for all  $\beta$ , then  $\beta = 0$ , respectively  $\alpha = 0$ .

Similarly, there is a pairing between  $\Omega^k(\partial Z)$  and  $\Omega^{n-1-k}(\partial Z)$  given by

$$\langle \beta | \alpha \rangle := \int_{\partial Z} \beta \wedge \alpha \quad (\text{A.1.32})$$

with  $\alpha \in \Omega^k(\partial Z)$ ,  $\beta \in \Omega^{n-1-k}(\partial Z)$ . Now let us define the linear space

$$\mathcal{F}_{p,q} := \Omega^p(Z) \times \Omega^q(Z) \times \Omega^{n-p}(\partial Z) \quad (\text{A.1.33})$$

for any pair  $p, q$  of positive integers satisfying

$$p + q = n + 1 \quad (\text{A.1.34})$$

and correspondingly let us define

$$E_{p,q} := \Omega^{n-p}(Z) \times \Omega^{n-q}(Z) \times \Omega^{n-q}(\partial Z) \quad (\text{A.1.35})$$

Then the pairing (A.1.31) and (A.1.32) yields a (non-degenerate) pairing between  $\mathcal{F}_{p,q}$  and  $E_{p,q}$ . Symmetrization of this pairing yields the following bilinear form on  $\mathcal{F}_{p,q} \times E_{p,q}$  with values in  $\mathbb{R}$ :

$$\begin{aligned} & \ll (f_p^1, f_q^1, f_b^1, e_p^1, e_q^1, e_b^1), (f_p^2, f_q^2, f_b^2, e_p^2, e_q^2, e_b^2) \gg := \\ & \int_Z [e_p^1 \wedge f_p^2 + e_q^1 \wedge f_q^2 + e_p^2 \wedge f_p^1 + e_q^2 \wedge f_q^1] \\ & + \int_{\partial Z} [e_b^1 \wedge f_b^2 + e_b^2 \wedge f_b^1] \end{aligned} \quad (\text{A.1.36})$$

where for  $i = 1, 2$

$$\begin{aligned} f_p^i & \in \Omega^p(Z), f_q^i \in \Omega^q(Z) \\ e_p^i & \in \Omega^{n-p}(Z), e_q^i \in \Omega^{n-q}(Z) \\ f_b^i & \in \Omega^{n-p}(\partial Z), e_b^i \in \Omega^{n-q}(\partial Z) \end{aligned} \quad (\text{A.1.37})$$

The spaces of differential forms  $\Omega^p(Z)$  and  $\Omega^q(Z)$  will represent the energy variables of two different physical energy domains interacting with each other, while  $\Omega^{n-p}(\partial Z)$  and  $\Omega^{n-q}(\partial Z)$  will denote the boundary variables whose (wedge) product represents the boundary energy flow.

**Theorem.** Consider  $\mathbb{F}_{p,q}$  and  $E_{p,q}$  given in (A.1.33), (A.1.35) with  $p, q$  satisfying (A.1.34), and bilinear form  $\langle\langle, \rangle\rangle$  given by (A.1.36). Define the following linear subspace  $D$  of  $\mathbb{F}_{p,q} \times E_{p,q}$

$$D = \left\{ (f_p, f_q, f_b, e_p, e_q, e_b) \in \mathbb{F}_{p,q} \times E_{p,q} \mid \begin{aligned} \begin{bmatrix} f_p \\ f_q \end{bmatrix} &= \begin{bmatrix} 0 & (-1)^r d \\ d & 0 \end{bmatrix} \begin{bmatrix} e_p \\ e_q \end{bmatrix}, \\ \begin{bmatrix} f_b \\ e_b \end{bmatrix} &= \begin{bmatrix} 1 & 0 \\ 0 & -(-1)^{n-q} \end{bmatrix} \begin{bmatrix} e_p|_{\partial Z} \\ e_q|_{\partial Z} \end{bmatrix} \end{aligned} \right\} \quad (\text{A.1.38})$$

where  $|_{\partial Z}$  denotes restriction to the boundary  $\partial Z$ , and  $r := pq + 1$ . Then  $D = D^\perp$ , that is,  $D$  is a *Dirac structure*.

### 2.3. Differential forms [Des 06], [Cou 90]

A *differential form* is an integrand, i.e., a quantity that can be integrated. It is the  $dx$  in  $\int dx$  and the  $dx dy$  in  $\int dx dy$ . More precisely, consider a smooth function  $F(x)$  over an interval in  $\mathbb{R}$ . Now, define  $f(x)$  to be its derivative, that is,

$$f(x) = \frac{dF}{dx} \quad (\text{A.1.39})$$

Rewriting this last equation (using slightly abusive notations for simplicity) yields  $dF = f(x)dx$ , which leads to:

$$\int_a^b dF = \int_a^b f(x)dx = F(b) - F(a) \quad (\text{A.1.40})$$

This last equation is known as the Newton-Leibnitz formula, or the first fundamental theorem of calculus. The integrand  $f(x)dx$  is called a *1-form*, because it can only be integrated over any 1-dimensional (1D) real interval. Similarly, for a function  $G(x,y,z)$ , we have:

$$dG = \frac{\partial G}{\partial x} dx + \frac{\partial G}{\partial y} dy + \frac{\partial G}{\partial z} dz \quad (\text{A.1.41})$$

which can be integrated over any 1D curve in  $\mathbb{R}^3$ , and is also a 1-form. More generally, a  $k$ -form can be described as an entity ready to be integrated on a  $kD$  (sub)region. Note that forms are valued zero on (sub)regions that are of higher or lower order dimension than the original space; for example, 4-forms are zero on  $\mathbb{R}^3$ .

Let consider the  $n$ -dimensional Euclidean space  $\mathbb{R}^n$ ,  $n \in \mathbb{N}$  and let  $M$  be an open region  $M \subset \mathbb{R}^n$ ;  $M$  is also called a  $n$ -manifold. The vector space  $T_x M$  consists of all the (tangent) vectors at a point  $x \in M$  and can be identified with  $\mathbb{R}^n$  itself. A  $k$ -form  $w^k$  is a rank- $k$ , skew-symmetric, tensor field over  $M$ . That is, at each point  $x \in M$ , it is a multi-linear map that takes  $k$  tangent vectors as input and returns a real number:

$$w^k : T_x M \times \dots \times T_x M \rightarrow \mathbb{R} \quad (\text{A.1.42})$$

which changes of sign when you switch two variables.

There are seven operators in Exterior Calculus:

- $d$ : the exterior derivatives, that extends the notion of the differential of a function to differential forms;
- $\star$ : the Hodge star, that transforms  $k$ -forms into  $(n-k)$ -forms;
- $\wedge$ : the wedge product, that extends the notion of exterior product to forms;
- $\sharp$  and  $\flat$ : the sharp and flat operators, that, given a metric, transforms a 1-form into a vector and vice-versa;
- $i_X$ : the interior product with respect to a vector field  $X$  (also called contraction operator), a concept dual to the exterior product;
- $L_X$ : the Lie derivative with respect to a vector field  $X$ , that extends the notion of directional derivative.

A  **$k$ -simplex** is a generic term to describe the simplest mesh element of dimension  $k$ - hence the name.

Let consider a three-dimensional mesh in space. This mesh is made of a series of adjacent tetrahedral. The vertices are said to form a 0-simplex. The edges form a 1-simplex; the faces form a 2-simplex. The adjacent tetrahedrals form a 3-simplex.

Formally, a  $k$ -simplex  $\sigma_k$  is the non-degenerate convex hull of  $k+1$  geometrically distinct points  $v_0, \dots, v_k \in \mathbb{R}^n$  with  $n \geq k$ . In other words, it is the intersection of all convex sets containing  $(v_0, \dots, v_k)$ ; namely:

$$\sigma_k = \left\{ x \in \mathbb{R}^n \mid x = \sum_{i=0}^k \alpha^i v_i \text{ with } \alpha^i \geq 0 \text{ and } \sum_{i=0}^k \alpha^i = 1 \right\} \quad (\text{A.1.43})$$

The entities  $v_0, \dots, v_k$  are called the *vertices* and  $k$  is called the dimension of the  $k$ -simplex, which we will denote as:

$$\sigma_k = \{v_0 v_1 \dots v_k\} \quad (\text{A.1.44})$$

An  $n$ -dimensional **discrete manifold**  $M$  is an  $n$ -dimensional simplicial complex that satisfies the following condition: for each simplex, the union of all the incident  $n$ -simplices forms an  $n$ -dimensional ball (i.e., a disk in  $2D$ , a ball in  $3D$ , etc.), or half a ball if the simplex is on the boundary. As a consequence, each  $(n-1)$ -simplex has exactly two adjacent  $n$ -simplices - or only one if it is on a boundary.

**Stokes' Theorem.**  $d$  applied to an arbitrary form  $w$  is evaluated on an arbitrary simplex  $\sigma$  as follows:

$$\int_{\sigma} dw = \int_{\partial\sigma} w \quad (\text{A.1.45})$$

The **wedge product**  $\wedge$  is an operation used to construct higher degree forms from lower degree ones. Let consider  $\alpha$  a 1-form and  $\beta$  a 2-form on a subset  $T \subset \mathbb{R}^4$ . Their wedge product  $\alpha \wedge \beta$  is a 3-form on  $T$ .

Given an inner product denoted  $\langle, \rangle$ , defined as the product of two  $k$ -forms  $\in \Omega^k(M)$ , which will measure in a way, the projection of one onto the other, the operator  $\star$ , called the **Hodge star**, maps a  $k$ -form to a complementary  $(n-k)$ -form:

$$\star: \Omega^k(M) \rightarrow \Omega^{n-k}(M) \quad (\text{A.1.46})$$

and is defined to satisfy the following equality:

$$\alpha \wedge \star \beta = \langle \alpha, \beta \rangle \mu^n \quad (\text{A.1.47})$$

for any pair of  $k$ -forms  $\alpha$  and  $\beta$  ( $\mu^n$  is the volume form).

## 2.4. Interpolation [Des 06]

### 2.4.1. Interpolating 0-forms

For linear interpolation of 0-forms to the whole space, we can use the vertex-based linear interpolation basis, the *hat function* in Finite Element literature. With each vertex  $v_i$  is associated a basis denoted as  $\varphi_i$ :

$$\varphi_i = 1 \quad \text{at } v_i, \quad \varphi_i = 0 \quad \text{at } v_j \neq v_i \quad (\text{A.1.48})$$

while  $\varphi_i$  linearly goes to zero in the one-ring neighborhood of  $v_i$ . These functions are the *barycentric coordinates*, introduced by Möbius in 1827 as mass points to define a coordinate-free geometry.

If we denote a vertex  $v_j$  by  $\sigma_j$ , with this basis we have:

$$\int_{v_j} \varphi_{v_i} = \int_{\sigma_j} \varphi_{\sigma_i} = \int_{\sigma_j} \varphi_i = \begin{cases} 1 & \text{if } i = j \\ 0 & \text{if } i \neq j \end{cases} \quad (\text{A.1.49})$$

### 2.4.2. Interpolating 1-forms

For the 1-forms interpolation we use the *Whitney* 1-form associated with an edge  $\sigma_{ij}$  between  $v_i$  and  $v_j$ .

$$\varphi_{\sigma_{ij}} = \varphi_i d\varphi_j - \varphi_j d\varphi_i \quad (\text{A.1.50})$$

We have:

$$\int_{\sigma_{kl}} \varphi_{\sigma_{ij}} = \begin{cases} 1 & \text{if } i = k \text{ and } j = l \\ -1 & \text{if } i = l \text{ and } j = k \\ 0 & \text{otherwise} \end{cases} \quad (\text{A.1.51})$$

This is zero when at least one vertex is not on the edge. Along the edge  $\sigma_{ij}$ , we have  $\varphi_i + \varphi_j = 1$ . Thus:

$$\int_{\sigma_{ij}} \varphi_{\sigma_{ij}} = \int_{\varphi_i=1}^{\varphi_i=0} (\varphi_i d(1-\varphi_i) - (1-\varphi_i) d\varphi_i) = \int_{\varphi_i=1}^{\varphi_i=0} (-d\varphi_i) = 1 \quad (\text{A.1.52})$$

## 2.5. Functionals [Kan 06]

An integral expression of the form:

$$I(u) = \int_a^b F(x, u, u') dx, \quad u = u(x), \quad u' = \frac{du}{dx} \quad (\text{A.1.53})$$

where the integrand  $F(x, u, u') dx$  is a given function with the argument  $x$ ,  $u$  and  $du/dx$ , is called a **functional**. The value  $I(u)$  of the integral depends on  $u$ ; hence the notation  $I(u)$  is appropriate. However, for a given  $u$ ,  $I(u)$  represents a scalar value. Mathematically, a functional is an operator  $I$  mapping  $u$  into a scalar  $I(u)$ .

### 2.5.1. The variational symbol

Consider the function  $F=F(x, u, u')$ . For an arbitrary fixed value of the independent variable  $x$ ,  $F$  depends on  $u$  and  $u'$ . The change  $\mu v$  in  $u$ , where  $\mu$  is a constant and  $v$  is a function, is called **the variation of  $u$**  and is denoted by  $\delta u$ :

$$\delta u = \mu v \quad (\text{A.1.54})$$

The operator  $\delta$  is called the **variational symbol**. The variation  $\delta u$  of a function  $u$  represents an admissible change in the function  $u(x)$  at a fixed value of the independent variable  $x$ . If  $u$  is specified at a point, the variation of  $u$  is zero there because the specified value cannot be varied, thus the variation of a function  $u$  should satisfy the homogenous form of the boundary conditions for  $u$ . The variation  $\delta u$  in  $u$  is a virtual

change. Associated with this change in  $u$ , there is a change in  $F$ . In analogy with the total differential of a function of two variables, the first variation of  $F$  at  $u$  is defined by

$$\delta F = \frac{\partial F}{\partial u} \delta u + \frac{\partial F}{\partial u'} \delta u' \quad (\text{A.1.55})$$

Note the analogy between the first variation (above) and the total differential of  $F$ ,

$$dF = \frac{\partial F}{\partial x} dx + \frac{\partial F}{\partial u} du + \frac{\partial F}{\partial u'} du' \quad (\text{A.1.56})$$

Since  $x$  is not varied during the variation of  $u$  to  $u + \delta u$ ,  $dx=0$  and the analogy between  $\delta F$  and  $dF$  becomes apparent. That is,  $\delta$  acts as a differential operator with respect to dependent variables. It can easily be verified that the laws of variation of sums, products, ratios, powers, and so forth are completely analogous to the corresponding laws of differentiation. For example, if  $F_1 = F_1(u)$  and  $F_2 = F_2(u)$  then

$$\delta(F_1 \pm F_2) = \delta F_1 \pm \delta F_2 \quad (\text{A.1.57})$$

$$\delta(F_1 F_2) = F_2 \delta F_1 + F_1 \delta F_2 \quad (\text{A.1.58})$$

$$\delta\left(\frac{F_1}{F_2}\right) = \frac{F_2 \delta F_1 - F_1 \delta F_2}{F_2^2} \quad (\text{A.1.59})$$

$$\delta[(F_1)^n] = n(F_1)^{n-1} \delta F_1 \quad (\text{A.1.60})$$

Furthermore, the variational operator can commute with differential and integral operators:

$$\frac{d}{dx}(\delta u) = \frac{d}{dx}(\mu v) = \mu \frac{dv}{dx} = \mu v' = \delta u' = \delta\left(\frac{du}{dx}\right) \quad (\text{A.1.61})$$

$$\delta \int_a^b u(x) dx = \int_a^b \delta u(x) dx \quad (\text{A.1.62})$$

### 2.5.2. Functional derivative

For a function with multiple arguments,  $f(x_1, x_2, \dots, x_n)$ , if the differential  $df$  can be written as,

$$df = \sum_{i=1}^n g_i(x_1, x_2, \dots, x_n) dx_i \quad (\text{A.1.63})$$

then the function  $g_i(x_1, \dots, x_n)$  is called the (partial) derivative of  $f$  with respect to  $x_i$ , for  $i = 1, \dots, n$ ,

$$\frac{\partial f}{\partial x_i} = g_i(x_1, \dots, x_n) \quad (\text{A.1.64})$$

Similarly, if the variation of a functional

$$I[y(x)] = \int_a^b F(y(x), y'(x)) dx \quad (\text{A.1.65})$$

can be written as,

$$\delta I = \int_a^b g(x) \delta y(x) dx \quad (\text{A.1.66})$$

then the functional derivative of  $I$  is

$$\frac{\delta I}{\delta y(x)} = g(x) \quad (\text{A.1.67})$$

The functional derivative of a functional  $I[y(x)]$  is a function  $g(x)$ .

## 2.6. The variational derivative [Sch 05]

Consider a density function  $\mathcal{H} : \Lambda^v(\Omega) \times \Omega \rightarrow \Lambda^n(\Omega)$  where  $v \in \{1, \dots, n\}$ . The variational derivative of the functional  $H = \int_{\Lambda} \mathcal{H} \in \mathbb{R}$

with respect to  $y \in \Lambda^v(\Omega)$  is the differential form  $\frac{\delta H}{\delta y} \in \Lambda^{n-v}(\Omega)$  which

satisfies for all  $\Delta y \in \Lambda^v(\Omega)$  and  $\varepsilon \in \mathbb{R}$ :

$$H(y + \varepsilon \Delta y) = \int_{\Omega} \mathcal{H}(y + \varepsilon \Delta y) = \int_{\Omega} \mathcal{H}(y) + \varepsilon \int_{\Omega} \left[ \frac{\delta H}{\delta y} \wedge \Delta y \right] + O(\varepsilon^2) \quad (\text{A.1.68})$$

where  $\mathcal{H} : \Lambda^v(\Omega) \times \Omega \rightarrow \Lambda^n(\Omega)$ ,  $v \in \{1, \dots, n\}$  is a density function.

